2013-07-23

Investigation of Robust Chatter Stability in Milling

Graham, Eldon

UNIVERSITY OF CALGARY

Investigation of Robust Chatter Stability in Milling

by

Eldon Graham

A THESIS

SUBMITTED TO THE FACULTY OF GRADUATE STUDIES

IN PARTIAL FULFILMENT OF THE REQUIREMENTS FOR THE

DEGREE OF MASTER OF SCIENCE

DEPARTMENT OF MECHANICAL & MANUFACTURING ENGINEERING

CALGARY, ALBERTA

JULY 2013

Abstract

In machining operations, self-excited regenerative chatter can develop due to a phase difference between overlapping cutting paths which results in oscillating chip thickness. Machine tool chatter decreases overall productivity and quality of manufactured parts due to excessive vibrations. Analytical models are used to predict the chatter stability lobe diagrams, which illustrate stable and unstable combinations of cutting depths and spindle speeds. The conventional chatter models, however, typically assume that parameters are constant, which leads to inaccuracy. Dynamics, including natural frequencies, damping ratios, and cutting coefficients are the primary parameters that are susceptible to uncertainty and can vary during real milling operations. Especially in micro milling, high spindle speeds can generate centrifugal forces, gyroscopic moments, and thermal effects in the spindle bearings, which can significantly affect tooltip dynamics. Cutting coefficients reflect how the cutting tool interacts with the workpiece material and due to the miniature tool size, material uniformity, tool geometry, and frictional effects, can all affect cutting coefficient values. In addition, cutting coefficients can also be affected by the two different cutting regimes, ploughing or shearing dominant that can exist depending upon the chip thickness with respect to the edge radius of tools. The effects of parameter uncertainty can be directly taken into consideration using the robust stability approaches. The objective of this study is to develop two robust formulations for predicting regenerative chatter stability in micro milling while considering the effects of three uncertain parameters: namely natural frequencies, damping ratios, and cutting coefficients. A frequency domain approach using the Edge theorem can analytically account for time invariant parameter uncertainty directly in the characteristic equation. Combined with the Zero Exclusion principle,

computation of stability regions can be efficiently checked graphically. Robust chatter stability can also be detected using Lyapunov stability subjected to linear matrix inequality (LMI) constraints. Experiments are conducted to demonstrate that, while both methods can conservatively predict system stability, the Edge theorem approach predicts the stability lobes faster. From an accuracy and computational time viewpoint, both robust stability approaches are compared for establishing micro milling chatter stability regions. Whereas the LMI approach can be extended to account for time varying parameter uncertainty.

Acknowledgements

I would like to thank Dr. Simon Park for his academic guidance and support. This project was funded by the Natural Sciences and Engineering Research Council - Canadian Network for Research and Innovation in Machining Technology (NSERC CANRIMT) and the Alberta Innovates Technology Futures (AITF). I would also like to acknowledge my colleagues in the Micro Engineering Dynamics Automation Laboratory (MEDAL) at the University of Calgary for their support, and I would especially like to thank Majid Mehrpouya for help reviewing and editing this thesis. Finally I would like to acknowledge Dr. Ryozo Nagamune from the University of British Columbia who collaborated in developing the LMI robust stability.

Table of Contents

List of Figures

List of Tables

List of Symbols

A , B , C , D	State space matrices for dynamics
A_T , B_T , C_T , D_T	State space matrices of Pade approximation
a	Cutting depth
α_{xx} , α_{xy} , α_{yx} , α_{yy}	Time invariant average directional factors
b_x , b_y	Number of modes in x and y directions
c_x , c_y	Damping coefficients in x (feed) and y directions
F_x , F_y	Cutting force in x (feed) and y directions
F_t	Cutting force tangential to cutting edge
F_r	Cutting force radial to cutting edge
f_t	Feed rate per tooth
G	Assembled structure FRF
H	Substructure FRF
h	Dynamic chip thickness
h_o	Static or desired chip thickness
I	Identity matrix
K_{tc}	Tangential cutting coefficient
K_{rc}	Radial cutting coefficient
K_{te}	Tangential edge coefficient
K_{re}	Radial edge coefficient
K_r	Ratio between radial and tangential cutting coefficients
k_x , k_y	Stiffness coefficients in x (feed) and y directions

M	System matrix
m	Number of uncertain parameters
m_x , m_y	Mass coefficients in x (feed) and y directions
N	Number of flutes
n	Spindle speed [rpm]
P	Lyapunov matrix
p	Extreme vertex polynomial
s	Laplace variable
T	Time delay
t	Time
V	Lyapunov function
$x(t)$, $y(t)$	Tool displacement in x (feed) and y directions
ε	Phase shift between cutting paths
Λ	Eigenvalue
ρ	Equivalent parametric bounds
υ	Fluid density
Φ_{xx} , Φ_{yy}	Transfer function of dynamics in x (feed) and y directions
ϕ	Immersion angle
ϕ_{st}	Start immersion angle
ϕ_{ex}	Exit immersion angle
ζ_x , ζ_y	Damping ratios in x (feed) and y directions
ω_c	Critical chatter frequency
$\omega_{n,x}$, $\omega_{n,y}$	Natural Frequencies in x (feed) and y directions

List of Abbreviations

2-DOF	Two Degree of Freedom
AE	Acoustic Emission
CNC	Computer Numerical Control
EMA	Experimental Modal Analysis
FFT	Fast Fourier Transform
FE	Finite Element
FRF	Frequency Response Function
LMI	Linear Matrix Inequality
MDOF	Multiple Degree of Freedom
RC	Receptance Coupling
RMS	Root Mean Square
SDOF	Single Degree of Freedom

CHAPTER 1. INTRODUCTION

Many industries are searching for more advanced machining solutions to meet increasing demands for accurate, high quality components. To stay competitive in a global market, aerospace manufacturers have concluded that high performance machining methods are needed to deliver high volumes of advanced, functional products, including airfoils and turbine engines [Kappmeyer et al. 2012]. Machining processes are widely used in modern industry to fabricate highly accurate three dimensional components. In manufacturing research, machining is a popular topic as manufacturers are keen to boost material removal rates and surface quality of components. Technology has advanced tremendously in recent years and this has opened up many new improvements manufacturers can take advantage of. Higher efficiency and reduced material wastage is now possible due to developments in computing and software technology, which allow for enhanced process optimization as well as in process monitoring. The increased accuracy of finished components has been made possible with developments in accurate positioning feed drives, rigid spindles, and enhanced cutting tools [Abele et al. 2010, Altintas et al. 2011]. Modern machining technology allows optimal process parameters to be identified to suit any particular machining setup.

Using miniaturized cutting tools, micro machining is increasingly being utilized for the fabrication of miniature components, which can range anywhere from a few micrometers to a few millimetres in size. Many of the same advantages associated with macro sized machining are also present in micro operations. These include fabrication of three dimensional (3D) parts, high dimensional accuracy, and few material limitations. However, the small size of the cutting tool, presents some challenges with cutting on a micro scale. Micro cutting tools are very fragile and

tool deflection is a critical issue. Especially in micro milling processes, intermittent cutting can decrease tool longevity and pose difficulties in controlling part tolerances [Chae et al. 2006]. Due to the high spindle speeds required, small amplitude measurement signals will contain high frequency components, which require high bandwidth sensors to detect and can be sensitive to sensor noise [Chae et al. 2007]. This presents many measurement and process monitoring challenges which are essential to improving productivity and minimizing vibrations.

Mechanical tool vibrations known as chatter are consistently recognized as the primary factor which limits the productivity and can have adverse effects upon part quality. Under certain conditions, interactions between the cutting tool and workpiece can specifically lead to self-excited vibrations, known as regenerative chatter [Altintas 2012, Schmitz et al. 2009]. As shown in Figure 1.1, chatter occurs when a phase difference between cutting paths left by the cutting tool on the workpiece surface produces an oscillating chip thickness. This causes amplification in tool deflections and can present serious limitations to the machining process.

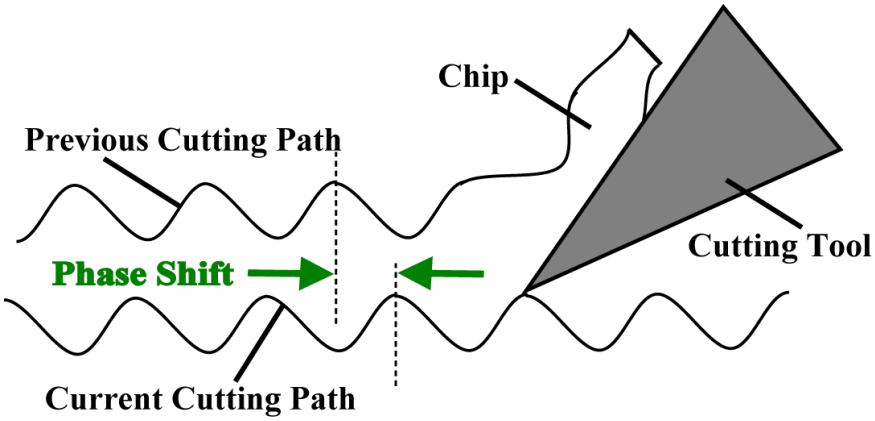

Figure 1.1 Regenerative chip thickness

Studies done by Tobias and Fishwick [1958] and Tlusty [1963] provided the framework of many of the early regenerative chatter stability models and the first descriptions of the self-excitation effect. Regenerative chatter receives much interest from the research community due

to its unique dynamic behaviour and the challenges it poses to machinists and manufacturers. Chatter limits material removal rates and in severe cases can result in wasted production time and energy, damage to the workpiece, and breakage of machine tools. In addition to restricting productivity, chatter produces poor surface finishes, dimensional inaccuracies, accelerated tool wear, and excessive noise [Quintana et al. 2011]. With these negative aspects, choosing suitable process parameters and eliminating chatter has become an integral part of optimizing machining operations.

For a given machine tool setup, chatter occurs at certain combinations of cutting depth and spindle speed. These combinations can be presented in stability lobe diagrams as shown in Figure 1.2, which graphically illustrate the boundary between unstable and stable cutting regions [Altintas et al. 2004]. Stability lobe diagrams can be easily predicted using analytical models, which use delay differential equations to describe the self-excited, regeneration effect [Altintas 2012]. A key feature of stability lobes are the peaks, which indicate that at certain spindle speeds, relatively large, chatter free depths of cut can be achieved. By identifying theses peak regions, machinists and manufacturers can identify process parameters to maximize their material removal rate without encountering unstable chatter [Budak 2006].

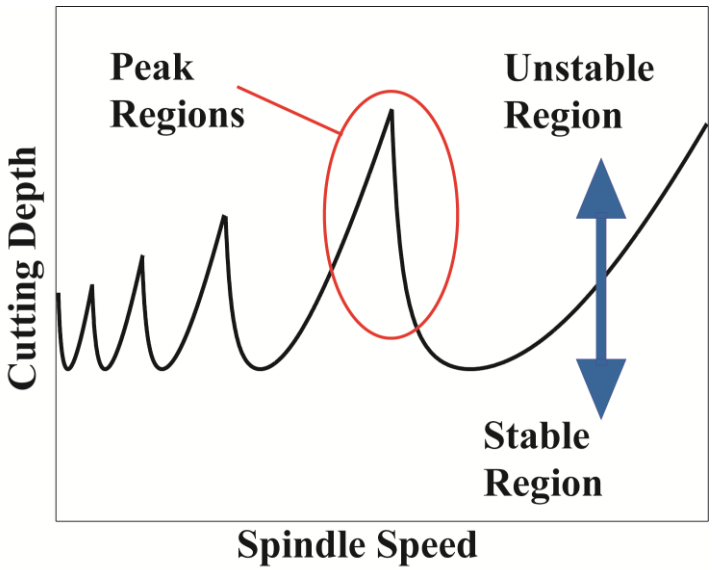

Figure 1.2 Chatter stability lobe diagram

Prediction of stability lobe boundaries partly involves experimental methods, which requires knowledge of both the machine tool system and a suitable mathematical model [Quintana et al. 2010]. Chatter stability depends upon structural dynamics of the machine tool system and the interaction behaviour between the cutting tool and workpiece material. Chatter vibrations occur near the natural frequencies of the tooltip, and therefore dynamic parameters must be acquired for a given milling machine and cutting tool. Mechanistic models are used to describe cutting forces and cutting coefficient parameters are needed to reflect how the chip thickness generated by the machining process relates to forces. Cutting coefficients are experimentally identified by measuring cutting forces for a given workpiece material and cutting tool. To enable stability lobe prediction, chatter stability models require system parameters to be accurately identified.

Implementing techniques to minimize and avoid chatter will be an important step towards meeting surface roughness and tolerance requirements in many industries. Due agility and flexibility, the use articulated robot arms for machining is a growing trend which some industries

have begun to embrace. However, due to varying dynamics and deflection issues, vibration and chatter analysis are crucial to the future success of implementing robot machining systems and in the fabrication of miniature components [Chen et al. 2012, Chae et al. 2006]. Excessive vibrations can lead to a complete loss of dimensional accuracy and increased cutting forces, which reduces tool longevity. Understanding chatter stability has become a vital to the future development of many advanced industries that rely on machining technologies.

1.1 Motivation

Proper selection of machining process parameters to avoid chatter can prevent tool breakage and damage to machine, reduce tool wear, and maximize material removal rates. Utilizing stability lobe diagrams prior to the actual cutting process has been a proven method of avoiding chatter [Altintas et al. 2004]. Conventional analytical models used to predict stability lobe diagrams; however, they assume that parameters are constant when in reality they are subject to uncertainty during machining operations [Park et al. 2007]. Uncertainties arise from modeling assumptions, experimental measurements, and parameter changes during the actual milling operation. If parameter uncertainty could be accounted for, then stability lobes could be more reliably predicted.

Dynamics, including natural frequencies and damping ratios, and cutting coefficients are the primary parameters that affect chatter stability. Chatter stability models are sensitive to variations in theses parameters, which result in inaccurate stability lobe diagrams that are ineffective in selecting optimal cutting depths and spindle speeds [Quintana et al. 2010]. The effects of material behaviour, thermal expansion, and other nonlinear behaviour that are known to occur during chip formation are complex and difficult to model [Quintana et al. 2011, Wiercigroch et al. 2001]. Often these effects are neglected in conventional chatter models or

approximated using linear models, which can also render stability lobes impractical to use [Stepan 2001].

In micro milling, excessive vibrations are detrimental to tolerances and parameter variations are known to occur during the process. High spindle speeds have been known to introduce variations in dynamic parameters, through changes in centrifugal forces and gyroscopic effects [Jorgensen et al. 1998, Movahhedy et al. 2006]. Spindle shafts cannot be perfectly balanced due to small mass imbalances and bearings can deform due to thermal effects [Abele et al. 2010]. Variations in cutting coefficients can arise due to material uniformity, tool wear, and tool geometry [Stepan 2001, Park et al. 2007]. In addition, two different cutting regimes, ploughing dominant and shearing dominant, have been shown to exist depending upon feed rate and chip thickness [Malekian et al. 2009]. Increased process damping effects due to ploughing, material elastic recovery, and friction also affect cutting forces and alter chatter stability lobes. At low spindle speeds, process damping effects dissipate energy and increase stability lobe boundaries [Rahnama et al. 2009].

Acquiring system parameters requires experimental methods to identify dynamic parameters for given spindle system, and cutting coefficients for a given tool-workpiece pair. Measurement uncertainty primarily enters when collecting the tool tip frequency response functions (FRFs) and cutting coefficients [Duncan et al. 2006]. Accurate parameter identification can be difficult to achieve since stationary tool dynamics can differ during actual cutting due to changing conditions [Cao et al. 2012]. Micro milling operations experience much higher frequency vibrations, compared to its macro scaled counterpart, and accurate measurements can be difficult to achieve due to limitations of different sensors. External factors, such as untrained

personal with insufficient knowledge, can also cause human errors when taking measurements [Quintana et al. 2010].

To overcome the challenges of predicting chatter stability lobes while considering parameter variations, the conventional analytical model for chatter stability can be formulated while considering robust stability theorems. The behaviour of many real systems is dominated by parameter uncertainty, and therefore robustness has become a major consideration in many processes. In control theory, a robust process is one that tries to resist the effects of uncertainty in order to meet performance or stability conditions [Safonov 2012]. It has been recognized that addressing the issue of robustness is paramount in preventing failures and improving reliability of engineering systems. This has been a major driver in behind the development of robust theories for design and analysis.

All models are approximations of real systems and modelling robustness depends upon a description of the uncertainty in the system. Uncertainty can be described using either a deterministic description involving extreme boundaries or a probabilistic description [Calafiore et al. 2011]. Using a deterministic description, uncertain parameters can be modelled as having any value between an upper and lower limit. Robust stability theorems based on this description attempt to ensure stability for all possible values. In contrast, using a probabilistic description models the uncertain parameters as having a statistical nature [Tempo et al. 2013]. Robust theorems using a probabilistic description cannot guarantee robust stability for all possible uncertain parameter values and as a result, there always exists a small risk of instability. In micro milling, both the process productivity and quality of fabricated components can be hindered in the presence of vibrations. The motivation is therefore to utilize a deterministic description of uncertain parameters with extreme bounds, which represents a worst case scenario.

Two different robust stability methods can be implemented and compared: a frequency domain approach involving the Edge theorem and polynomial equations, and a Lyapunov stability approach using linear matrix inequality (LMI) constraints. There are many sources of uncertainty that affect chatter stability, however, provided that both the system parameters and the upper and lower bounds on these parameters can be quantitatively determined, then the effects of uncertainties can be accounted for using robust theorems. Robust stability theorems are ideally suited to the chatter problem and uncertain parameters can be analytically incorporated directly into stability models. By developing new robust chatter stability models and algorithms, stability lobes can be predicted with higher accuracy and guaranteed stability.

1.2 Objectives

Advanced manufacturing requires new reliable chatter theories to enable optimal process parameter selection. The primary objective of this thesis is to develop an improved approach to chatter avoidance that accounts for the effects of parameter variations and uncertainties in micro milling operations. Using robust stability theories, conventional chatter models can be expanded to predict stable and unstable regions when parameter uncertainty is known. There have been previous studies which utilized robust stability theorems in the prediction of chatter lobe diagrams. For macro milling operations, Park et al. [2007] used the Edge theorem and Zero Exclusion principle to predict stability lobes. Park et al. [2009] extended the method for micro milling operations and included the effects of process damping. There are two main limitations these studies. Both only considered variations in two parameters, the natural frequency and cutting coefficients. When modeling robust systems to include more uncertain parameters, the issue of increased computational time must be addressed. Efficient algorithms, coding practices, and selection of computer hardware become important to consider. To predict robust stability

lobe diagrams, these studies only considered the pseudo single degree of freedom (SDOF) stability model. While this model is simple to implement, this model may be inadequate for milling operations especially at full immersion conditions [Altintas et al. 2004]. This study looks into developing a robust stability model which considers the effects of three uncertain parameters and is based on the two degree of freedom (2-DOF) regenerative chatter stability model, developed by Altintas and Budak specifically for milling operations [Altintas et al. 1995].

Two different robust approaches are described, and while both are derived considering three uncertain parameters, either can be generalized for any number of uncertain parameters. For uncertain parameters that are known to vary between given maximum and minimum values, stable cutting conditions can be predicted. Using the Edge theorem, robust stability can be found with a geometric approach. Combined with the Zero Exclusion principle, chatter stability can be efficiently checked graphically. The second approach is based upon Lyapunov theory, and while there are some challenges associated with finding Lyapunov functions, stability can be established for a wide range of different types of systems. With extensions of Lyapunov theory, robust chatter stability can be established by imposing constraints on the system in the form of linear matrix inequality (LMI) equations. The effects of varying parameters are critical for stability in micro milling operations. Robust stability methods can minimize chatter and provide a way to achieve high quality finished components. The objectives of this research are:

i. *Investigate varying parameters during micro milling operations:*

Especially during micro milling operations, parameter uncertainty due to both high spindle speeds and the miniature size of the cutting tool, can pose major difficulties in finding optimal cutting conditions. The dynamics of miniature cutting tools are highly influenced by the development of dynamic and thermal effects in the spindle at high

speeds. The size of the cutting tool edge, relative to the chip thickness is more comparable in micro milling, which leads to more uncertainty in cutting coefficient values. Different material behaviour and cutting mechanisms are present which affect how chip formation relates to cutting forces. In addition, the presence of grain boundaries and other material defects can cause variations. Changes in parameters can cause shifts in predicted stability lobe diagrams and in reality, dynamic parameters and cutting coefficients can only be known approximately. However, if the upper and lower bounds on the uncertain parameters can be determined, then robust stability theorems can be applied and chatter stability lobes, more reliably predicted. For this study, three varying parameters are considered: the natural frequency, damping ratio, and cutting coefficients. For a real micro milling system, parameter variations are artificially introduced and the effects of parameter variations are investigated. Tooltip dynamics are changed in real time during actual micro milling operations by attaching liquid reservoirs to the spindle and varying the liquid levels. Variations can be introduced into the cutting coefficient parameters through micro milling of free machining brass, which has a coarse grained microstructure. Dynamic and cutting coefficient parameters with their respective uncertainty bounds are experimentally identified and utilized in robust chatter stability lobe predictions.

ii. *Develop a robust chatter stability approach involving the Edge theorem:*

Edge theorem provides a means for incorporating the effects of parameter uncertainty in establishing system stability. Historically, Edge theorem is an extension of Kharitonov's theorem, which was the first robust stability theorem to present the idea of finding stability using extreme boundaries. A robust formulation of the characteristic

equation utilized in the 2-DOF analytical chatter stability model for milling processes is presented using the Edge theorem. By evaluating the characteristic equation at only the extreme combinations of uncertain parameters, the problem of determining robust stability is transformed into a graphical problem. Along with the Zero Exclusion condition, an algorithm for establishing robust stability for micro milling operations in the frequency domain is described for three uncertain parameters.

iii. *Develop a robust chatter stability approach involving LMIs:*

Lyapunov stability theory determines stability by examining the trajectory of system states. Stability for an entire system can be determined by finding appropriate Lyapunov functions without having to solve complicated differential equations. While finding Lyapunov functions presents a major challenge, there has been increased interest due to the theory's applicability to a wide range of problems and advanced computational techniques. Linear matrix inequality equations are being utilized in modern control theory literature. They represent constraints placed upon a system and can be solved using convex optimization methods. In this study, a robust extension of Lyapunov stability theory involving LMIs is utilized in the formulation of the 2-DOF robust chatter model for micro milling while considering three uncertain parameters.

While most robust stability theorems assume that uncertain parameters are time invariant, in reality this is a simplification of the more general case of time varying uncertainty where the rates of parameter variation are considered. During actual milling operations, parameters vary in time and robust stability theorems involving LMIs can be used to account for time varying uncertainty. In this study, an investigation is also

performed into whether including time varying effects of uncertain parameters may lead to more accurate stability lobes.

iv. *Compare both robust approaches presented:*

While the combination of the Edge theorem and the Zero Exclusion principle is geometric approach to establishing robust stability, the LMI approach relies on Lyapunov stability. Both methods present different mathematical approaches to solving robust problems and can be compared in terms of accuracy and performance. Uncertainty modeling is an important step when utilizing robust theorems and both approaches can consider uncertain parameters that are only known approximately.

The contributions of this thesis are achieved through development and verification of robust chatter stability models. Robust stability theorems are incorporated into the 2-DOF conventional stability model in the context of three uncertain parameters. For supporting experimental work, parameters and uncertainty bounds are identified for a real micro milling system. The spindle is equipped with liquid reservoirs and the liquid level is varied during actual cutting to change the dynamics. Dynamic parameters and variations of the tooltip are indirectly found using a combination of Experimental Modal Analysis and Receptance Coupling. Cutting coefficient parameters are obtained through measuring cutting forces and optimizing with a linear mechanistic force model. After nominal values for all three uncertain parameters, natural frequency, damping ratio, and cutting coefficients, and their uncertainties are identified experimentally, chatter stability lobes using both robust approaches are predicted. The stability lobe predictions compared to actual detected chatter points and the conventional chatter stability model which considers no parameter variations.

1.3 Thesis Organization

This thesis contains six chapters that are organized as follows:

Chapter two contains a literature review of chatter stability in milling operations. It covers a brief history of the development of analytical regenerative chatter stability models and a summary of the sources of uncertainty that affect micro milling chatter stability. It also covers an overview of the two different robust control approaches to stability that utilize a deterministic description of parameter uncertainty.

Chapter three outlines the experimental setup and procedure used to obtain parameters and uncertainty bounds. Experimental Modal Analysis (EMA) and Receptance Coupling (RC) were used to acquire dynamic parameters including natural frequencies, and damping ratios. Two different computer numerical controlled (CNC) milling machines were used to obtain cutting coefficients and perform chatter experiments.

Chapter four describes the robust stability formulation using a frequency domain approach, combining the Edge theorem and the Zero Exclusion condition. The two degree of freedom (2-DOF) analytical chatter stability milling model and the automated procedure for plotting robust stability lobes with changing parameters is described. Detected chatter points were compared to predicted stability lobes to verify the robustly predicted lobes. The prediction is verified through experiments.

In Chapter five, the robust formulation involving a linear matrix inequality (LMI) approach is described. The state space form of the 2-DOF chatter stability is first derived using a Pade approximation of the delay term. Based upon Lyapunov stability theory, three different sets of LMIs are described depending upon the system modeling, and compared. The LMI and Edge theorem methods are also compared and contrasted.

Chapter six concludes the thesis. It includes a summary, discussion of assumptions and limitations, and a description of future works that could improve the future research. This final section also summarizes the novel scientific contributions.

CHAPTER 2. LITERATURE REVIEW

In this chapter an overview of the basic chatter stability models used in milling are described. Chatter stability theory has seen extensive developments since Tobias and Tlusty first described the fundamental aspects of the regenerative effect in the 1950's [Altintas et al. 2004]. Altintas and Budak [1995] developed a successful linear analytical model, which is more accurate for milling operations and is employed by many researchers today. Modal parameters of the spindle and tooltip, and cutting coefficients are the primary parameters that contribute to dynamic chatter behaviour. These parameters are, however, subject to many sources of uncertainty which affect stability lobe predictions. Implementing robust stability techniques is one solution to address the issue of parameter uncertainty.

2.1 Conventional Chatter Stability in Milling

Tlusty et al. [1975] and Tobias and Fishwick [1958], first described the contact mechanism between tool and workpiece and introduced a basic regenerative chatter stability theory for single degree of freedom (SDOF) systems. At certain cutting depths and spindle speeds, vibrational modes of the cutting tool can excite and cause a wavy surface to be cut into the workpiece surface. Regenerative chatter occurs when this wavy surface is imprinted onto the workpiece surface over successive, overlapping cuts of the cutting tool [Schmitz et al. 2009]. The phase difference between current and previous cutting paths generates variations in chip thicknesses and amplification in vibrations. The oscillating chip thickness may grow exponentially when the critical chatter frequency is close to the dominant structural frequency

[Altintas 2012, Schmitz et al. 2009]. As shown in Figure 2.1, this differs from forced vibrations where subsequent cuts are in phase and the chip thickness is constant [Huo et al. 2009].

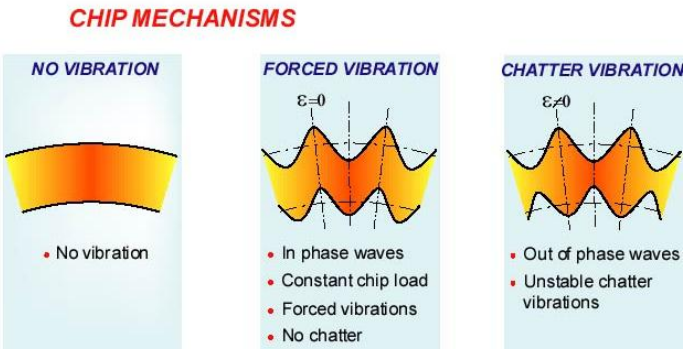

Figure 2.1 Chip mechanisms [Altintas 2012]

In milling the phase shift occurs as each tooth on the milling cutter passes over the surface. By considering the true kinematics of an end mill, including chip formation mechanisms, tool geometry, and runout effects, chatter analysis can be accomplished using numerical time domain simulations [Han et al. 2012]. However, analytical frequency domain models are preferable due to faster computation [Wiercigroch et al. 2001]. As shown in Figure 2.2, end mills are modeled with two degrees of freedom (2-DOF) [Altintas 2012]. For flat end mills a 2-DOF model is sufficient since forces are considerably less along the bottom face and the tool is much stiffer in the vertical direction. The end mill is consider to be rotating with angular speed of n, with N number of teeth, and is fed into the workpiece along the x axis at a given immersion condition.

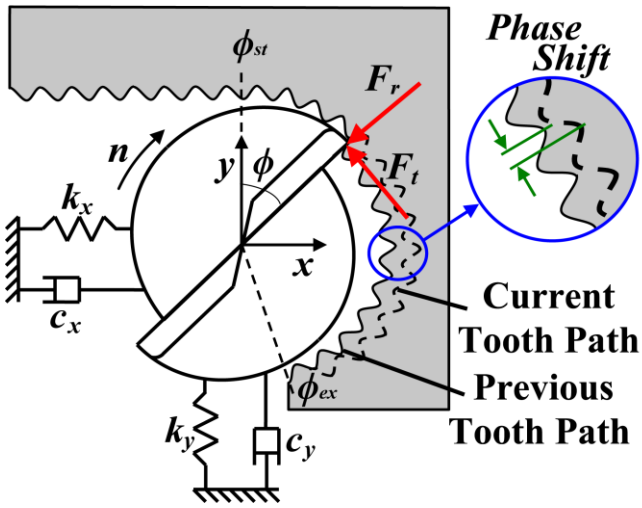

Figure 2.2 2-DOF Milling model for chatter analysis

With two independent, orthogonal degrees of freedom, and mass, stiffness and damping coefficients given by m_x, m_y, k_x, k_y, c_x, and c_y, the equations of motion for the 2-DOF milling system can be written as:

$$\begin{aligned} m_x\ddot{x} + c_x\dot{x} + k_x x &= \sum_{i=1}^{N} F_{x,i} \\ m_y\ddot{y} + c_y\dot{y} + k_y y &= \sum_{i=1}^{N} F_{y,i} \end{aligned} \tag{2.1}$$

The cutting forces in the tangential and radial directions given by F_t and F_r, initially excite each tooth i, imparting a wavy surface onto the workpiece surface. With each successive cutting edge overlapping the previously cut surface with period T, an oscillating chip develops leading self-excited vibrations. The total dynamic chip thickness, h, is given by [Altintas et al. 2004]:

$$h(t) = g_i\left[f_t \sin(\phi_i) + \Delta x(t)\sin(\phi_i) + \Delta y(t)\cos(\phi_i)\right] \tag{2.2}$$

where f_t is the feed per tooth, $\Delta x(t)=x(t)-x(t-T)$ and $\Delta y(t)=y(t)-y(t-T)$ are the changes in end mill displacements between the present and previous cuts. The delay between the successive passes of the cutting edges is related to the spindle speed:

$$T = \frac{60}{Nn} \tag{2.3}$$

With the immersion angle, given as a function of time $\phi_i(t)= nt$, the function, g_i, determines whether each tooth is engaged in the workpiece and lies between the entry, ϕ_{st}, and exit, ϕ_{ex}, immersion angles:

$$g_i = g(\phi_i) = \begin{cases} 1 & \phi_{st} < \phi_i < \phi_{ex} \\ 0 & else \end{cases} \tag{2.4}$$

The static chip thickness, $f_t sin(\phi_i)$, represented by the first term in Equation 2.2, does not contribute to the dynamic behaviour [Altintas 2012].

Proper selection of cutting parameters is important since they affect cutting forces. Modeling of cutting forces provides a better and more in-depth understanding of tool longevity, tool wear, and final quality of machined components. For macro cutting operations, cutting force models are based upon a sharp cutting edge theory first presented by Merchant [1945]. For shearing dominant cutting the mechanistic cutting forces for conventional milling can be formulated as [Tlusty et al. 1975, Altintas 2012]:

$$\begin{aligned} F_{t,i} &= K_{tc} ah + aK_{te} = K_{tc} ah \\ F_{r,i} &= K_{rc} ah + aK_{re} = K_r F_{t,i} \end{aligned} \tag{2.5}$$

where a is the depth of cut, K_{tc}, K_{te}, K_{rc}, and K_{re} are the cutting and edge coefficients in the tangential and radial directions, respectively, and $K_r=K_{rc}/K_{tc}$ is the ratio between radial and tangential cutting coefficients. The edge coefficient terms represent friction between the tool and workpiece and with the linear model, friction forces are assumed to be constant [Park et al.

2009]. In chatter analysis, the static edge coefficient terms are dropped since they do not contribute to the dynamic behaviour. Cutting coefficients are found experimentally by measuring forces at different feed rates and optimizing with theoretically found cutting forces [Altintas et al. 2004].

The cutting forces and responses in the x and y directions are coupled through transfer functions that represent the dynamics of the system. Frequency response functions (FRFs) are identified through either conventional Experimental Modal Analysis (EMA) techniques or indirectly with the Receptance Coupling (RC) method [Mascardelli et al. 2008]. The direct transfer functions, Φ_{xx} and Φ_{yy}, consist of k_x, k_y, ζ_x, ζ_y, $\omega_{n,x}$, and $\omega_{n,y}$, which are the modal stiffness, damping ratios, and natural frequencies in the x and y directions. For b_x and b_y number of modes in each direction, the transfer functions in both directions can be written as:

$$\begin{aligned} \Phi_{xx} &= \sum_{i=1}^{b_x} \frac{\omega_{n,,x,i}{}^2 / k_{x,i}}{s^2 + 2\zeta_{x,i}\omega_{n,x,i}s + \omega_{n,x,i}^2} \\ \Phi_{yy} &= \sum_{i=1}^{b_y} \frac{\omega_{n,y,i}{}^2 / k_{y,i}}{s^2 + 2\zeta_{y,i}\omega_{n,y,i}s + \omega_{n,y,i}^2} \end{aligned} \tag{2.6}$$

where $s=j\omega$ is the Laplace variable.

To illustrate the relationship between cutting process dynamics, which includes cutting force model and modal dynamics of the machine tool structure, Merritt [1965] presented the block diagram, shown in Figure 2.3.

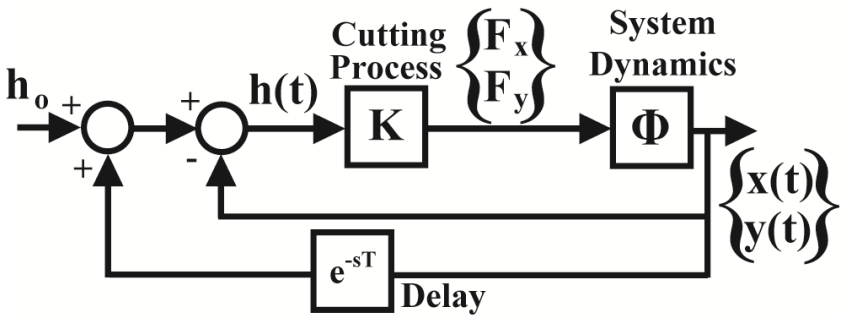

Figure 2.3 Block diagram of regenerative chatter process

For a desired chip thickness, h_o, the cutting process, which depends the depth of cut, cutting coefficients and tool geometry, produces cutting forces, F_x and F_y. The inner feedback loop represents the current displacement, *x(t)* and *y(t),* and when it is out of phase with the previous cutting path, *x(t-T)* and *y(t-T),* regenerative chatter occurs. In milling the time delay of the outer feedback loop occurs between cutting teeth shown in Equation 2.3. The dynamic chip thickness, *h(t),* oscillates in size and produces the self excited effect.

Modeling of chatter stability in milling is made difficult due to the changing direction of the cutting forces since chip thickness is dependent upon the immersion angle [Schmitz et al. 2009]. Tlusty presented a basic model which dealt with the time variance in the cutting force direction by projecting the cutting forces and vibrations into a single direction [Tlusty 1978]. Alternatively, Altintas and Budak used a truncated Fourier series and eigenvalue approach to deal with the time varying effects [Altintas et al. 1995, Altintas et al. 1999].

2.1.1 Pseudo SDOF Chatter Model

A pseudo SDOF characteristic equation can be derived to describe the chatter stability for multiple degree of freedom (MDOF) machining systems [Tlusty 2000]. While originally developed for orthogonal cutting operations, the theory has been extended to include milling

operations. The tangential and radial force components, Equation 2.5, can be expressed as a resultant force as a function of radial immersion angle, given by [Altintas et al. 2004]:

$$F_s(\phi) = K_s a h(\phi) \tag{2.7}$$

where i is the tooth number and K_s is the resultant cutting coefficient found using tangential and radial coefficients:

$$K_s = K_{tc}\sqrt{1+K_r{}^2} \tag{2.8}$$

Cutting forces in the feed and normal directions can be expressed in terms of the resultant force:

$$\begin{aligned} F_x(\phi) &= -F_s(\phi)\cos(\phi-\theta) \\ F_y(\phi) &= F_s(\phi)\sin(\phi-\theta) \end{aligned} \tag{2.9}$$

where angle θ is calculated using the ratio between radial and tangential forces by:

$$\theta = \tan^{-1}\left(\frac{F_r}{F_t}\right) \tag{2.10}$$

When cutting coefficients are assumed to be constant, chatter stability depends upon the depth of cut, a, and the time delay between cutting teeth, T, given in Equation 2.3 [Tlusty 2000, Altintas 2012]. At stability lobe boundaries, chatter occurs at a critical frequency, ω_c, and the characteristic equation can be derived as [Schmitz et al. 2009, Altintas et al. 2004]:

$$1+\left(1-e^{-j\omega_c T}\right)K_s a_{\lim}\Phi(\omega_c) = 0 \tag{2.11}$$

where a_{lim} is the maximum depth of cut for stable, chatter free milling, and Φ is the oriented transfer function:

$$\Phi = u_x\Phi_{xx} + u_y\Phi_{yy} \tag{2.12}$$

For milling, Tlusty used time invariant transfer functions, Equation 2.6, which he combined into a single directional, time invariant oriented transfer function [Altintas et al. 2004]. By calculating the geometric mean of the immersion angle, ϕ_o, he derived orientation factors, u_x

and u_y. Opitz presented an extension of Tlusty's model by considering the average periodic directional functions in deriving the orientated transfer function instead [Opitz 1969]. The orientation factors are defined as:

Tlusty's Method

$$\begin{aligned} u_x &= \sin(\phi_o)\cos(\phi_o - \theta) \\ u_y &= -\cos(\phi_o)\sin(\phi_o - \theta) \\ \phi_o &= \phi_{st} + \frac{\phi_{ex} - \phi_{st}}{2} \end{aligned} \tag{2.13a}$$

Opitz's Method

$$\begin{aligned} u_x &= \frac{N}{2\pi}\int_{\phi_{st}}^{\phi_{ex}} \sin(\phi)\cos(\phi - \theta)d\phi \\ u_y &= \frac{N}{2\pi}\int_{\phi_{st}}^{\phi_{ex}} -\cos(\phi)\sin(\phi - \theta)d\phi \end{aligned} \tag{2.13b}$$

The SDOF characteristic equation, Equation 2.11, was first solved by Tlusty et al. [1963], Tobias et al. [1958], and Merritt [1965], who all presented similar solutions. The characteristic equation can be split into a real part, which yields the maximum cutting depth, a_{lim}, and an imaginary part, which can be solved for phase shift, ε, between current and previous wavy cutting paths [Altintas 2012]. Stability lobes can be plotted by scanning through a range of frequencies around the natural frequency of the machine tool structure and solving the equations [Altintas et al. 2004]:

$$
\begin{aligned}
a_{\lim} &= \frac{-1}{2K_s \,\mathrm{Re}[\Phi(\omega)]m_N} \\
n &= \frac{60}{TN} \\
T &= \frac{2\pi k + \varepsilon}{\omega_c} \\
\varepsilon &= 3\pi + 2\psi \\
\psi &= \tan^{-1}\left(\frac{\mathrm{Im}[\Phi(\omega)]}{\mathrm{Re}[\Phi(\omega)]}\right)
\end{aligned}
\tag{2.14}
$$

where $Re[\Phi(\omega)]$ and $Im[\Phi(\omega)]$ are the real and imaginary parts of the oriented transfer function, k is an integer number of vibration waves, ψ is the phase shift of the transfer function, and $m_N=N(\phi_{ex}-\phi_{st})/2\pi$ is the average number of teeth in cut.

The projection of the cutting forces into one direction is a major modeling assumption, which may be suitable for orthogonal cutting. While simple to implement, in milling this approximation leads to inaccuracies depending upon the immersion conditions [Altintas et al. 2004]. For milling, some of the inaccuracies of using an oriented transfer function are avoided when considering analytical eigenvalue model for chatter stability.

2.1.2 2-DOF Chatter Model

Chatter stability in milling was further studied by Altintas and Budak who presented a pure 2-DOF analytical chatter stability model [Altintas et al. 1995]. Instead of projecting dynamic transfer functions onto a single plane as in the pseudo SDOF model, Altintas and Budak used an eigenvalue analysis to solve the 2-DOF milling system in the frequency domain.

The tangential and radial cutting forces, Equation 2.5, can be transformed to the feed and normal directions through the immersion angle [Altintas 2012]:

$$F_x = \sum_{i=1}^{N} - F_{t,i}\cos(\phi_i) - F_{r,i}\sin(\phi_i)$$
$$F_y = \sum_{i=1}^{N} F_{t,i}\sin(\phi_i) - F_{r,i}\cos(\phi_i) \tag{2.15}$$

The chip thickness, given in Equation 2.2, can be substituted into the *x* and *y* cutting forces, and expressed in matrix form:

$$F(t) = \begin{Bmatrix} F_x(t) \\ F_y(t) \end{Bmatrix} = \frac{1}{2} a K_{tc} \begin{bmatrix} a_{xx} & a_{xy} \\ a_{yx} & a_{yy} \end{bmatrix} \begin{Bmatrix} \Delta x(t) \\ \Delta y(t) \end{Bmatrix} \tag{2.16}$$

Since the immersion angle is a function of time $\phi_i(t)$, the time varying directional factors are:

$$a_{xx} = \sum_{i=1}^{N} - g_i \left[\sin 2\phi_i + K_r(1 - \cos 2\phi_i)\right]$$
$$a_{xy} = \sum_{i=1}^{N} - g_i \left[(1 + \cos 2\phi_i) + K_r \sin 2\phi_i\right]$$
$$a_{yx} = \sum_{i=1}^{N} g_i \left[(1 - \cos 2\phi_i) - K_r \sin 2\phi_i\right] \tag{2.17}$$
$$a_{yy} = \sum_{i=1}^{N} g_i \left[\sin 2\phi_i - K_r(1 + \cos 2\phi_i)\right]$$

Cutting forces in milling are periodic with respect to the tooth passing frequency. To eliminate the time dependence on the directional factors, Altintas and Budak expanded Equation 2.16 with a Fourier series and expressed them as a function of the harmonics of the tooth passing frequency [Altintas et al. 1995]. Provided that radial immersion conditions where large enough, higher harmonics can be ignored [Budak 2006]. The simplest solution considers only the mean component of the Fourier series expansion (i.e. the zero order solution) [Altintas et al. 1999]. The cutting forces can be reduced to:

$$F(t) = \begin{Bmatrix} F_x(t) \\ F_y(t) \end{Bmatrix} = \frac{1}{2} a K_{tc} A_o \begin{Bmatrix} \Delta x(t) \\ \Delta y(t) \end{Bmatrix} \tag{2.18}$$

$$A_o = \frac{N}{2\pi}\begin{bmatrix} \alpha_{xx} & \alpha_{xy} \\ \alpha_{yx} & \alpha_{yy} \end{bmatrix} \tag{2.19}$$

where the time invariant average directional factors are given as:

$$\begin{aligned} \alpha_{xx} &= \frac{1}{2}[\cos 2\phi - 2K_r + K_r \sin 2\phi]_{\phi_{st}}^{\phi_{ex}} \\ \alpha_{xy} &= \frac{1}{2}[-\sin 2\phi - 2\phi + K_r \cos 2\phi]_{\phi_{st}}^{\phi_{ex}} \\ \alpha_{yx} &= \frac{1}{2}[-\sin 2\phi + 2\phi + K_r \cos 2\phi]_{\phi_{st}}^{\phi_{ex}} \\ \alpha_{yy} &= \frac{1}{2}[-\cos 2\phi - 2K_r - K_r \sin 2\phi]_{\phi_{st}}^{\phi_{ex}} \end{aligned} \tag{2.20}$$

The transfer function matrix can be identified in the Laplace domain where the direct transfer functions are given in Equation 2.6. If only two orthogonal degrees of freedom are considered, then cross transfer functions can be assumed to be zero (Φ_{xy}=Φ_{yx}=0) [Budak 2006]. Cross transfer functions can become important to consider depending upon tool geometry, type of cutting, or other dynamic effects. Altintas et al. [2006] discussed the importance of including cross terms for plunge milling operations and Cao et al. [2012] reported that significant gyroscopic effects can increase the impact cross terms have on chatter stability. The transfer functions and the cutting forces can be substituted after taking the difference between the present and previous cutting paths. The following quadratic characteristic equation, at the critical chatter frequency, can be derived after an eigenvalue analysis is performed:

$$a_0\Lambda^2 + a_1\Lambda + 1 = 0 \tag{2.21}$$

where the coefficients, a_0 and a_1, and the eigenvalue, Λ, are:

$$\begin{aligned} a_0 &= \Phi_{xx}(\omega_c)\Phi_{yy}(\omega_c)\left(\alpha_{xx}\alpha_{yy} - \alpha_{xy}\alpha_{yx}\right) \\ a_1 &= \alpha_{xx}\Phi_{xx}(\omega_c) + \alpha_{yy}\Phi_{yy}(\omega_c) \end{aligned} \tag{2.22}$$

$$\Lambda = -\frac{N}{4\pi} a K_{tc} (1 - e^{-j\omega_c T}) \tag{2.23}$$

Using the quadratic formula, the eigenvalue can also be obtained from Equation 2.21, showing that the eigenvalue is also a function of the coefficients in Equation 2.22 and therefore depends on the dynamic transfer functions and can be split into real, Λ_{Re}, and imaginary, Λ_{Im}, parts:

$$\Lambda = -\frac{1}{2a_0}\left(a_1 \pm \sqrt{a_1^{\,2} - 4a_0}\right) = \Lambda_{\mathrm{Re}} + j\Lambda_{\mathrm{Im}} \tag{2.24}$$

Equating both eigenvalue expressions, the maximum chatter free depth of cut, a_{lim}, and corresponding phase shift, ε, between cutting paths can be solved for [Altintas 2012, Schmitz et al. 2009]. Since Equation 2.24 provides two eigenvalues, the one that yields the lowest critical cutting depth is used [Budak 2006]. Chatter stability lobes can be calculated by scanning through frequencies and solving the following equations:

$$\begin{aligned}
a_{\mathrm{lim}} &= -\frac{2\pi\Lambda_{\mathrm{Re}}}{NK_{tc}}(1+\kappa^2) \\
n &= \frac{60}{TN} \\
T &= \frac{2\pi k + \varepsilon}{\omega_c} \\
\varepsilon &= \pi - 2\tan^{-1}(\kappa) \\
\kappa &= \frac{\Lambda_{\mathrm{Im}}}{\Lambda_{\mathrm{Re}}}
\end{aligned} \tag{2.25}$$

where k is an integer number of waves.

The 2-DOF analytical chatter stability model has shown to be an accurate, versatile model and has been successful extended to other milling chatter applications. Beyond cylindrical end milling, the model has been modified for ball end mills [Altintas et al. 1999], and bull nosed end mills [Campa et al. 2011]. Shamoto et al. [2009] utilized the same procedure to include

inclination angle in predicting chatter stability for ball end mills. Budak et al. [2010] utilized this chatter model as part of a new procedure for identifying process damping effects.

Chatter stability analysis is mainly performed using frequency domain models to generate graphical stability lobes, and optimal spindle speeds and cutting depths can be selected by taking advantage of peak regions in predicted diagrams, whereby large material removal rates can be achieved. While these parameters are typically assumed to be constant, variations in these parameters can occur during micro milling operations. Parameter uncertainty can lead to instabilities during the machining process and render any initial stability lobe predictions inaccurate.

2.2 Parameter Uncertainty

Cutting coefficients and modal dynamics are the key parameters that must be identified in order to predict stability lobes, however, in reality these parameters can only be known approximately. Measurement errors, assumptions in modeling, and variations during actual cutting processes all contribute to overall parameter uncertainty, and are important to consider in chatter analysis [Duncan et al. 2006].

2.2.1 Variations in Dynamics

Dynamics of the tool and spindle system are important in chatter stability analysis and proper measurement of natural frequencies, damping ratios, and stiffness, are critical for predicting accurate stability lobes. Tool dynamics are dependent upon dynamics of the tool holder, spindle, the overall machine structure, and even the workpiece when milling flexible components [Budak 2006, Budak et al. 2012]. Dynamics can also change with material removal [Budak et al. 2012] and changes in stage and workpiece positioning [Altintas et al. 2011]. High

spindle speeds required by micro milling operations, are known to cause and even amplify variations in tool dynamics [Tlusty 1993, Cao et al. 2012].

Bearings have the greatest influence on spindle performance and many researchers have studied how different bearing related effects that occur can give rise to changes in tool dynamics during milling [Movahhedy et al. 2006]. Changes in bearing stiffness and nonlinear bearing behaviour have been largely attributed to both thermal effects and high spindle speeds [Abele et al. 2010]. In contact ball bearings, Shin [1992] reported that high speeds can cause thermal expansion resulting in decreased stiffness, in an event known as bearing softening. This shifts the contact angle of the bearings resulting in changes in centrifugal forces as shown in Figure 2.4. Bearing preloads have also been shown to have an effect on modal parameters at high spindle speeds by influencing the contact angle of bearings [Gunduz et al. 2012, Cao et al. 2012].

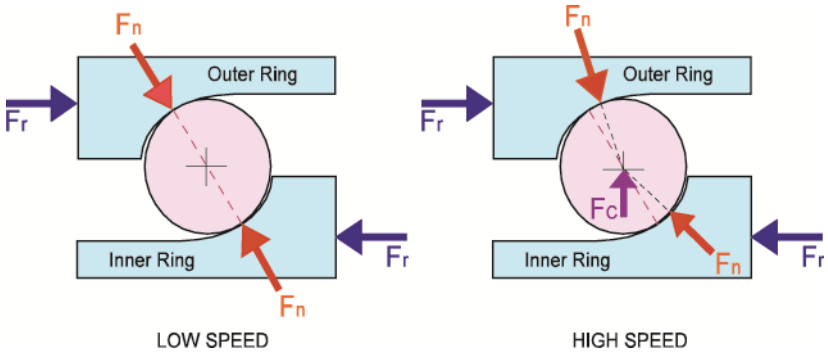

Figure 2.4 High speed effects on contact bearings [Abele et al. 2003]

General thermal effects and temperature changes of the entire spindle system also cause changes in dynamics [Mayr et al. 2012]. Friction in bearings, heat transferred from machining materials with low thermal conductivity, and power losses in the motor have all been identified as potential heat sources in spindles [Abele et al. 2010].

Jorgensen et al. [1998] investigated spindles with ball bearings and concluded that centrifugal effects play a critical role to the spindle and tool dynamics. In reality, ball bearings

and spindle shafts cannot be perfectly balanced, and even small unbalanced masses may amplify centrifugal forces. Gyroscopic effects occur when torque is generated perpendicular to the axis of spindle rotation, and have also been shown to affect spindle dynamics [Stepan 2001, Abele et al. 2010]. Both Xiong et al. [2003] and Movahhedy et al. [2006] concluded that gyroscopic effects are significant at high spindle speeds and affect both the critical chatter frequency and cutting depth in chatter stability.

Accurately measuring the tooltip frequency response function (FRF) is vital for stability analysis [Abele et al. 2010]. Since dynamics are known to change during milling, FRFs acquired on stationary machines prior to the operation may not be completely accurate [Cao et al. 2012]. Variations in FRFs can arise due to variations in impact locations when hammer testing [Mascardelli et al. 2008]. Hammer testing itself also requires some skill and knowledge of vibrations and untrained personal may not be qualified to perform modal testing [Quintana et al. 2010]. Uncertainties in modal parameters also arise due to modeling errors and many researchers have recognized the importance of including centrifugal, gyroscopic, and other speed varying effects into the analytical modeling of chatter stability [Cao et al. 2012]. However, errors can be produced while curve fitting data during EMA, and finite element models (FEM) depend on quality of computer model [Campa et al. 2011]. The dynamic effects of spindle systems at high rotational speeds can exhibit highly nonlinear behaviour and can be difficult to model completely [Quintana et al. 2011].

2.2.2 Variations in Cutting Coefficients

Chatter heavily depends upon the interaction between the workpiece and the cutting edge of the tool. Cutting coefficients are central to many mechanistic cutting models and depend on the relation between cutting forces and chip thicknesses [Gonzalo et al. 2010]. Whether certain

aspects of chip formation are included in cutting models can lead to uncertainties in cutting coefficient values. For conventional milling operations, the chip thickness predicted by the linear cutting model developed by Tlusty et al. [1975], assumes a circular cutting edge trajectory. In reality, cutting edges follow a trochoidal path and this leads to differences in predicted chip thickness [Bao et al. 2000]. Nonlinear chip formation mechanisms due to effects of strain, material behaviour, and temperature, can result in changes in cutting forces during milling [Wiercigroch et al. 2001, Stepan 2001].

In micro milling, both shearing and ploughing cutting mechanisms are present since the cutting edge radius of micro tools is comparable to chip thicknesses [Malekian et al. 2009], shown in Figure 2.5. When the uncut chip thickness is below a critical value, material deforms under the cutting edge and then elastically recovers. During this ploughing dominated regime, the edge radius results in a large effective negative rake angle and elasto-plastic material effects. Cutting force models describing a shearing based on Merchant's sharp cutting edge theory that are typically used for macro scale operations are no longer valid [Chae et al. 2007]. At higher feed rates, the cutting mechanism becomes more shearing dominated, material is removed, and the ploughing mechanism becomes negligible as chip thickness increases. In micro end milling, each flute actually switches between both cutting mechanisms and in addition must interact with ploughed areas left from previous flutes.

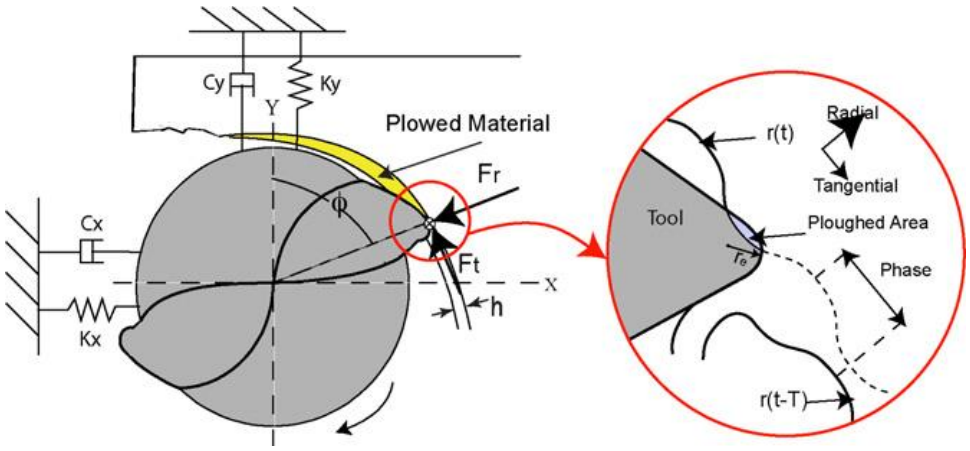

Figure 2.5 Ploughing effect in micro milling [Park et al. 2009]

Wearing of the cutting edge can change the tool geometry can affect the cutting process and lead to errors in cutting coefficients [Altintas et al. 2008]. The cutting process itself can generate work hardening effects and residual stresses which can cause tool wear and variations in the cutting coefficients [Li et al. 2007]. Especially at low spindle speeds, process damping effects have been shown to increase chatter stability [Altintas et al. 2008, Budak et al. 2010]. The use of cutting fluids which affect friction between chip and cutting tool are also known to introduce changes in cutting forces [Childs 2006].

The effects of material grain size on micro milling have also been studied. Increased tool wear and surface roughness can result when the cutting edge radius of micro end mills are comparable to grain size and interact with grain boundaries [Popov et al. 2006, Mian et al. 2009]. Feed rates, minimum chip thickness effects, process damping due to elastic recovery of material and rubbing along the flank face of the tool, and other size effects have also been shown to cause variations and affect the micro cutting process [Filiz et al. 2007, Rahnama et al. 2010, Vollertsen et al. 2009]. Cutting coefficients depend on both the properties of the workpiece material and any

non-uniformity of the workpiece material can cause uncertainties in the cutting coefficient values [Vogler et al. 2004].

Milling in general is a dynamic process and the effects of parameter uncertainty in modal dynamics and cutting coefficients are all known to affect chatter stability. Many advanced machining operations today rely on extensive computer modeling to determine optimal cutting parameters and tool paths prior to actual operations. However, computer modeling depends upon the quality of analytical models used and often requires physical parameters to be known. The accurate prediction of stability lobes is limited during cutting operations due to changing parameters and therefore uncertainties need to be considered in chatter stability analysis.

2.3 Robust Stability

Analyzing and modeling real systems is made difficult due to parameter uncertainties. Developed from control theories, robust stability theorems provide a means to analytically account for uncertainties in analysis and design. A parametric approach is used when the physical parameters of a system are known to fall between some upper and lower bounds [Fu et al. 1989], and there are several deterministic theories which can be used to establish stability for uncertain systems. In general, these methods all determine stability through calculating the extreme bounds, within which the parameters can vary [Bhattacharyya et al. 1995]. These stability theorems attempt to ensure robust stability within these bounds. Historically, the area of robust stability has seen many developments, beginning with the ideas of Kharitonov's theorem and utilizing characteristic polynomials [Kharitonov 1979, Fu et al. 1989]. More modern methods involve linear matrix inequality (LMI) formulations based on Lyapunov stability theory [Henrion et al. 2001].

2.3.1 Edge Theorem and Zero Exclusion Condition

The development of Kharitonov theorem in the late 1970's has been the inspiration behind the continued advancement of robust stability [Barmish 1994]. Classical control theory approaches to establishing stability are ineffective for systems with uncertain parameters. Parameter uncertainty directly affects coefficient values and the roots of characteristic polynomials, which govern stability and are continuously dependent upon these values [Fu et al. 1989]. When physical parameters are allowed to vary, the characteristic equation can be expressed as a family of polynomials. Unlike classical control approaches, robust stability methods seek to establish stability for a set of polynomials.

The most basic robust stability theory is Kharitonov theorem, which states that a system is robustly stable if its four Kharitonov polynomials are stable [Barmish 1989]. These Kharitonov polynomials are formed using the system's characteristic equation and only the upper and lower bounds of the uncertain parameters [Bhattacharyya et al. 1995]. This established the fundamental idea that stability for uncertain systems could be guaranteed by only testing a finite number of polynomials [Fu et al. 1989, Barmish 1994]. Unfortunately, Kharitonov's theorem is restricted to continuous time systems and cannot be implemented by either discrete time or time delay systems [Barmish 1989, Bhattacharyya et al. 1995].

Bartlett et al. [1987] first developed the Edge theorem by extending the ideas of Kharitonov's theorem to determine robust stability for a wider class of uncertain polynomials. Edge theorem addresses the problem of robust stability more generally than Kharitonov's theorem by dealing with individual uncertain parameters as opposed to strictly focusing on polynomial coefficients [Bhattacharyya et al. 1995].

Evaluating the characteristic polynomial for a system at all combinations of the upper and lower bounds on the uncertain parameters yields a family of extreme vertex polynomials. The Edge theorem says that a system is robustly stable if the edges between each pair of polynomial vertices are stable [Barmish 1994]. These edges will form a shape in the complex plane the Zero Exclusion condition can be used to check stability. If the origin lies outside the edges then the system is robustly stable [Matusu 2011]. This guarantees system stability for any combination of the uncertain parameter values, which must lie within the area between the edges.

The combination of Edge theorem and the Zero Exclusion condition can be used to improve the speed at which robust stability can be determined [Park et al. 2007]. Both Edge theorem and the Zero Exclusion condition can be applied to a wide range of problems, including continuous time systems, time delay systems, and thus the regenerative chatter problem [Matusu 2011, Park et al. 2007]. The analytical 2-DOF stability lobe prediction directly depends upon a characteristic equation in Equation 2.21 and therefore robust theorems based on polynomials, an ideal choice to use.

2.3.2 LMI's and Lyapunov Stability

LMI's have become powerful analysis and design tools in modern control engineering. LMI's can be used to formulate many problems and be solved using numerical solvers and computer algorithms. In general, an LMI is a matrix inequality equation that represents constraints, such as stability criteria, performance requirements and design specifications, which are imposed on a system [Ostertag 2011]. Uncertain systems can be easily expressed in matrix form using state space formulations and when combined with Lyapunov stability theory, robust stability can be determined [Grman et al. 2003].

Formally, an LMI is an equation of the form [Boyd et al. 1994, Ostertag 2011]:

$$F(x) = F_o + \sum_{i=1}^{n} x_i F_i > 0 \tag{2.26}$$

where x=[x_1 x_2 x_3 ... x_n] is a vector of state variables, and $F_i=F_i^T>0$ are symmetric, positive definite matrices representing constraints placed upon the state variables. Often LMI problems are formulated using matrices as variables, such as with the Lyapunov's stability criteria [Boyd et al. 1994, Grman et al. 2003].

Lyapunov's second method determines stability for dynamic systems, described by differential equations, by finding or proving the existence Lyapunov functions which have certain properties [Ostertag 2011]. This is a sufficient condition for asymptotic stability and indicates that the solutions of differential equations converge to equilibrium [Franklin et al. 2002]. Stability for a homogeneous, continuous linear system of the form:

$$\dot{x} = Ax \tag{2.27}$$

where A is the system matrix and x is the state vector. The system is said to be asymptotically stable if and only if there exists a positive definite matrix $P=P^T>0$ that satisfies the following LMI [Ostertag 2011]:

$$A^T P + PA < 0 \tag{2.28}$$

The existence of P is sufficient to establish stability, and ensure $V(x)=x^TPx$ will be a quadratic Lyapunov function. The search for suitable matrix, P is known as an LMI feasibility problem [Boyd et al. 1994]. Failure to find a Lyapunov function does not indicate instability, but says that stability cannot be established using Lyapunov's second method.

For uncertain linear systems, Horisberger et al. [1976] performed initial work by extending Lyapunov theory for the robust case of quadratic stability. The simplest robust formulation seeks to find a common quadratic Lyapunov function to satisfy a set of Lyapunov LMI equations [Barmish 1994]. While this is a sufficient condition for robust stability, it is

known to be highly conservative. Historically, this has been the motivation to develop parameterized Lyapunov functions where multiple Lyapunov matrices are found, each one dependent upon an extreme parameter combination [Dasgupta et al. 1994, Neto 1999]. This set of Lyapunov matrices can then be combined into a parameter dependent Lyapunov function. Parameter dependent quadratic stability has also been used to handle both time invariant or time varying parameter uncertainty [Dasgupta et al. 1994, Gahinet et al. 1996]. While it can be a challenge finding appropriate Lyapunov functions for quadratic stability approaches, there are techniques which can be implemented.

Quadratic stability is a robust extension of basic Lyapunov theory and can be efficiently solved using numerical algorithms based on convex optimization techniques, which are available in many commercial software and programming packages. Convex optimization refers to a large class of optimization methods, which include well known least squares and steepest descent algorithms [Boyd et al. 2004]. Since the 1980s it has been recognized that many LMIs and other control problems can be solved using convex optimization [Boyd et al. 1994]. Much of the modern control literature focuses upon a matrix approach to robust stability as opposed to a polynomial approach presented in the previous section.

2.4 Summary

This chapter presented a literature review and outline of the fundamental concepts used in regenerative chatter for milling processes and robust stability. A review of the two basic analytical methods used in describing chatter stability were presented and importance of both modal parameters and cutting coefficients to stability lobe prediction was discussed. While stability lobes can be utilized to predict stable cutting conditions in real milling operations, they are highly sensitive to parameter uncertainties. Robust stability theorems provide a means for

accounting for parameter variations directly in the mathematical formulations for chatter stability.

CHAPTER 3. EXPERIMENTAL SETUP

This chapter outlines the experimental methods and describes the different tools and sensors used. There are three main parts to the procedure. The first is acquiring modal parameters through Experimental Modal Analysis (EMA) and Receptance Coupling (RC) techniques. Next, cutting coefficients are acquired through measuring cutting forces and optimizing with an analytical cutting force model. In order to verify robust prediction of chatter stability, uncertainties must be deliberately introduced and quantified. Lastly, chatter tests were performed to detect actual chatter conditions for comparison with stability lobe diagrams.

3.1 Milling Machines and Chatter Detection

The majority of experimental tests were performed on a three axis, computer numerical controlled (CNC) micro milling machine, as shown in Figure 3.1a. The system is secured to a vibration isolation table, which prevents ground signals from corrupting experiments. Three linear stages (Parker Daedal 10600) are driven by stepper motors (*x* and *y* axis stages driven by ZETA57-51 and *z* axis stage by ZETAS67-83) connected to micro-stepping drivers (Parker ZETA ζ Drive), which can be fine-tuned to adjust the current and damping settings. Stage movement is controlled by a motion control system (National Instrument PXI-1042Q). An electric, high speed spindle (NSK Astro-E 800Z) is equipped with ceramic ball bearings and is capable of providing rotational speeds anywhere from 0 to 80000 rpm.

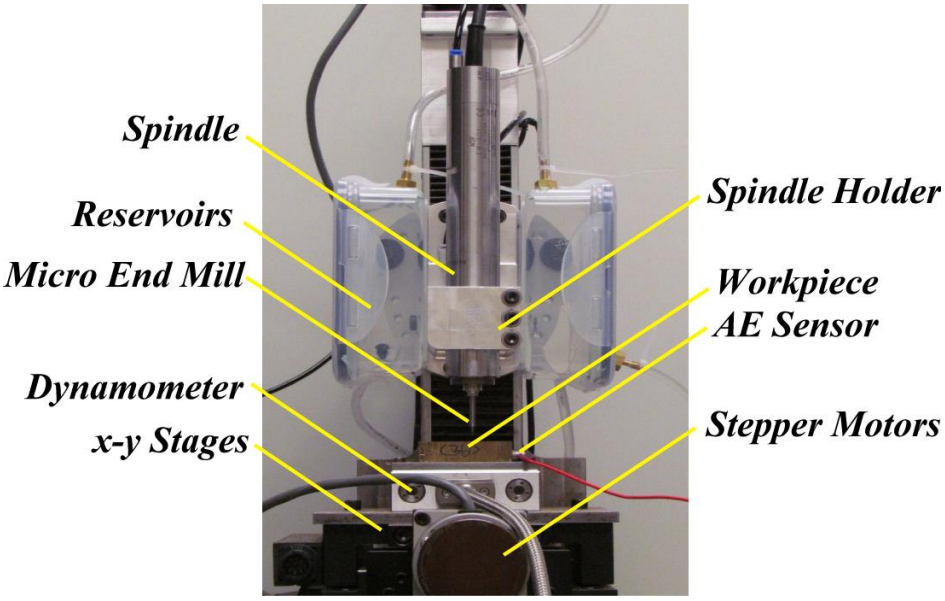

a) 3-Axis micro milling machine

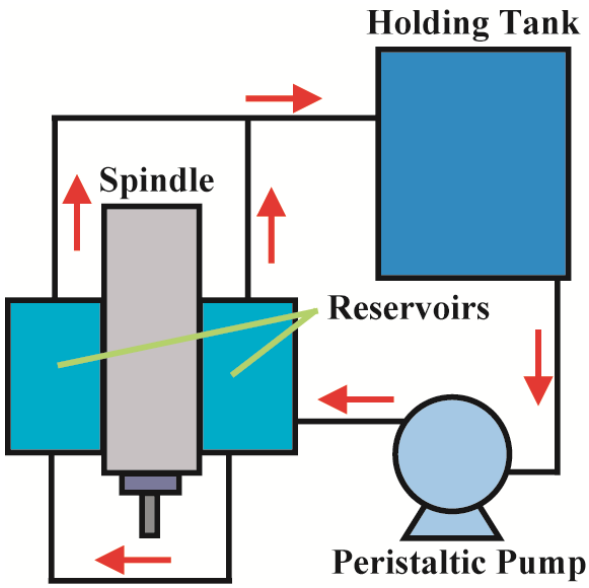

b) Schematic of liquid reservoirs

Figure 3.1 Experimental setup

The spindle holder has been equipped with reservoirs on both sides, which were used to influence the dynamics of the system by adjusting the liquid levels and changing the overall mass. As shown in Figure 3.1b, the reservoirs can be filled or emptied via peristaltic pump (Cole

Parmer 77200-50), with a flow rate range from 0.8 to 480 mL/min, connected with 0.25" OD tubing, and draws fluid from a holding tank. Water, with a nominal density of 1000 kg/m^3 and viscosity of 1 mPa×s, was used as the working fluid in this study. When the reservoirs are completely filled, excess fluid is allowed to drain back into the holding tank. Both hammer testing and chatter tests were performed on this machine.

Cutting coefficient identification tests were performed on a 5 axis micro machining center (KERN Micro 2255), shown in Figure 3.2, with spindle speeds that range from 60000 up to 160000 rpm.

Figure 3.2 Kern Micro milling machine

Chatter is identified by performing cutting tests at different spindle speeds and cutting depths, and using sensors to detect its frequency signature. A variety of different sensors have been implemented by researchers including accelerometers, microphones, dynamometers, acoustic emission sensors, and others [Kuljanic et al. 2008, Park et al. 2010]. A common approach is to utilize an acoustic emission sensors (AE) attached directly to the workpiece to detect chatter signals. AE sensors have a wide bandwidth and can be utilized to detect high

frequency vibrations phenomena in micro milling [Teti et al. 2010]. As suggested by Kuljanic et al. [2008], multiple sensors are preferable for more accuracy and reliability. Two AE sensors (Acoustics Emission Nano 30) were used in this study to detect chatter signals. A Fast Fourier transform (FFT) can be performed on the AE signals and the magnitude used to compare the strength of different signals. During unstable conditions, higher peaks will appear near the dominant natural frequencies of tooltip, indicating chatter [Park et al. 2010]. The limited bandwidth of the dynamometer prevents it from capturing chatter signals, however unstable force signals was used to provide secondary evidence of chatter.

3.2 Dynamic Testing

Chatter stability mainly depends upon the tooltip dynamics, which in turn are highly influenced by the spindle, especially at high rotational speeds [Movahhedy et al. 2006, Abele et al. 2010]. For accurate chatter prediction these parameters must be found experimentally for the milling system shown in Figure 3.1a. With micro end mills, a combination of EMA, and RC must be employed to identify tool tip dynamics.

EMA is a practical method of acquiring dynamic parameters for mechanical systems. Either shakers or impact hammers are used to deliver initial exciting forces to the system and the response is measured using sensors [Altintas 2012]. Shakers excite the system using constant amplitude and frequency vibrations, while piezoelectric impact force hammers deliver a quick impulse. The response is measured using either displacement sensors or accelerometers, and analyzed with data acquisition software to obtain the frequency response functions (FRF). Measured FRFs are then curve fitted with Equation 3.1 to estimate modal parameters.

$$\Phi(\omega) = \sum_{i=1}^{q} \frac{\omega_{n,,i}{}^{2} / k_i}{\omega^2 - \omega_{n,i}^2 + 2\zeta_i \omega_{n,i} \omega} \tag{3.1}$$

where q is the number of modes.

Modern modal testing software is equipped with computational tools to perform Fourier analysis and obtain the measured FRF, Φ [Altintas 2012]:

$$\Phi(\omega) = \frac{X(\omega)}{F(\omega)} \tag{3.2}$$

where ω is frequency, $X(\omega)$ and $F(\omega)$ are the Fourier transforms of the measured displacement and input force signals, respectively. Due to the presence of noise in the force and response signals, the coherence function, $C_{XF}(\omega)$, is also evaluated by modal software:

$$C_{XF}(\omega) = \frac{\left|S_{XF}(\omega)\right|^2}{S_{FF}(\omega) S_{XX}(\omega)} \tag{3.3}$$

where $S_{XF}(\omega)$ is the average cross power spectrum of displacement and force spectra, $S_{XX}(\omega)$ and $S_{FF}(\omega)$ are the average auto power spectrum of the displacement and force signals, respectively [Altintas 2012]. This represents the portion of the response which is due to the applied excitation, and good quality FRF signals will have low measurement noise and coherence functions close to unity. Although EMA and hammer testing can be time consuming to perform, the technique is widely used due to mobility of the hammer and accurate identification of modal parameters.

For the dynamics of the cutting tool, impact hammer testing cannot be applied and direct measurement of tooltip response is often not practical since accelerometers cannot be effectively attached [Mascardelli et al. 2008]. Acquiring modal parameters for micro tools is challenging task due to the fragility of micro tools. Receptance Coupling (RC) can be used to combine EMA results of the spindle and a finite element (FE) model of the miniature tool, to obtain the

dynamics at the tool tip. For the chatter tests, the dynamics for a 2 fluted, tungsten carbide 500 µm diameter end mill, with a 25 mm overhang length, and a 3 mm shank diameter needs to be obtained. To apply the RC method, the end mill is modelled into two parts as shown in Figure 3.3, a lower substructure A containing the cutting portion and an upper part, Substructure B.

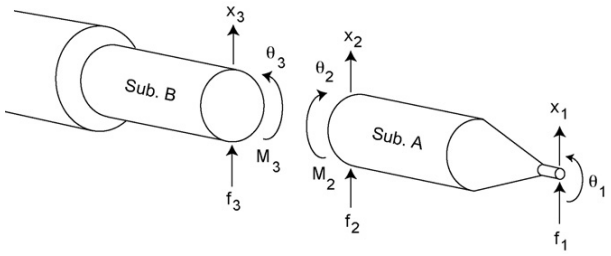

Figure 3.3 Receptance coupling modeling of end mill [Park et al. 2009]

Dynamics of Substructure B are obtained using EMA with an impact hammer (PCB 30722, sensitivity 23.76mV/N) as shown in Figure 3.4. Multiple tests were performed to ensure both reliability and unity coherence functions, and the results averaged to reduce noise [Park et al. 2003]. Rotational dynamics cannot be ignored, but they can be obtained indirectly using the procedure outline in Mascardelli et al. [2008]. Two blank end mills (cylinders) made of the same material as the actual end mill are used. Each blank cylinder was inserted into the spindle at 10 mm and 15 mm overhangs, and EMA performed at the free ends. After modeling the last 5 mm of the second blank end mill using FE analysis, the rotational dynamics at point 3 in Figure 3.3, can be extracted.

Using FE analysis, the dynamics of the cutting tool, Substructure A, can be found in free-free boundary conditions. The bottom 15 mm portion of the cutting tool is modeled as three sections using Timoshenko beam theory: the cylindrical shank is modeled as a cylindrical beam

with 10 elements, the tapered section is modelled using 10 elements, and the fluted section with the helix is modeled by a cylinder with an equivalent diameter 68% of the cutter diameter [Rahnama et al. 2010]. The material parameters for tungsten carbide end mills used in the FE analysis are: Young's Modulus=580 GPa, density=14300 kg/m^3, Poisson's ratio=0.28, and damping ratio=0.01 [Mascardelli et al. 2008].

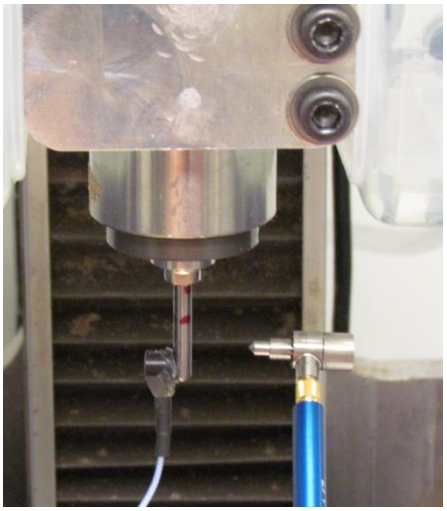

Figure 3.4 Hammer testing of blank end mill

Dynamics are then coupled mathematically using compatibility conditions of the joint. Tool tip dynamics are obtained with [Park et al. 2003]:

$$G_{11} = \frac{X_1}{F_1} = H_{11} - H_{12}(H_{22} + H_{33})^{-1} H_{21} \tag{3.4}$$

where G is the assembled structure's FRF and H's are the substructure's FRFs. H_{33} is acquired directly using EMA and the rest are obtained using FE analysis. Due to the symmetrical shape the cylindrical micro end mill, tool tip dynamics were assumed to be the same in both the x and y directions. Figure 3.5 shows the combined FRF of the acquired tool tip dynamics which is then

curve fitted using Equation 3.1 to the modal parameters of tool tip which are summarized in Table 3.1.

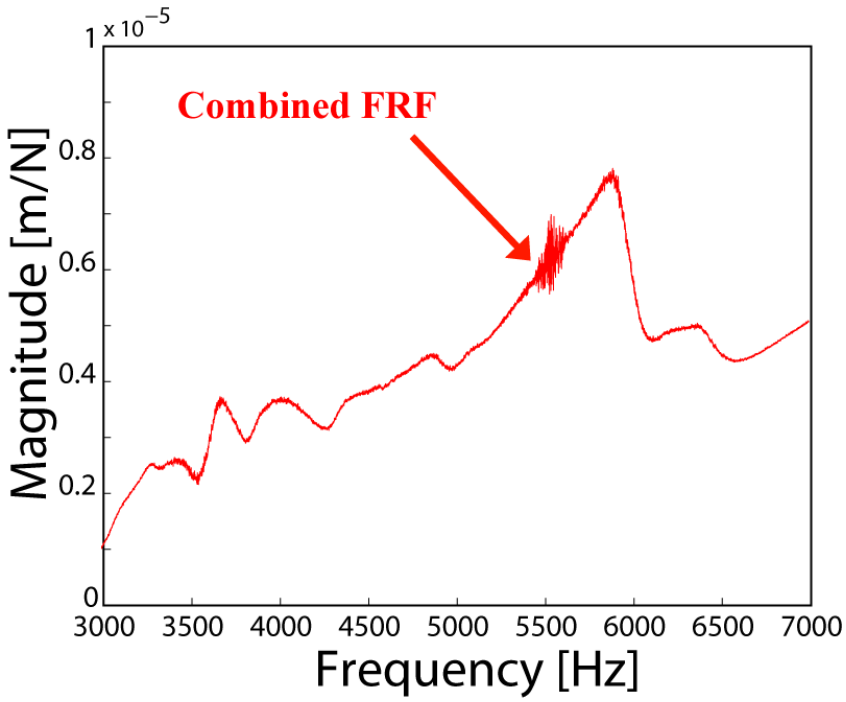

Figure 3.5 Combined tool tip FRF

As shown in Figure 3.1, variations were introduced in the dynamic parameters through the use of two 350 mL (2”×3.5”×1.5”) liquid reservoirs secured to the spindle structure of the micro milling system. The dynamics at the tool tip contain the dominant vibrational modes that contribute to chatter. Variations in the spindle dynamics were considered to be equivalent to changes in tool dynamics. By varying the volume flow rate, the reservoirs can be filled or emptied at different rates and thus change spindle dynamics during actual milling operations. This can be used to simulate time varying dynamics while simultaneously milling and detecting chatter.

Dynamics were acquired for the spindle structure through impact hammer testing (PCB 2222, sensitivity 1.86 mV/N). Responses to excitations applied to the spindle structure in both *x* and *y* directions were measured using an accelerometer (Kistler 8778A500), and curve fitted using Equation 3.1. Modal parameters can change at high spindles speeds and therefore hammer testing was performed on both full and empty reservoirs over a 0 to 60000 rpm spindle speed range to identify the maximum and minimum bounds on the dynamics. Multiple hammer tests were performed to accurately identify FRFs and ensure coherence functions as close to unity as possible, and the modes and uncertainty intervals of the spindle structure were found by averaging the data. The uncertainty bounds around the most dominant spindle mode were applied to all other modes, including at the tool tip. Variations in natural frequencies and damping ratios in the *x* and *y* directions are outlined in Table 3.1.

Table 3.1 Dynamic parameters at the tool tip

Direction	Mode	Natural Frequency [Hz]		Damping Ratio		Stiffness [N/m]
x	1	3722	±3.1%	0.009	±16.0%	8.01E+07
	2	4115.6		0.024		3.30E+07
	3	4990.5		0.064		5.60E+06
	4	5934		0.022		5.20E+06
y	1	3722	±5.0%	0.009	±10.6%	8.01E+07
	2	4115.6		0.024		3.30E+07
	3	4990.5		0.064		5.60E+06
	4	5934		0.022		5.20E+06

3.3 Cutting Coefficients

Mechanistic force models require cutting coefficients which reflect the contributions of the workpiece material and cutting conditions to forces. Cutting coefficients are therefore unique for a given cutting tool and workpiece material and must be found experimentally [Altintas 2012]. Cutting tests were performed on a high speed micro CNC machining center (Kern Micro) with a two fluted, 500 μm diameter carbide end mill (Mitsubishi VC-2MS) on a brass (C360) workpiece. Cutting force measurements were acquired using a piezo-electric table dynamometer (Kistler 9256C) capable of measuring forces in three axes. All cutting forces were measured at stable, chatter free cutting conditions, which was checked by using an acoustic emission (AE) sensor (Physical Acoustics Nano 30) [Park et al. 2009]. Data was acquired using a data acquisition system (NI cDAQ-9215) and anti-aliasing filters (Krohn Hite 3364). Forces were measured at constant spindle speed of 60000 rpm, constant cutting depth of 200 μm, at full immersion cutting, with a minimal 10 mm tool overhang to limit tool deflection.

Cutting coefficients are identified through experimental tests at different feed rates. Forces measured with the dynamometer were curve fitted with theoretically predicted forces to find coefficient values. Using the steepest descent algorithm, the error between measured forces, F_{exp}, and theoretical forces, F_{theo} is minimized [Malekian et al. 2009]:

$$e = \sum_{i=1}^{n} \sum_{j=1}^{m} (F_{\exp,i,j} - F_{theo})^2 \tag{3.5}$$

where n is the number of feed rates tested and m is the number of samples acquired. Forces were also measured at down milling cutting and compared to the theoretical prediction using the optimized coefficient values to verify.

Chip thicknesses in milling vary with both feed rate and immersion angle. While the cutting mechanism is mainly shearing, a ploughing effect can be observed if the feed rate is below a critical value [Malekian et al. 2009]. For this study rather than consider ploughing and size effects separately, experimental force measurements were curve fitted using the linear mechanistic cutting force model in Equation 3.6:

$$\begin{aligned} F_t &= K_{tc} a h + a K_{te} \\ F_r &= K_{rc} a h + a K_{re} \end{aligned} \tag{3.6}$$

The workpiece material was selected to be brass C360 which has a nominal composition of 61.5% Cu 35.5% Zn 3.0% Pb [Davis 2001]. Brass C360 is known as a free machining brass, which means that it has been alloyed with small concentrations of lead. As seen in Figure 3.6, this introduces small particles of lead into the grains, which at the macro scale act like stress concentrations during chip formation resulting in smaller chips and lower cutting power required [Davis 2001]. However, during micro milling, grain boundaries and the coarse microstructure can affect cutting forces since the edge radius of micro tools are comparable in size [Popov et al. 2006, Vogler et al. 2004]. The edge radius of the micro end mill used is approximately 2 μm [Malekian et al. 2009].]. These mechanisms which cause variations can be accounted for in predicting chatter stability using linear coefficients with uncertainties.

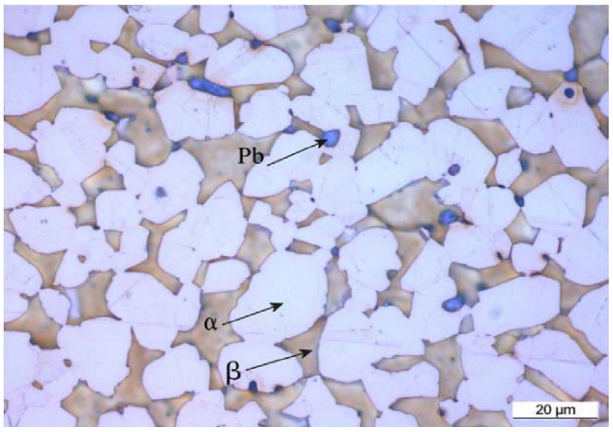

Figure 3.6 Microstructure of leaded brass [Garcia et al. 2010]

As shown in Figure 3.7, the root mean square (RMS) of the resultant force after optimization with Equation 3.6, is plotted against feed rate. In comparison to the optimized forces, the measured forces are scattered with respect to feed rate and variations in the cutting coefficients are assumed to be the dominant contributing factor. Table 3.2 summarizes the nominal cutting and edge coefficients and average variations in tangential and radial cutting coefficients need to cover the spread in the forces. Since the edge coefficients represent the component of cutting forces that do not contribute to cutting, they are not included in the subsequent chatter models [Budak 2006]. However, they must be included when curve fitting the experimental and theoretical forces to identify accurate cutting coefficients.

Table 3.2 Optimized mechanistic coefficients for brass C360

Tangential Cutting, K_{tc} [N/mm^2]		Radial Cutting, K_{rc} [N/mm^2]		Tangential Edge, K_{te} [N/mm]	Radial Edge, K_{re} [N/mm]
4203	+21.5%	1483	+23.3%	2.96	1.11
	-19.0%		-22.0%		

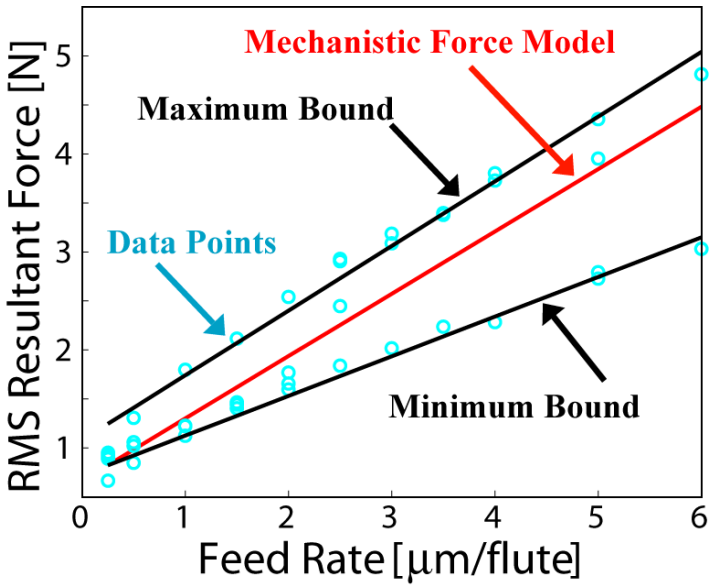

Figure 3.7 RMS resultant forces versus feed rate for micro milling of brass C360

3.4 Summary

The micro milling setup implemented used in this study and the methods used to identify the system parameters and their uncertainties were presented in this chapter. Dynamics were acquired using a combination of EMA and RC technique and variations were introduced by changing spindle speeds and a liquid reservoir system which alters the mass of the spindle structure. Fitting a linear mechanistic force model to experimentally measured cutting forces over both ploughing and shearing dominant cutting regimes, and micro milling of free machining brass with material non-uniformities provided variations in cutting force data. These experimental parameters were utilized in the subsequent chapters for chatter analysis.

CHAPTER 4. ROBUST CHATTER STABILITY WITH EDGE THEOREM

Chatter stability analysis involves using analytical models in the frequency domain to generate graphical stability lobes, which reveal stable and unstable regions for different combinations of spindle speeds and cutting depths. For two uncertain parameters, the Edge theorem has been studied previously for robust stability [Park et al. 2007, Park et al. 2010], however these attempts used the pseudo SDOF chatter stability model, which is known to inaccurate for milling operation at full immersion conditions [Altintas et al 2004]. The conventional frequency domain approach for (two degree of freedom) 2-DOF milling stability originally developed by Altintas and Budak [Altintas et al. 1995] can be extended to also include parameter uncertainties. For the first time, this chapter presents a robust chatter stability model for 2-DOF milling operations using the combination of the Edge theorem and the Zero Exclusion principle that accounts for three uncertain parameters, namely the natural frequency, damping ratio, and cutting coefficient. Using the robust formulation, an algorithm is described for finding critical cutting depth using a bisection algorithm to plot robust chatter stability lobe diagrams. Robust stability lobes are predicted and compared to the conventional stability model and experimentally detected chatter points using the identified parameters and uncertainties described in Chapter 3.

4.1 Robust Modeling

The 2-DOF analytical chatter model for milling, as shown in Figure 4.1 [Altintas 2012, Altintas et al. 2004, Schmitz et al. 2009], can be derived by considering the general equations of

motion. As outlined in Chapter 2, the characteristic equation, in Equations 2.21 -2.23, governs chatter stability.

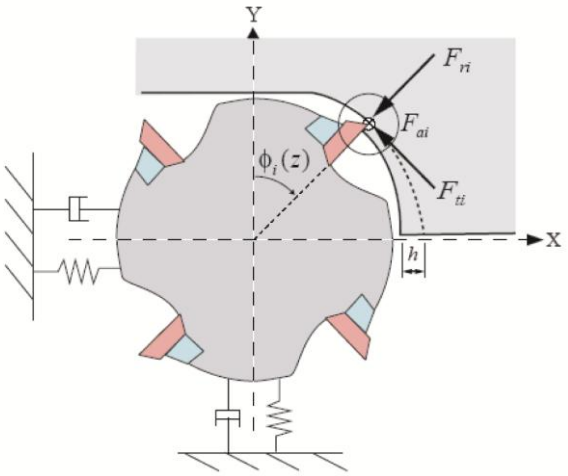

Figure 4.1 2-DOF Milling Model [Park et al. 2007]

The characteristic equation, Equation 2.21, must first be rearranged before Edge theorem can be directly applied [Park et al. 2007]. The transfer functions, Equation 2.6, the coefficients, Equation 2.22, and the eigenvalue, Λ, Equation 2.23, can be substituted into Equation 2.21, yielding:

$$\begin{aligned} 0 = {} & \Phi_{xx}(s,\omega_n,\zeta)\Phi_{yy}(s,\omega_n,\zeta)\left(\alpha_{xx}\alpha_{yy}-\alpha_{xy}\alpha_{yx}\right)\left(-\frac{N}{4\pi}aK_{tc}(1-e^{-sT})\right)^2 \\ & +\left(\alpha_{xx}\Phi_{xx}(s,\omega_n,\zeta)+\alpha_{yy}\Phi_{yy}(s,\omega_n,\zeta)\right)\left(-\frac{N}{4\pi}aK_{tc}(1-e^{-sT})\right)+1 \end{aligned} \tag{4.1}$$

where s is the Laplace variable, a is the axial depth of cut, K_{tc} is the tangential cutting coefficient, $T=60/Nn$ is the time delay between flutes, n is the spindle speed [rpm], N is the number of flutes, $\Phi_{xx}(s)$ and $\Phi_{yy}(s)$ are the direct transfer functions in the x and y directions, α_{xx}, α_{xy}, α_{yx}, α_{yy} are the time invariant average directional factors, ζ_x, ζ_y, are damping ratios and, $\omega_{n,x}$, $\omega_{n,y}$, are natural frequencies in the x and y directions, respectively. The cross transfer functions are assumed to be

negligible ($\Phi_{xy}(s)= \Phi_{xy}(s)=0$). Since the critical chatter frequency occurs bear the dominant tooltip modes of the system, the characteristic equation is then multiplied on both sides by the denominator of the transfer function with the most dominant mode and Equation 4.1 can be expressed as [Park et al. 2007]:

$$0 = \left[\Phi_x(s,\omega_n,\zeta)\Phi_y(s,\omega_n,\zeta)\left(\alpha_{xx}\alpha_{yy} - \alpha_{xy}\alpha_{yx}\right)\left(-\frac{N}{4\pi} aK_{tc}(1-e^{-sT})\right)^2 \right.$$
$$\left. + \left(\alpha_{xx}\Phi_x(s,\omega_n,\zeta) + \alpha_{yy}\Phi_y(s,\omega_n,\zeta)\right)\left(-\frac{N}{4\pi} aK_{tc}(1-e^{-sT})\right) + 1 \right](s^2 + 2\zeta_i\omega_{n,i}s + \omega_{n,i}^2) \tag{4.2}$$

This puts the characteristic equation into a final quasi-polynomial form with time delay terms. For real systems, parameter values can never be known precisely and can even vary during cutting operations thus affecting stability of the milling system.

Chatter stability can be established by incorporating robust control theorems into the 2-DOF model, while accounting for uncertainty in the natural frequency, ω_n, damping ratio, ξ, and cutting coefficients, K_c. For time invariant parameters, stability can be detected using both Edge theorem and the Zero Exclusion condition [Bhattacharyya et al. 1995].

In robust literature, uncertain parameters are described as belonging to an uncertainty set, Q where each uncertain parameter is bounded by a maximum and minimum value [Matusu 2011]:

$$Q = \left\{\omega_n \in [\omega_{n(\min)}, \omega_{n(\max)}], \zeta \in [\zeta_{\min}, \zeta_{\max}], K_{tc} \in [K_{tc(\min)}.K_{tc(\max)}]\right\} \tag{4.3}$$

Graphically shown in Figure 4.2, for m number of uncertain parameters the uncertainty set Q forms an m-dimensional box, where each vertex is an extreme combination of the parameter bounds.

It is assumed that the dynamics in both the x and y directions vary together and reach their maximums and minimums simultaneously. Evaluating the characteristic polynomial,

Equation 4.2, over the entire uncertainty set, Q, (i.e. at all combinations of the uncertain parameters) yields a family of polynomials, P:

$$P = \{p(s, \omega_n, \xi, K_c) : \omega_n, \zeta, K_c \in Q\} \tag{4.4}$$

While this represents an infinite number of systems, only the equations evaluated at the extreme upper and lower bounds of the uncertain parameters are needed to establish robust stability. Each extreme vertex equation becomes:

$$\begin{aligned} p_q(s) = & \left[\Phi_{xx}(s, \omega_{n(\min,\max)}, \zeta_{(\max,\min)})\Phi_{yy}(s, \omega_{n(\min,\max)}, \zeta_{(\max,\min)})(\alpha_{xx}\alpha_{yy} - \alpha_{xy}\alpha_{yx})(\Lambda(K_{tc(\max,\min)}))^2\right. \\ & + (\alpha_{xx}\Phi_{xx}(s, \omega_{n(\min,\max)}, \zeta_{(\max,\min)}) + \alpha_{yy}\Phi_{yy}(s, \omega_{n(\min,\max)}, \zeta_{(\max,\min)}))\Lambda(K_{tc(\max,\min)}) \\ & \left. + 1\right](s^2 + 2\zeta_{i(\min,\max)}\omega_{n,i(\min,\max)}s + \omega_{n,i(\min,\max)}^2) \end{aligned} \tag{4.5}$$

where $q=1...2^m$ ($m=3$ for three uncertain parameters) represents the polynomial number. When the eight characteristic polynomials in Equation 4.5 are evaluated at a given frequency, $s=j\omega$, this gives vertex points in the complex plane, as shown in Figure 4.2.

Effectively, the characteristic equation represents a mapping of uncertain parameters into a closed shape in the two dimensional complex plane. The Edge theorem says that a system is robustly stable if the edges between each pair of polynomial vertices are stable [Barmish 1994]. These edges correspond to edges in Q and can be expressed in the complex plane as:

$$E_n = (1-\lambda)p_i(s, v_i) + \lambda p_j(s, v_j) \tag{4.6}$$

where E_n, represents an edge polynomial, $n=1,2,...,m2^{m-1}$, and $1 \leq i,j \leq 2^m$. Analytically if these edge equations are found to be stable for all $\lambda \epsilon [0,1]$ then the system is robustly stable and this is both a necessary and sufficient condition [Bhattacharyya et al. 1995, Fu et al. 1989]. Establishing stability for an uncertain system is reduced to establishing stability for a set of edge polynomials, which are now a function of a single uncertain parameter, λ. This guarantees system stability for

any combination of the uncertain parameter values, which must be mapped to the area between the edges.

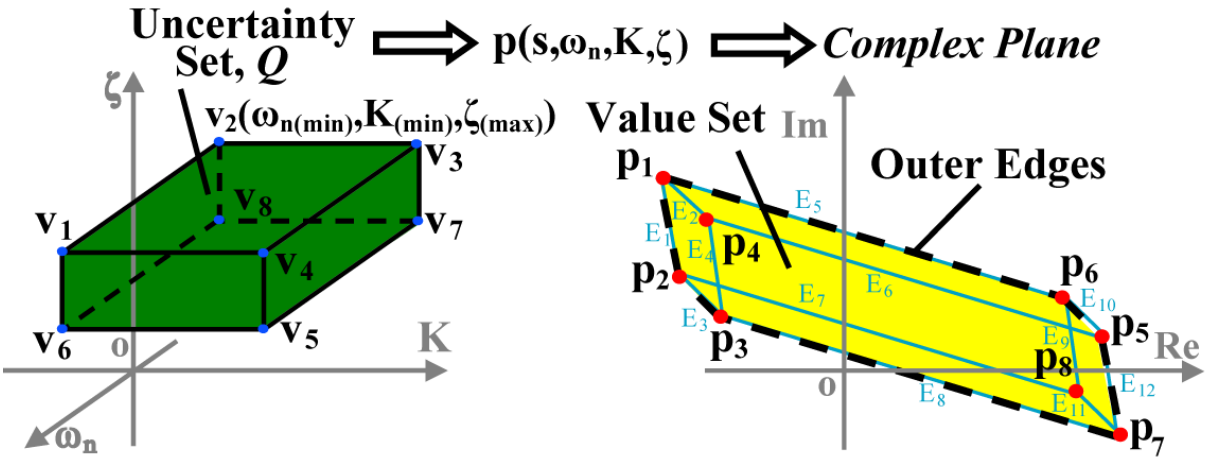

Figure 4.2 Mapping of uncertainty into complex plane (*m*=3 uncertain parameters)

The underlying principle of the Edge theorem is the value set concept [Barmish 1994]. The value set is all the points in the complex plane mapped from the entire uncertainty set, *Q*, by the characteristic equation at a given frequency [Matusu 2011]. The Zero Exclusion condition says that if the origin is excluded from the value set, then the system is robustly stable, as shown in Figure 4.3 [Barmish 1994]. This is a general graphical approach that is even applicable to complicated systems with a time delay systems [Matusu 2011]. However, evaluating the characteristic equation for all uncertain parameter combinations is time consuming and highly impractical.

Computation can be made more efficient by using a combination of both Edge theorem and the Zero Exclusion condition. The vertices and edges of the value set shape directly correspond to vertex and edge polynomials described by the Edge theorem, as shown in Figure 4.2 [Bhattacharyya et al. 1995]. By connecting the outermost vertices with edges then the

polygonal shape of the value set (also known as a polytope) can be found [Barmish 1994]. Instead of directly finding the entire value set, stability can be established graphically with the Zero exclusion condition using only the outer vertices and edges, shown in Figure 4.3; the interior is not actually needed. In addition, only eight extreme vertex equations in Equation 4.5 need to be evaluated instead of directly employing Equation 4.6 and finding twelve edge equations. The edges of the uncertainty set, *Q*, do not have to map into the edges of the value set [Barmish 1994].

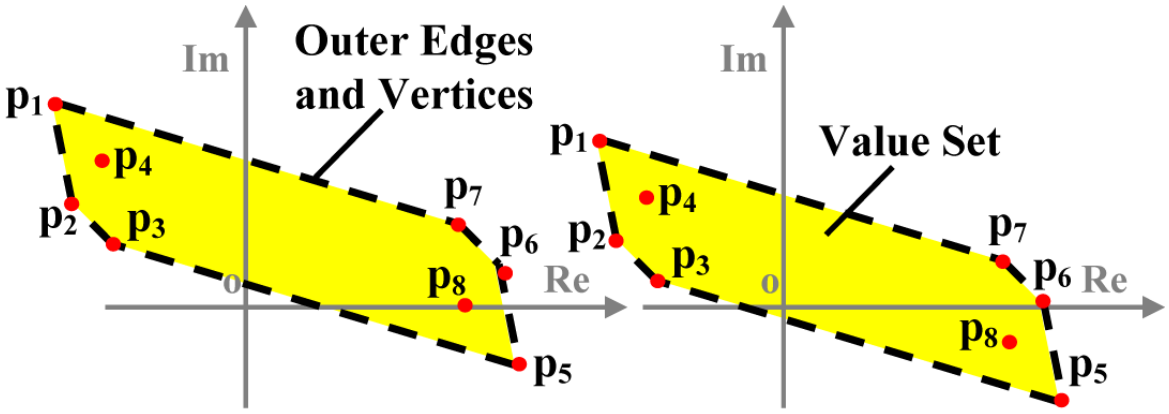

Figure 4.3 Zero Exclusion for three uncertain parameters in stable (left) and unstable (right) configurations

Robust stability is established by ensuring the entire set of equations, represented in Equation 4.4, is stable over all admissible values of the uncertain parameters. The combination of Zero Exclusion method and Edge theorem is a frequency domain approach of establishing robust stability by using only extreme parameter combinations to graphically establish stability boundaries. For a given spindle speed, cutting depth, and range of frequencies, the characteristic equation for 2-DOF milling chatter stability can be evaluated at the extreme parameter combinations. Geometrically, the outer shape of the value set can be found and if the origin is

excluded from outer shape, then by the Zero Exclusion principle the system is robustly stable. This method simplifies the computational complexity of determining stability for systems with uncertain parameters.

4.2 Robust Stability Algorithm

An algorithm for plotting robust stability lobes was implemented in Matlab™ and Figure 4.4 shows flowchart of the algorithm used. Robust stability lobe diagrams are plotted by converging upon the cutting depth with a bisection algorithm that utilizes the Edge theorem and Zero Exclusion robust stability criteria at a given spindle speed.

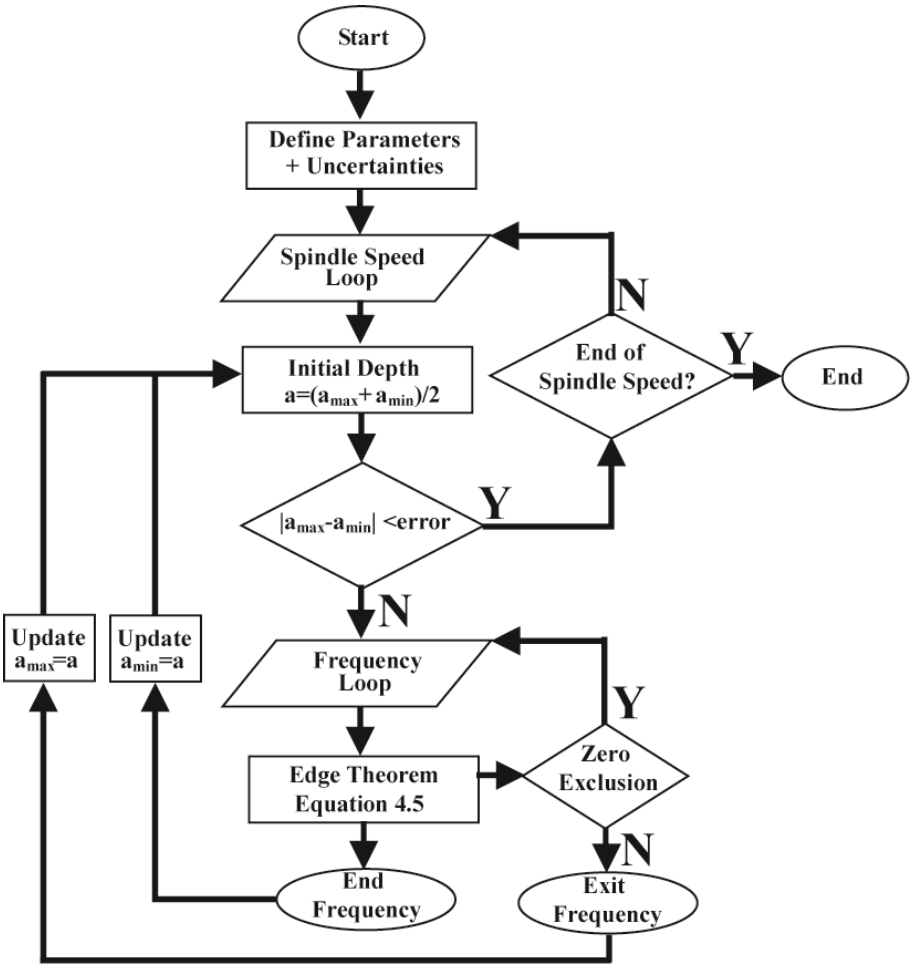

Figure 4.4 Robust stability algorithm flowchart

After parameters and uncertainties are defined, an initial cutting depth is determined by specifying a minimum value, a_{min} (taken to be zero since cutting depth is a real, positive value), and a maximum value, a_{max}, and finding an average. The algorithm then proceeds in to a frequency loop, where stability is established by applying the Edge theorem and the Zero Exclusion condition over a range of chatter frequencies. This frequency range must include the natural frequencies of the dominant tool tip modes. At a given frequency, Equation 4.5 is evaluated eight times for all extreme uncertain parameter combinations. The outermost vertices are identified using the Matlab™ "*convhull*" function which finds the largest straight edged polygon that fits the eight points. This polygon represents the outer shape of the value set. Zero Exclusion criteria is applied and whether the origin lies inside that polygon is determined using Matlab™ "*inpolygon*" function. This function uses the identified outermost vertices and checks whether a specified point lies inside. If the origin is excluded at all frequencies then the system is robustly stable and the current cutting depth is assign to be the minimum value for the next iteration. If the origin is included then the frequency loop is stopped and the current depth is assigned as the maximum value. This procedure is repeated at all speed, cutting depth, and frequency combinations since the polygonal shape and position of the value set changes in the complex plane. Once the cutting depth is found to be within a defined tolerance, and then the algorithm moves on to the next spindle speed iteration.

The combination of Edge theorem and Zero Exclusion condition simplifies the problem of determining stability for a set of polynomials, to a geometric problem. Computational time depends upon the extent of the speed, depth, and chatter frequency ranges that need to be swept. Computational time can be improved at the expense of computer memory using a parallel programming structure, which can simultaneously performs several spindle speed iterations.

4.3 Experimental Results

Experimental tests were performed on the in-house built micro milling system, to verify the robust stability lobe prediction. Cutting coefficients for free machining brass C360, tooltip dynamics, and parameter bounds were experimentally identified, as outlined in Chapter 3, and used to predict chatter lobes. Figure 4.5 shows a comparison between robust predicted stability lobes using algorithm shown in Figure 4.4 at eight extreme parameter combinations, the experimental chatter points, and a summary of the experimental conditions. Chatter tests were performed over a range of cutting depths and spindle speeds at full immersion conditions, at 2 μm/flute feed rate, while varying the liquid level at a 240 mL/min flow rate to change dynamics. Based on the AE sensor data acquired in the frequency domain, the occurrence of chatter was determined for each spindle speed and cutting depth combination tested. The conventional 2-DOF chatter stability lodes were also plotted at the average parameter values to compare with the robust lobes and illustrate the effectiveness of robust stability. All lobes were plotted over the same speed and cutting depth range as the chatter tests, and iterated by sweeping a frequency range from 100 Hz to 6500 Hz, which covers all the dominant frequencies of the tool and spindle.

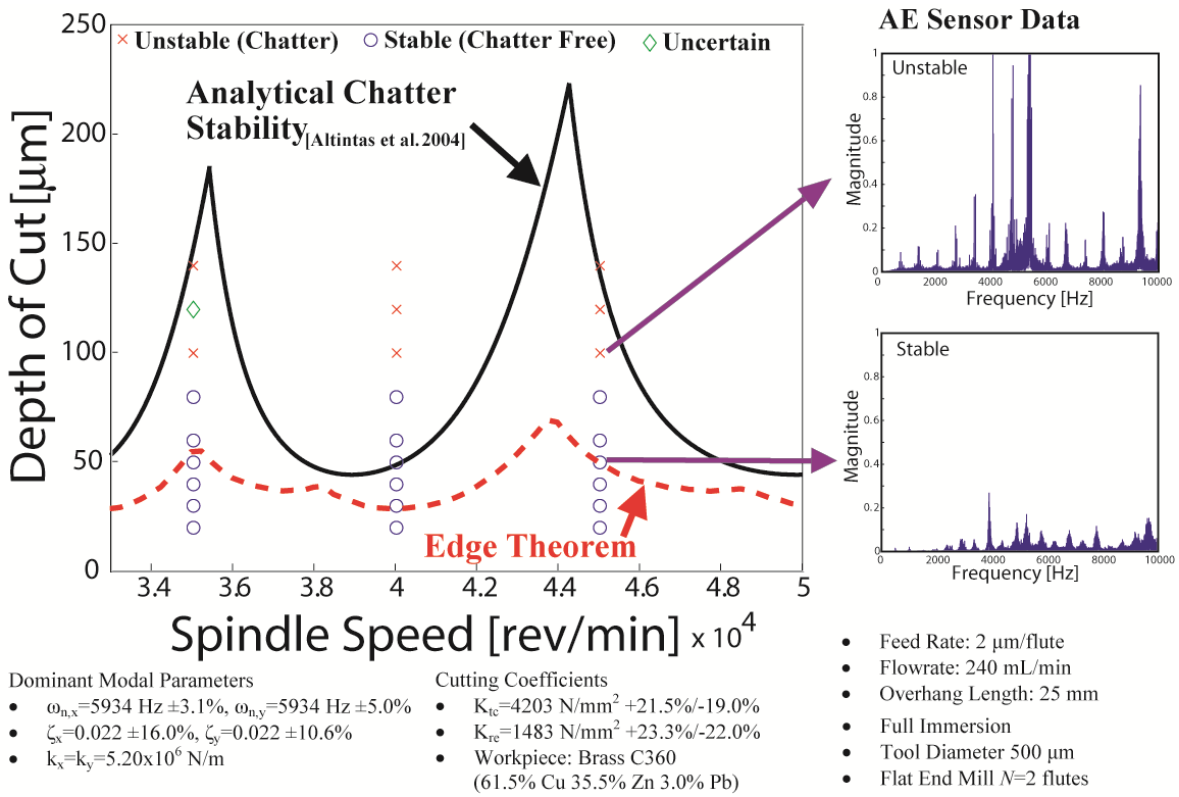

Figure 4.5 Comparison of stability lobes and measured chatter points

Figure 4.5 shows a good correlation between the experimental chatter tests and the predicted robust stability lobes with the majority of chatter free points below the robust boundary. It can be observed that many of the unstable points that were detected occur below the lobes predicted by the analytical chatter stability model. This outlines the central advantage of predicting chatter stability using the robust method in that it gives a more conservative prediction. During machining, system parameters may fall anywhere within a given range, and as such the analytical chatter stability model may shift and not adequately predict a stable cutting regime. Robust stability accounts for the full range over which the parameters can vary, whereas the conventional stability lobes only accounts for a constant value of the parameters.

Using conventional chatter stability, shifts in stability lobes can be observed when parameters are changed. Figure 4.6 compares the result obtained by the Edge theorem approach

and the conventional chatter stability lobes plotted at different extreme parameter combinations and at the nominal experimental parameters. While there are eight extreme parameter combinations for three uncertain parameters, only the two extreme combinations which shift conventional stability lobes closest to the robust lobes are shown.

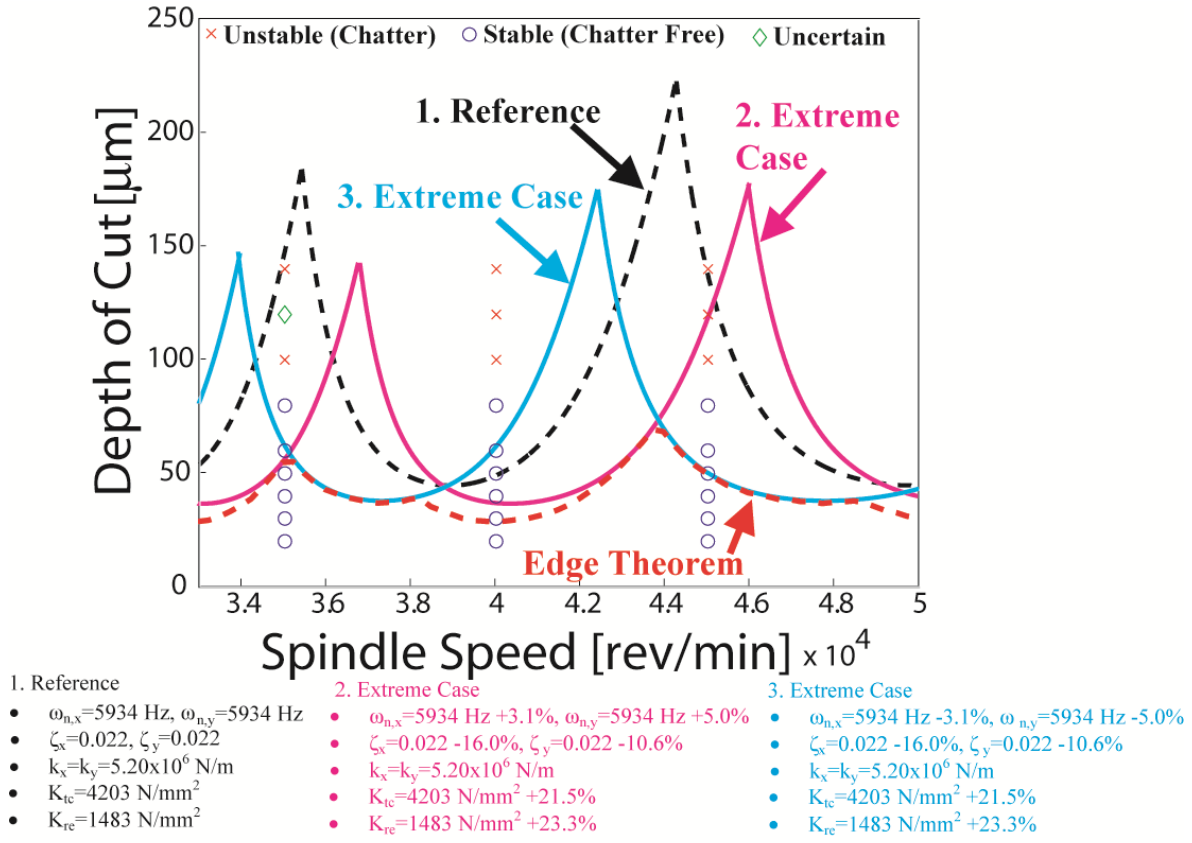

Figure 4.6 Comparison with two extreme parameter combinations

From Figure 4.6 it can be observed that robust stability tends to follow the most conservative boundary at the lowest cutting depths of the combined conventional lobes. Conventional stability lobes that are individually plotted at different extreme parameter combinations do not guarantee stability for parameters that lie between the extremes and unstable points may still be found below the lobes.

Depending upon the immersion condition, the pseudo SDOF model and the 2-DOF model for chatter stability will give different predictions [Altintas et al. 2004]. For full immersion conditions, the pseudo SDOF model yields a poor prediction for chatter stability. Full immersion conditions were used for the experimental work and Figure 4.7 compares conventional model without uncertainties to the measured chatter points.

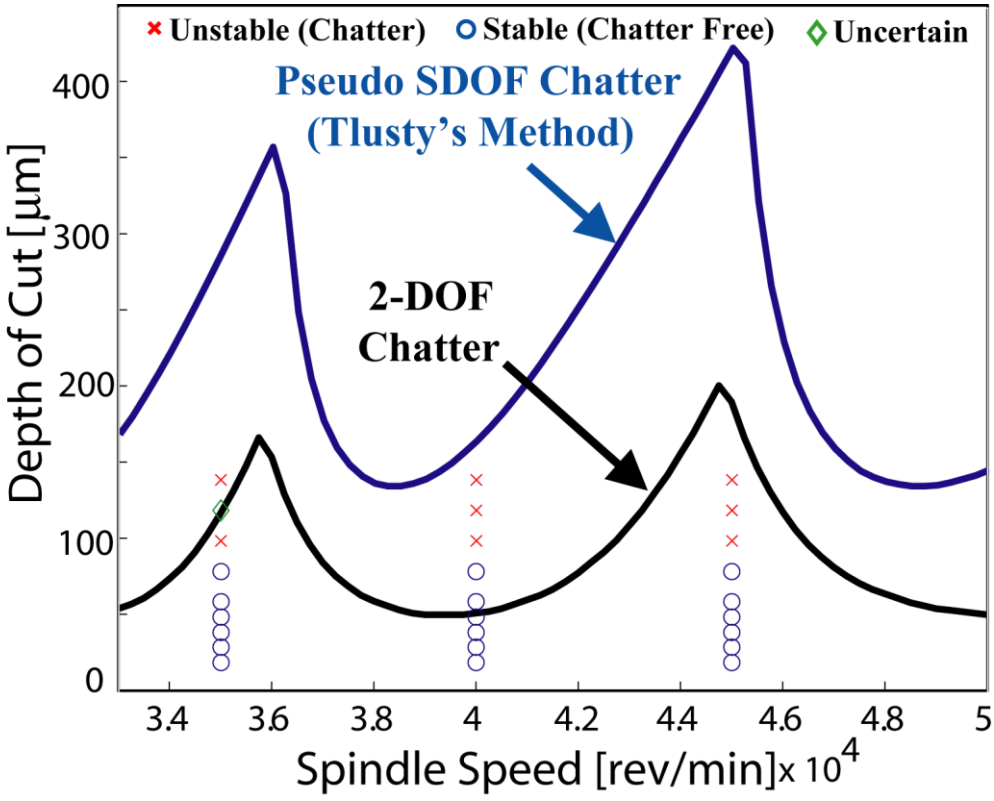

Dominant Modal Parameters

- $\omega_{n,x}$=5934 Hz, $\omega_{n,y}$=5934 Hz
- ζ_x=0.022, ζ_y =0.022
- k_x=k_y=5.20x10^6 N/m

Cutting Coefficients

- K_{tc}=4203 N/mm^2
- K_{re}=1483 N/mm^2
- Workpiece: Brass C360 (61.5% Cu 35.5% Zn 3.0% Pb)

- Feed Rate: 2 µm/flute
- Flowrate: 240 mL/min
- Overhang Length: 25 mm
- Full Immersion
- Tool Diameter 500 µm
- Flat End Mill *N*=2 flutes

Figure 4.7 Comparison between 2-DOF and pseudo SDOF chatter

As illustrated in Figure 4.7, the pseudo SDOF models cannot reliably predict stability lobes. Tlusty's method forces the resultant cutting force to act at the geometric mean of the immersion angle, given by the directional factors in Equation 2.13. In both cases when full immersion conditions are applied, the formulation simplifies resulting in an inaccurate prediction [Altintas et al. 2004]. Whereas the vibrations are coupled in the 2-DOF model through the cutting forces, shown in directional factors in Equation 2.19.

The combination of Edge theorem and the Zero Exclusion condition, in theory, requires that a frequency range must be swept from zero to infinity. In practice, this frequency range can be restricted with knowledge of the given system [Matusu et al. 2011]. Provided that the frequency range swept contains all the dominant tooltip modes, robust stability can be established. The number of uncertain parameters considered is also an important consideration when implementing robust theorems. With m uncertain parameters, 2^m extreme polynomials are needed, which can greatly increase computational requirements.

4.4 Summary

In this chapter, a frequency domain approach involving a combination of the Edge theorem and the Zero Exclusion condition was presented for the 2-DOF analytical chatter model, which is used to predict chatter stability lobe diagrams specifically for milling operations. For the first time three uncertain parameters were accounted for: the natural frequency, damping ratio, and the cutting coefficient. For time invariant parameters which have known upper and lower bounds, a basic algorithm was described for plotting robust stability lobes. A range of spindle speeds are scanned, and the cutting depth corresponding to the stability boundary was found using a bisection method and employing the robust stability approach. Dynamics and cutting coefficients were experimentally measured for a real micro milling system. Uncertainties

in the parameters were deliberately introduced and the upper and lower bounds were quantified. Through experiments it was shown that robust stability can be used to give a conservative prediction by comparing to detected chatter points and conventional chatter stability lobes.

CHAPTER 5. ROBUST CHATTER STABILITY WITH LINEAR MATRIX INEQUALITIES

Chatter stability with parameter uncertainty can be checked using Lyapunov's stability criteria, which can be formulated as a set of linear matrix inequality (LMI) equations. Matrix and state space approaches to robust problems have dominated control theory literature in recent years and LMI equations can be used to represent constraints placed on complex systems. LMIs can be used to represent constraints on system stability and provide a versatile approach to modeling uncertain systems which can accommodate both time invariant and time varying uncertainties.

Until now, the use of Lyapunov LMIs for predicting regenerative chatter stability lobes in milling operations while considering parameter uncertainty has not been investigated. This chapter presents three LMI formulations for 2-DOF milling chatter stability based on robust Lyapunov stability. For time invariant uncertainty, two formulations are presented and consider both a parameter independent and parameter dependent Lyapunov functions for three uncertain parameters. Unlike the Edge theorem approach from Chapter 4, which can only deal with time invariant uncertain parameters, the LMI approach can be made to handle time varying uncertain parameters. The third method therefore considers parameter dependent Lyapunov functions for time varying uncertainties. Time varying uncertainty represents the most general case and requires the bounds on parameters time derivatives in addition to the parameter bounds [Francesco 2006]. Although challenging, Lyapunov functions can be found using convex optimization techniques [Boyd et al. 1994]. A comparative study is performed with the robust LMI formulations and the Edge theorem approach, described in Chapter 4.

5.1 Robust Chatter Stability with LMI

The state space model and the robust Lyapunov theorems are derived for a continuous time 2-DOF chatter system. Basic Lyapunov stability requires a system matrix, and for regenerative chatter this system matrix can be derived by considering the individual state space descriptions of the dynamics and the delay term:

$$\begin{array}{ll} \textit{Dynamics} & \textit{Delay} \\ \dot{z}_d = Az_d + Bu & \dot{z}_T = A_T z_T + B_T w \\ w = Cz_d + Du & w_T = C_T z_T + D_T w \end{array} \tag{5.1}$$

where u is the input to the dynamics z_d, z_T, w, w_T, are the state variable and output vectors, A, B, C, D are the state space descriptions of the dynamics, and A_T, B_T, C_T, D_T, are the state space descriptions of the exponential time delay term. The closed loop block diagram is shown in Figure 5.1 using the zero order solution for 2-DOF milling stability.

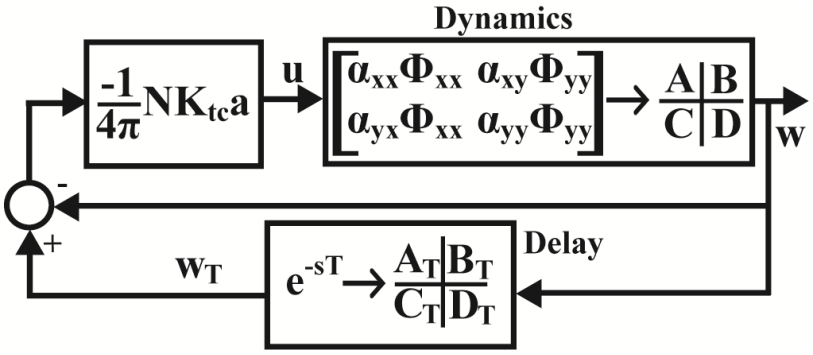

Figure 5.1 2-DOF Regenerative chatter block diagram

The difference between the current and previous displacement drives the regenerative chatter effect. Assuming cross transfer functions are negligible, the 2-DOF state space descriptions of the dynamics shown in Equation 5.1, with b_x and b_y number of modes in the x and y directions respectively, can be expressed as:

$$A=\begin{bmatrix}\begin{bmatrix}A_{x,1} & 0 & 0\\ 0 & \ddots & 0\\ 0 & 0 & A_{x,b_x}\end{bmatrix} & \mathbf{0}_{2b_x x 2b_y}\\ \mathbf{0}_{2b_y x 2b_x} & \begin{bmatrix}A_{y,1} & 0 & 0\\ 0 & \ddots & 0\\ 0 & 0 & A_{y,b_y}\end{bmatrix}\end{bmatrix} \quad B=\begin{bmatrix}B_{x,1}\\ \vdots\\ B_{x,b_x}\\ B_{y,1}\\ \vdots\\ B_{y,b_y}\end{bmatrix}$$
$$C=[C_{x,1} \quad \cdots \quad C_{x,b_x} \quad C_{y,1} \quad \cdots \quad C_{y,b_y}] \quad D=\begin{bmatrix}0 & 0\\ 0 & 0\end{bmatrix} \tag{5.2}$$

The sub matrices in Equation 5.2 are:

$$A_{x,i}=\begin{bmatrix}0 & 1\\ -\omega_{n,x,i}^{\ 2} & -2\zeta_{x,i}\omega_{n,x,i}\end{bmatrix} \quad A_{y,i}=\begin{bmatrix}0 & 1\\ -\omega_{n,y,i}^{\ 2} & -2\zeta_{y,i}\omega_{n,y,i}\end{bmatrix}$$
$$B_{x,i}=\begin{bmatrix}0 & 0\\ \alpha_{xx}\dfrac{\omega_{n,x,i}^{\ 2}}{k_{x,i}} & \alpha_{xy}\dfrac{\omega_{n,x,i}^{\ 2}}{k_{x,i}}\end{bmatrix} \quad B_{y,i}=\begin{bmatrix}0 & 0\\ \alpha_{yx}\dfrac{\omega_{n,y,i}^{\ 2}}{k_{y,i}} & \alpha_{yy}\dfrac{\omega_{n,y,i}^{\ 2}}{k_{y,i}}\end{bmatrix} \tag{5.3}$$
$$C_{x,i}=C_{y,i}=\begin{bmatrix}1 & 0\\ 0 & 0\end{bmatrix}$$

where $i=1,2,...b_x$ and $i=1,2,...b_y$ for each direction.

A Pade approximation can be used to replace the exponential time delay term with a series expansion of a rational transfer function that in turn can be transformed into equivalent state space system. The Pade approximant can be truncated to a desired degree of accuracy by specifying the approximation order, *r*. While the order of the numerator and denominator can be different, it is common to specify the same order to avoid numerical errors when finding coefficients [Baker et al. 1996]. The Pade approximant for time delay, *T*, is calculated by expanding and equating both the exponential delay term with a truncated McLauren series (i.e. a Taylor series about zero) and a rational expression for a desired order [Baker et al. 1996]:

$$e^{-sT} \approx 1-(sT)+\frac{(sT)^2}{2}+\cdots(-1)^r\frac{(sT)^r}{r!}=\frac{\sum_{l=0}^{r}\beta_l(sT)^l}{1+\sum_{j=1}^{r}\chi_j(sT)^j} \tag{5.4}$$

where β_l and χ_j are constant coefficients found after matching terms. After these constants can be multiplied with time delay values, T, and normalized to get constant coefficients, g and d, for the numerator and denominator, the polynomials can then be converted into a first companion state space form [Friedland 1986]:

$$\frac{g_r + g_{r-1}s + \cdots + g_0 s^r}{d_r + d_{r-1}s + \cdots d_1 s^{r-1} + s^r} \rightarrow$$

$$A_P = \begin{bmatrix} 0 & 1 & \cdots & 0 & 0 \\ 0 & 0 & 1 & 0 & 0 \\ \cdots & \cdots & \cdots & \cdots & \cdots \\ 0 & \cdots & 0 & 0 & 1 \\ -d_r & \cdots & -d_3 & -d_2 & -d_1 \end{bmatrix} \quad B_P = \begin{bmatrix} 0 \\ 0 \\ \vdots \\ 0 \\ 1 \end{bmatrix} \tag{5.5}$$

$$C_P = \begin{bmatrix} g_r - d_r g_0 & \cdots & \cdots & g_2 - d_2 g_0 & g_1 - d_1 g_0 \end{bmatrix} \quad D_P = \begin{bmatrix} g_0 \end{bmatrix}$$

The time delay affects chatter behaviour in both the x and y directions, and therefore the overall state space matrices for the delay, shown in Equation 5.1, are comprised of the matrices from Equation 5.5, and given by:

$$A_{T(2rx2r)} = \begin{bmatrix} A_P & \mathbf{0}_{rxr} \\ \mathbf{0}_{rxr} & A_P \end{bmatrix} \quad B_{T(2rx2)} = \begin{bmatrix} B_P & \mathbf{0}_{rx1} \\ \mathbf{0}_{rx1} & B_P \end{bmatrix}$$

$$C_{T(2x2r)} = \begin{bmatrix} C_P & \mathbf{0}_{1xr} \\ \mathbf{0}_{1xr} & C_P \end{bmatrix} \quad D_{T(2x2)} = \begin{bmatrix} D_P & 0 \\ 0 & D_P \end{bmatrix} \tag{5.6}$$

In general, Pade approximations work best at small time delays since lower orders are required. Selecting a higher order can improve the accuracy of the approximation but can cause the matrices in Equation 5.6 can become large and slow down computation [Richard 2003]. In addition, for a sufficient stability prediction, the order of the Pade approximation must also be selected such that phase of the exponential delay term matches the phase of the rational function approximation at the dominant natural frequencies of the spindle-tool assembly. This issue is mitigated, however, by the fact that micro milling operations require high spindle speeds and as speed increases, the time delay between cutting flutes becomes smaller as shown by:

$$T = \frac{60}{nN} \tag{5.7}$$

From the block diagram in Figure 5.1, the input signal, *u*, to the dynamics is written as:

$$u = \frac{-1}{4\pi} NK_{tc} a\left(w_T - w\right) \tag{5.8}$$

For linear vibrational systems, the feed through matrix of the dynamics will be zero, *D=0*, and after substitution of the output equations from Equation 5.1 into Equation 5.8, signal *u* can be expressed as:

$$u = \frac{-1}{4\pi} NK_{tc} aC(D_T - I)z_d + \frac{-1}{4\pi} NK_{tc} aC_T z_T \tag{5.9}$$

where *I* is the identity matrix. Recognizing that the output signal, *w*, is the input to the time delay, this and Equation 5.9 can be substituted into the state variable equations from Equation 5.1 to yield:

$$\begin{aligned} \dot{z}_d &= \left(A + \frac{-1}{4\pi} NK_{tc} aB(D_T - I)C \right) z_d + \frac{-1}{4\pi} NK_{tc} aBC_T z_T \\ \dot{z}_T &= B_T C z_d + A_T z_T \end{aligned} \tag{5.10}$$

Equation 5.10 can be expressed as a matrix and the homogeneous state space description of the 2-DOF chatter system becomes:

$$\dot{z} = Mz \tag{5.11}$$

where $z=[z_d\ z_T]$ is a vector of state variables and *M* is the system matrix:

$$M = \begin{bmatrix} A + \frac{-1}{4\pi} NaK_{tc} B(D_T - I)C & \frac{-1}{4\pi} NaK_{tc} BC_T \\ B_T C & A_T \end{bmatrix} \tag{5.12}$$

Lyapunov's second method can be applied directly to Equation 5.12 at different spindle speed and cutting depth combinations to find conventional stability lobes with no variations. Equation 5.12 forms the basic state space structure for applying robust theorems involving LMI's.

The system matrix, $M(\omega_n, \zeta, K_{tc})$, is a function of the three varying parameters: the natural frequency, damping ratio, and cutting coefficients which are known to lie between an upper and lower bound:

$$\omega_n \in [\omega_{n(\min)}, \omega_{n(\max)}] \quad \zeta \in [\zeta_{(\min)}, \zeta_{(\max)}] \quad K_{tc} \in [K_{tc(\min)}.K_{tc(\max)}] \tag{5.13}$$

With three uncertain parameters, a total of eight extreme system matrices can be evaluated using Equation 5.12, and Lyapunov stability theories applied. Depending upon whether parameterized Lyapunov functions are used and whether time invariant or time varying uncertainty is considered, three different LMI formulations can be utilized.

5.1.1 Quadratic Stability

Time invariant uncertain parameters are described as either being fixed and known approximately or undergo slow variations within an uncertainty interval. For state space systems, quadratic stability is the most straightforward method which applies to the time invariant case. An uncertain system is said to be quadratically stable if and only if there exists a common positive definite matrix $P=P^T>0$ that satisfies the following set of LMIs [Barmish 1994]:

$$P > 0$$

$$M_q{}^T P + P M_q < 0 \tag{5.14}$$

$$for \quad q = 1 \cdots 2^m$$

where $m=3$ is the number of uncertain parameters and M_q ($q=1...8$) are the extreme matrices, Equation 5.12, evaluated at all extreme parameter combinations. If a single Lyapunov matrix, P, can be found, then $V(z)=z^TPz$ will be a quadratic Lyapunov function for the system.

While this guarantees robust stability for a system it is known to be highly conservative [Grman et al. 2003]. In addition if the parameter uncertainty intervals are too wide, determining

the feasibility for the LMI set becomes a very restrictive problem and potentially unrealizable [Barmish 1994]. Nevertheless, Equation 5.14 represents the basic structure involving a convex set of LMI equations, which is numerically solvable using convex optimization [Gahinet et al. 1996]. The issue of conservatism can be reduced by using parameterized Lyapunov functions that depend on the uncertain parameters [Barmish 1994].

5.1.2 Parameter Dependent Quadratic Stability for Time Invariant Uncertainty

At the expense of increased computation, imposing more constraints on the Lyapunov function can reduce the conservatism that arises naturally in Equation 5.14 [Gahinet et al 1996]. For uncertain time invariant systems, the system matrix can also be expressed as a convex combination of extreme matrices [Barmish et al. 1986, Gahinet et al. 1996]:

$$\begin{aligned} M(\alpha) &= \sum_{q=1}^{2^m} \alpha_q M_q \\ where \quad \sum_{q}^{2^m} \alpha_q &= 1 \quad |\alpha_q| \geq 0 \end{aligned} \tag{5.15}$$

where M_q are the extreme matrices. In other words, the system matrix at any parameter combination can be expressed as a weighted sum of the extreme matrices in terms of the known constants, α_q. For m=3 uncertain parameters the system is quadratically stable if there exists eight positive definite matrices, P_q, that satisfies the set of LMIs [Ramos et al. 2002]:

$$\begin{aligned} P_q &> 0 \\ M_q{}^T P_q + P_q M_q &< -I \\ M_q{}^T P_v + P_v M_q + M_v{}^T P_q + P_q M_v &< \frac{2}{2^m - 1} I \\ for \quad q = 1 \cdots 2^m - 1 \quad v &= q+1 \cdots 2^m \end{aligned} \tag{5.16}$$

where each P_q, is a Lyapunov matrix associated with the corresponding extreme matrix M_q. To build the full LMI set, the indices q and v must be iterated through. It should be noted that there are only 2^m extreme matrices and that M_q is the same as M_v when $q=v$. This is a sufficient condition for robust stability. The individual Lyapunov matrices can be combined into a convex combination:

$$P(\alpha) = \sum_{q=1}^{2^m} \alpha_q P_q \tag{5.17}$$

and therefore the Lyapunov function becomes $V(z)=z^T P(\alpha)z$. If $P(\alpha)$ is taken to be constant, then Equation 5.16 reduces to the basic quadratic stability in Equation 5.14.

To establish stability only the eight individual Lyapunov matrices, P_q, need to be found; the constants, α_q, are not directly needed [Ramos et al. 2002]. The feasibility of the LMI set in Equation 5.16 can be solved using convex optimization methods. Conservatism is reduced by searching for multiple matrices, each one weighted to a specific extreme parameter combination. The LMI systems in both Equations 5.14 and 5.16 assume that parameter uncertainty is time invariant; meaning that the rates at which parameters vary within their uncertainty intervals is not accounted for.

5.1.3 Parameter Dependent Quadratic Stability for Time Varying Uncertainty

For real systems where parameters can vary in time, Lyapunov theories may be the only approaches available to establish stability [Francesco 2006]. By imposing further constraints, parameter dependent quadratic stability can be extended to include time varying uncertain parameters by expressing the system matrix in Equation 5.15 as a time varying convex combination of extreme matrices. Montagner et al. [2003] showed that a time varying system is quadratically stable if there exists Lyapunov matrices that satisfy the following set of LMIs:

$$P_q > 0$$

$$M_q{}^T P_q + P_q M_q + \sum_{b=1}^{2^m} \pm \rho_b P_b < 0$$

$$M_q{}^T P_v + P_v M_q + M_v{}^T P_q + P_q M_v + 2\sum_{b=1}^{2^m} \pm \rho_b P_b < 0 \tag{5.18}$$

$$for \quad q = 1 \cdots 2^m - 1 \quad v = q+1 \cdots 2^m$$

where ρ_v ($v=1...m-1$) are the equivalent parametric bounds on the time derivatives of the uncertain parameters and the parameterized Lyapunov function is shown in Equation 5.17. The LMI set must be built by iterating through all indices q, v, and b and at both positive and negative values of each ρ_v. This represents a sufficient condition for quadratic stability for time varying uncertainty.

The set of LMIs represents a general case for establishing quadratic stability for uncertain systems. For the time invariant case, the equivalent parametric bounds become zero, $\rho_v=0$, and Equation 5.18 reduces to Equation 5.16 [Montagner et al. 2004]. With the additional LMI constraints, increased computational resources are a practical issue that must be addressed. In order to implement, bounds on the rate of parameter variations are required, which may be difficult to identify in practice [Montagner et al. 2003, Francesco 2006].

5.2 Robust LMI Algorithm

A similar bisection algorithm as described in Chapter 4, can be used to establish chatter stability 2-DOF milling systems and implemented in Matlab™. Figure 5.2 outlines a similar algorithm where by iterating through a range of spindle speeds, the cutting robust chatter stability lobe boundaries are found using a bisection method and one of the three LMI robust stability formulations.

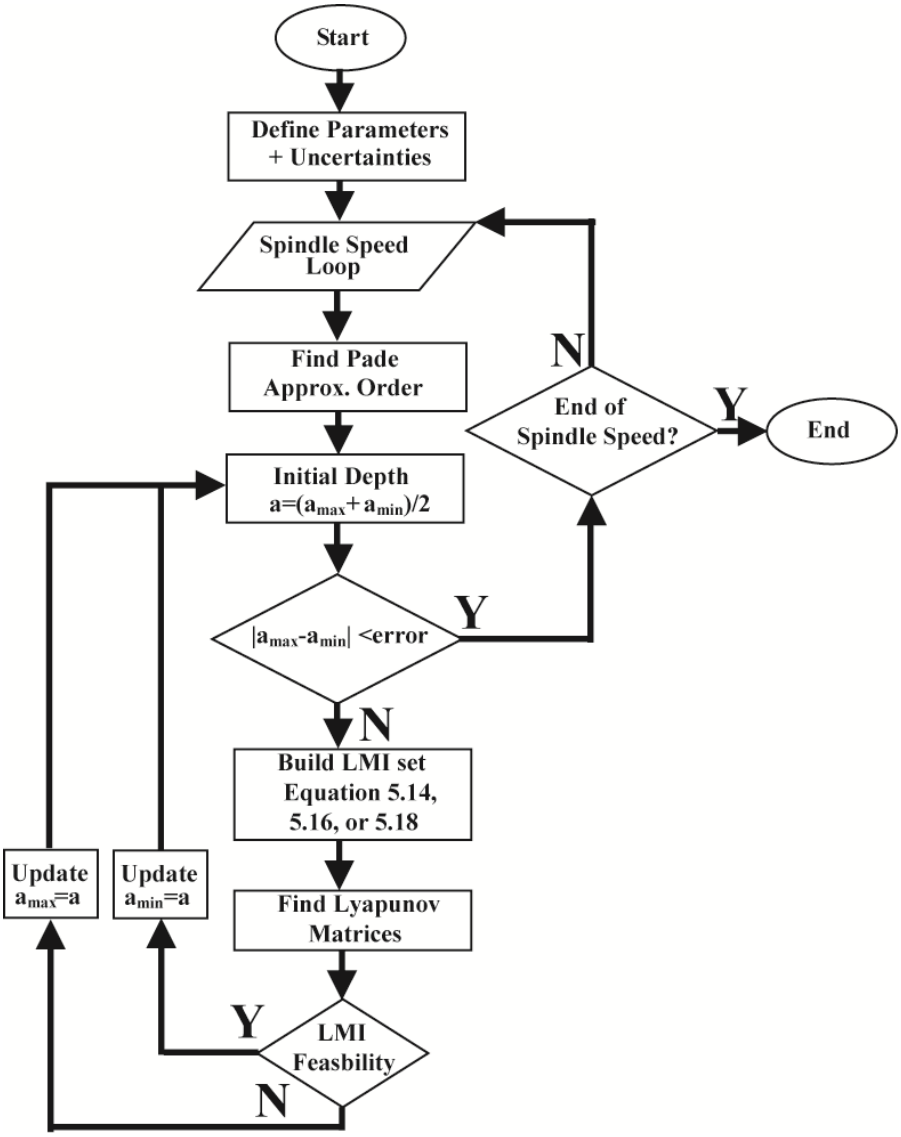

Figure 5.2 Bisection algorithm flowchart

Identified system parameters and uncertainties are first defined and a sufficient Pade approximation order is found by ensuring the phase of delay term at the highest natural frequency is accurately approximated. At a given speed (i.e. time delay), the approximation order is incremented until the phase of the transfer function built using Matlab™ "*pade*" function matches the phase of an exponential term of the same delay, at the highest, dominant natural frequency. This improves computational speed since stability at higher spindle speeds can be

determined with a lower order. Using the highest tooltip frequency at 5934 Hz with a maximum of +5.0%, as outlined in Chapter 3, the minimum Pade orders needed to find stability for the experimental system are 14 and 21 for spindle speeds of 50000 rpm and 30000 rpm, respectively. Since chatter does not necessarily occur exactly at the natural frequencies orders are incremented by one to ensure the approximation matches.

After finding a suitable approximation, the minimum and maximum bounds on the cutting depth are specified to get an initial starting point for the bisection algorithm. The extreme system matrices are then constructed with the state space descriptions of the approximated delay term and extreme parameters. One of the LMI sets given in Equations 5.14, 5.16, or 5.18 can then be specified and the feasibility of the LMI system solved using convex optimization solvers. If the feasibility problem is satisfied, the system is quadratically stable and the minimum cutting depth value is updated with the current cutting depth. If not stable, then the maximum cutting depth value is updated. The algorithm moves to the next spindle speed once the bisection algorithm reaches a specified tolerance.

Solving LMIs is a convex optimization problem and many commercial software programs contain different types of numerical solvers which can be applied to a variety of problems [Boyd et al. 1994]. Quadratic stability in Equation 5.14 was solved using LMI solver "*feasp*", which uses the Projective Method developed by Nemirovskii et al. [1999], and is found in the Matlab™ Robust Control Toolbox. The LMI feasibility problems involving parameter dependent formulations, Equations 5.16 and 5.18, were solved using the CVX package [CVX Research, Grant et al. 2008]. This software allows LMI constraints to be directly written using Matlab™ syntax and provides numerical solvers needed to handle convex optimization problems. While Equations 5.16 and 5.18 can be solved using the default solvers in Matlab™,

the CVX package was found to perform faster and complicated problems can be programmed easier.

Due to the difference in the size of LMI sets, parameter dependent quadratic stability requires more computational resources and time. Table 5.1 summarizes the number of LMIs in the above equations.

Table 5.1 Number if LMIs for m number of uncertain parameters and $\eta=2^m$ extreme parameter combinations

Method and Equation	Number of LMI Equations	Example With m=3 and η=8
Quadratic Stability with Time Invariant Uncertainty, Equation 5.14	$\eta+1$	9
Parameter Dependent Quadratic Stability with Time Invariant Uncertainty, Equation 5.16	$2\eta+\frac{\eta}{2}(\eta-1)$	44
Parameter Dependent Quadratic Stability with Time Varying Uncertainty, Equation 5.18	$\eta+\eta 2^{\eta}+\eta(\eta-1)2^{\eta-1}$	9224

The total number of LMI equations is determined by the number of uncertain parameters and the type of constraints imposed upon the system. Consideration of either time varying parameters versus time invariant parameters, or parameterized Lyapunov matrices over a single matrix, leads to larger LMI systems. Based on the flowchart in Figure 5.2, the set of LMIs will be evaluated multiple times at a given spindle speed to converge on the predicted robust stability lobe boundary. When implementing robust analysis, it is therefore important to consider the complexity of the robust model since the trade off is increased computational resources.

5.3 Results

Robust stability lobes were predicted with the LMI formulations were compared to the Edge theorem approach described in Chapter 4 and to the actual experimental chatter conditions using the micro milling setup described earlier in Chapter 3.

5.3.1 Simulation with Edge theorem

The LMI approaches which consider time invariant uncertainties, were compared to the combined Edge theorem and Zero Exclusion approach described in Chapter 4. Figure 5.3 shows a simulated comparison between the robust methods which consider ±3% uncertainty for time invariant parameters, and conventional stability lobe methods. Both the analytical chatter stability in the frequency domain [Altintas 2012] and conventional time domain simulations consider no uncertainties. Time domain simulations consider the exact kinematics of an end mill and are a good reference for comparison [Altintas et al. 2004]. Table 5.2 compares the computational time required by each prediction using a 2.90 GHz processor (Intel Core i5-2310) computer. The simulations were performed using Matlab^{TM} software with the exception of the time domain simulation, which was performed using machining software Cutpro 9.0^{TM}.

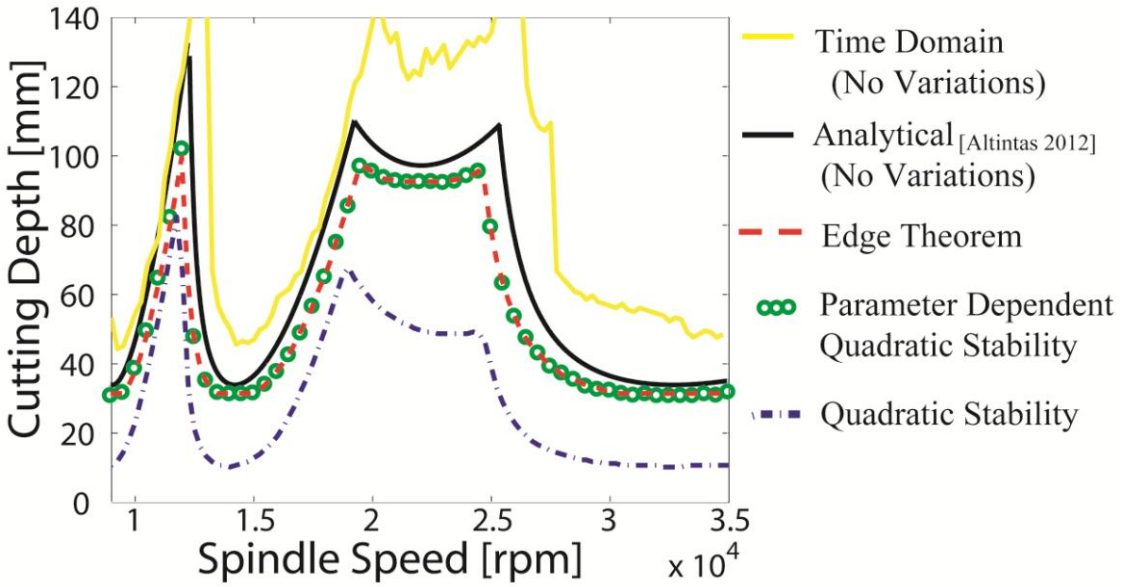

Figure 5.3 Stability lobe comparison

The robust methods in Figure 5.3 give a conservative prediction of chatter stability compared to the conventional approaches. Quadratic stability, from Equation 5.14, gives a highly conservative prediction as indicated in the theory [Grman et al. 2003]. A conservative robust theorem can benefit chatter stability lobes by ensuring a degree of reliability despite the presence of uncertainties. Many robust theorems based on a deterministic description of uncertainty, naturally have some conservatism [Calafiore et al. 2011]. By predicting stability lobes based upon extreme parameter boundaries, a reliable selection of cutting depth and spindle speed could be made. However, highly conservative theorems such as the quadratic stability condition can be restrictive and depending upon the width of the uncertainty intervals, may not always be realizable. For the same simulation parameters, the degree of conservatism is reduced using Equation 5.16 which considers parameterized Lyapunov functions, and matches the Edge theorem approach. However, there is a difference in computational performance between the two methods.

Table 5.2 Computational time comparison

Method	Time
Conventional Stability	0.59 [sec.]
Quadratic Stability	18 [min.]
Edge Theorem and Zero Exclusion	9.0 [min.]
Time Domain (Cutpro 9.0)	51 [min.]
Parameter Dependent Quadratic Stability	8 [hrs.]

From Table 5.2 it can be observed that the LMI approach is computationally more time consuming to implement, especially the parameter dependent quadratic stability. The LMI approaches require complex numerical algorithms to solve the LMI feasibility problem and in addition, the difficulty in finding parameter dependent Lyapunov matrices arises naturally from basic Lyapunov stability [Grman et al. 2003]. Lyapunov's second method outlines that system stability can be established if certain matrices can be found, but does not give a definitive method of finding these matrices. Lyapunov matrices are not unique and the theory holds for any matrix that satisfies the LMI equations. Rather than solving the convex LMI feasibility problem every iteration, Lyapunov matrices from the previous iteration could be used to check. Unfortunately previous results are unlikely to work, due to the complexity of the state space matrices for the 2-DOF system, the Pade approximation, and the number of Lyapunov matrices required, for Equation 5.16, and results in increased computational effort. The LMI formulation also depends upon an approximation of the delay term. When setting the order of Pade approximation, there is a trade-off between accuracy and increased matrix size which also leads to more computational effort for the LMI approach. Robust stability for relatively small uncertainty intervals can be more quickly realized using the Edge theorem method.

In Table 5.1, the simulation time for the Edge theorem approach and the quadratic stability from Equation 5.14, was achieved using parallel computing feature of Matlab^{TM} which makes better use of multi-core processor computers. The Edge theorem approach requires a lot of iterations over three variables, the spindle speed, cutting depth, and frequency using relatively simpler geometric calculations. The LMI approaches, in contrast, use convex optimization methods which require more complex calculations and computer memory. Without parallel computing, the Edge theorem approach requires 45 min and the quadratic stability requires about 32 min of simulation time to predict the stability lobes in Figure 5.3. By performing multiple iterations simultaneously, parallel computing can provide significant performance improvements; for the Edge theorem and quadratic stability approaches, respectively, there was about an 80% and 44% improvement in speed.

Parallel computing increases performance at the expense of computer memory and may not be adequate for the parameter dependent quadratic stability in Equation 5.16, due to the large number of LMI equations needed and the convex techniques needed to search for Lyapunov matrices. Overall computational performance of robust methods depends upon the extent and resolution of the spindle speed and cutting depth ranges, width of uncertainty intervals, and the available computer hardware. Stability lobes are predicted prior to a machining process, and therefore computation does not need to be performed in real time.

5.3.2 Experimental Comparison

The parameter dependent quadratic stability condition for time invariant uncertainty from Equation 5.16 was predicted using the algorithm outlined in Figure 5.2. In Figure 5.6 they are compared to the Edge theorem prediction using the experimental results, the measured chatter

points, and the conventional 2-DOF prediction computed using the average parameter values with no uncertainties. This is the same experimental setup described in Chapters 3 and 4.

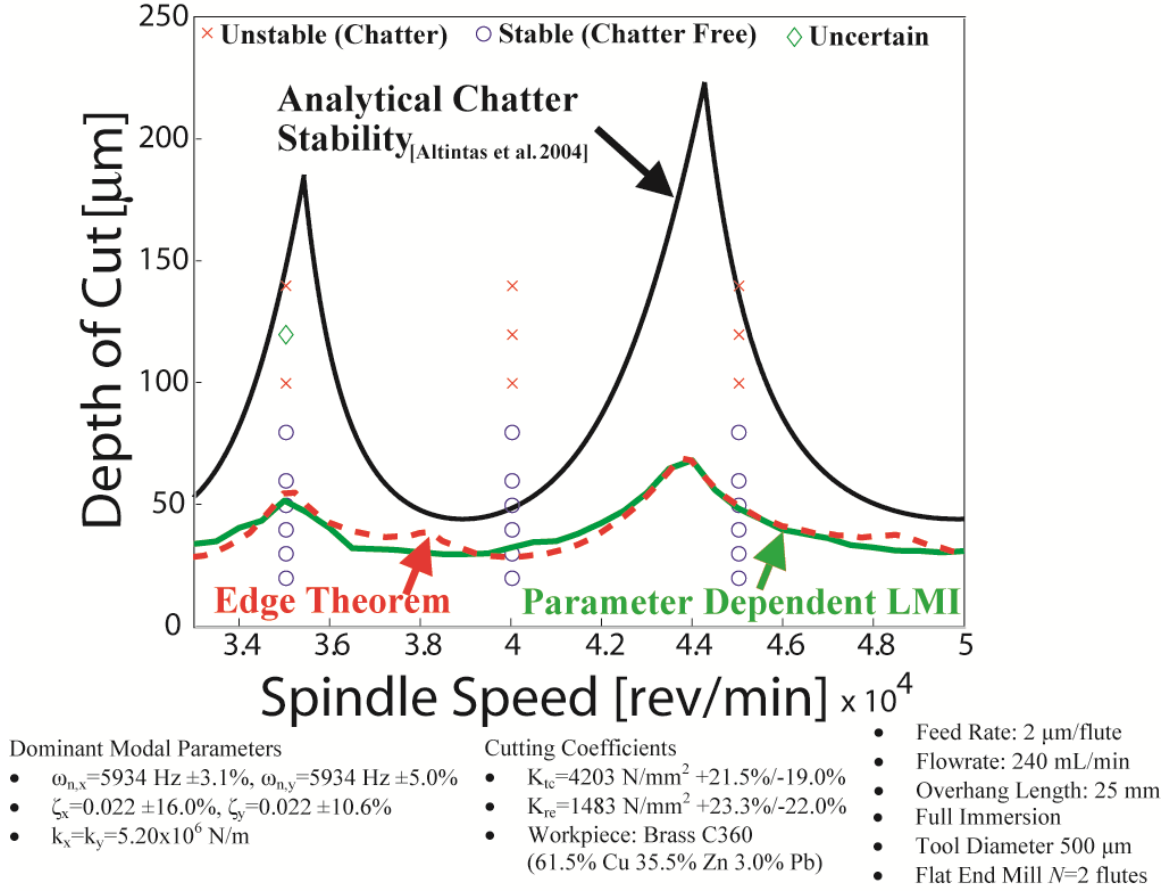

Figure 5.4 Robust LMI chatter prediction comparison with 3 uncertain parameters

The parameter dependent LMI approach gives a similar conservative prediction as the Edge theorem method. Basic quadratic stability, from Equation 5.14, could not be predicted using experimental parameters due to the relatively wide parameter uncertainty intervals. When uncertainty intervals are too wide, finding one common Lyapunov matrix is computationally difficult to achieve and in some cases not even possible [Barmish 1994].

In the saddle regions of the lobes there are some differences between the Edge theorem and LMI results. This is due to differences in formulation between the two methods. The LMI

approach is a sufficient condition based upon Lyapunov stability, which determines whether the system states go to a bounded equilibrium. Failure to find Lyapunov functions does not necessarily indicate that the system is unstable, and stable points may very likely be found above the stability lobe boundaries.

The combined Edge theorem and Zero Exclusion approach depends upon the shape of the value set and the ability to approximate that shape with a straight edged polygon and as shown in Figure 5.5, this may not always hold. Figure 5.5 shows value sets and their predicted outer edges at different points on the robust stability lobe boundary. At 38000 rpm, the outer edges do not accurately reflect the outer shape of the value set and at 40000 rpm they match.

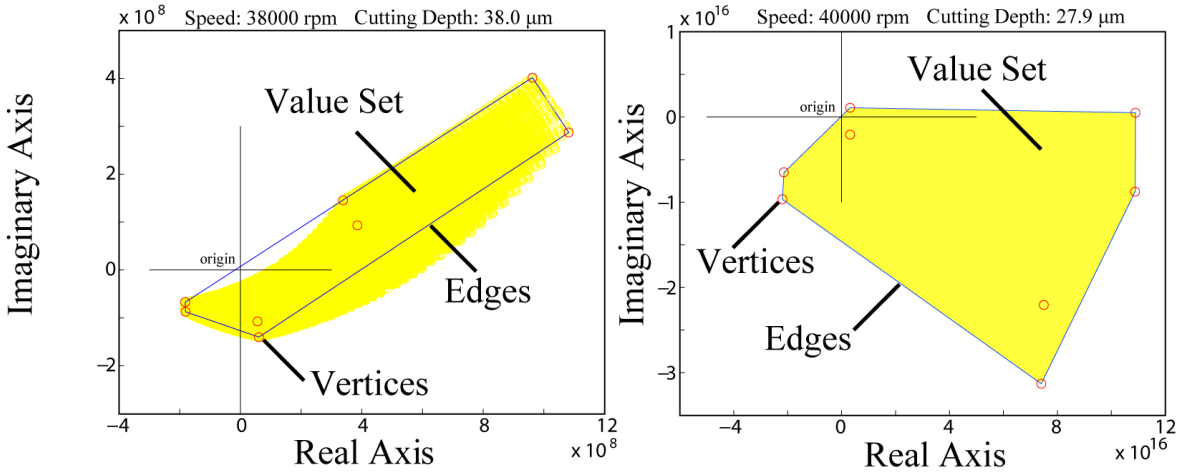

Figure 5.5 Value sets of Edge theorem approach at critical stability lobe boundary

At relatively wide uncertainty intervals the value set my no longer be straight edged polygon [Bhattacharyya et al. 1995]. For the case at 38000 rpm, the Zero Exclusion criteria indicates the system is not robustly stable with the outer edges, however the origin is not actually within the value set which represents the true stability region [Barmish 1994]. As such, the method is highly dependent upon the mathematical structure of the characteristic equation and the extent of the parameter uncertainty bounds. Although this is a minor issue for the experimental work

presented, any practical implementation of the Edge theorem method would require sufficient knowledge of its limitations.

In general, the effectiveness of different robust theories is limited by the width of the uncertainty intervals on the unknown parameters [Bhattacharyya et al. 1995]. Large uncertainty intervals can result in conservative lobes (i.e. lobes shift downward) or can become computationally difficult to realize. Even the selection of the number of uncertain parameters is vital as more uncertain parameters require a greater number of characteristic polynomials or system matrices that need to be evaluated and greater computational time. Adequate stability modeling and accurate identification of parameter uncertainties are critical for suitable implementation of robust chatter stability.

5.3.3 Time Varying Uncertainty

Due to the computational resources required, this study considers only two varying parameters when dealing with the time varying case in Equation 5.18. For time varying parameter uncertainty, the bounds on the time derivatives of the parameters are required [Montagner et al. 2004]:

$$\dot{\omega}_n \in [\dot{\omega}_{n(\min)}, \dot{\omega}_{n(\max)}] \quad \dot{K}_{tc} \in [\dot{K}_{tc(\min)}, \dot{K}_{tc(\max)}] \tag{5.19}$$

The bounds on the rates of parameter variations can be used to find the equivalent parametric bounds on the time derivatives, ρ_v. With two uncertain parameters, a total of four equivalent bounds are needed. Since the bounds are not directly available, the maximum and minimum bounds on the parameter variations were estimated using the experimental parameters.

Variations in the rate of change of the natural frequency were assumed to be related to the changing mass of the reservoirs. During chatter experiments, these reservoirs were filled with liquid at a constant flow rate and by finding an approximate relation with the dominant tooltip

natural frequency, an estimate of the bounds on the time variation can be found. For mechanical systems, natural frequency is related to both mass and stiffness. Assuming natural frequency and mass are functions of time:

$$\omega_n(t)^2 = \frac{k}{m(t)} \tag{5.20}$$

If the reservoirs are filled at a constant flow rate, *dV/dt*, then the mass flow rate can be related to liquid density, υ. After taking the time derivative of both sides of Equation 5.20, and substituting in for the mass flow rate, the minimum and maximum rates of natural frequency variation can be expressed as:

$$\begin{aligned} \dot{\omega}_{n(\min)} &= \frac{1}{2}\frac{\omega_n^{\,3}}{k}\upsilon\left(dV/dt\right)_{(\min)} \\ \dot{\omega}_{n(\max)} &= \frac{1}{2}\frac{\omega_n^{\,3}}{k}\upsilon\left(dV/dt\right)_{(\max)} \end{aligned} \tag{5.21}$$

where ω_n is the dominant tooltip natural frequency, *k* is the corresponding modal stiffness, and $(dV/dt)_{(min)}$ and $(dV/dt)_{(max)}$ are the minimum and maximum flow rate range of the pump. The modal parameters and flow rate range were identified and outlined in Chapter 3.

Changes in the cutting forces were assumed to be attributed to changes in cutting coefficients values. As described in Chapter 3, cutting coefficient values were found by optimizing experimental forces with the linear cutting force model. Along with their identified uncertainties, these values are assumed to contain the effects of ploughing, material non-uniformity, and other phenomena which cause variations. In micro milling, as shown in Figure 5.6, chip thickness changes with both the immersion angle of each tooth and the cutting regime.

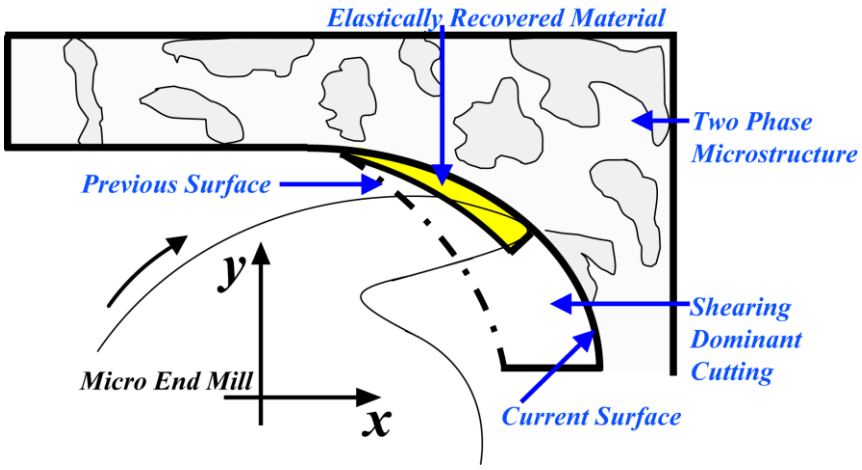

Figure 5.6 Chip thickness in micro milling

Cutting coefficient variations will occur as chip thickness changes with immersion conditions. Assuming these variations are also linear with respect to immersion angle, the cutting coefficient, per flute, can be approximated by:

$$K_{tc}(t) \approx \frac{K_{tc(\max)} - K_{tc(\min)}}{N\Delta\phi}\phi(t) \tag{5.22}$$

where $\Delta\phi=\phi_{ex}-\phi_{st}$ is the difference between exiting and staring immersion angles, and N is the number of teeth. The rate of change of the immersion angle is the spindle speed. Taking the time derivative of sides, the upper and lower bounds on the cutting coefficient variations can be expressed as:

$$\begin{aligned}\dot{K}_{tc(\min)} &= \frac{K_{tc(\max)} - K_{tc(\min)}}{N\Delta\phi}\frac{2\pi n_{lower}}{60} \\ \dot{K}_{tc(\min)} &= \frac{K_{tc(\max)} - K_{tc(\min)}}{N\Delta\phi}\frac{2\pi n_{upper}}{60}\end{aligned} \tag{5.23}$$

where n_{lower} and n_{upper} respectively are the lowest and highest spindle speeds [rpm] over which the variations in spindle dynamics were measured (i.e. 0 to 60000 rpm). Cutting coefficients are

outlined in Chapter 3. A two flute end mill at full immersion cutting conditions were utilized for chatter experiments.

Numerical optimization can be used to find the equivalent parametric bounds, ρ_v [Montagner et al. 2004]. For two uncertain parameters, the parametric bounds are found to satisfy the following:

$$\begin{aligned} &\dot{\omega}_{n(\min)} \le (\rho_1 + \rho_2)\omega_{n(\min)} + (\rho_3 + \rho_4)\omega_{n(\max)} \le \dot{\omega}_{n(\max)} \\ &\dot{K}_{tc(\min)} \le (\rho_1 + \rho_3)K_{tc(\min)} + (\rho_2 + \rho_4)K_{tc(\max)} \le \dot{K}_{tc(\max)} \\ &\left|\sum_{i=1}^{4} \rho_i\right| = 0 \end{aligned} \tag{5.24}$$

Prior to implementation of the chatter algorithm, when system parameters are defined, see Figure 5.2, Equation 5.24 can be solved using the same CVX toolbox in Matlab™. Accounting for time varying uncertainty is difficult since bounds on rates of change of the parameters are not always available.

The time varying parameter dependent LMI in Equation 5.18, was computed only considering two uncertain parameters, the natural frequency and cutting coefficients, due to limitations of computational resources. From Table 5.1, considering three uncertain parameters would lead to a significant number of LMI equations. As shown in Figure 5.7, this was compared to the parameter dependent time invariant case using Equation 5.16 also for two uncertain parameters. With two uncertain parameters, Equation 5.18 represents 164 LMIs in the time varying and Equation 5.16 represents 14 LMIs. By including the bounds on the rate of change of the uncertain parameters, the time varying LMI system gives a more conservative prediction when compared to the time invariant LMI approach for two uncertain parameters.

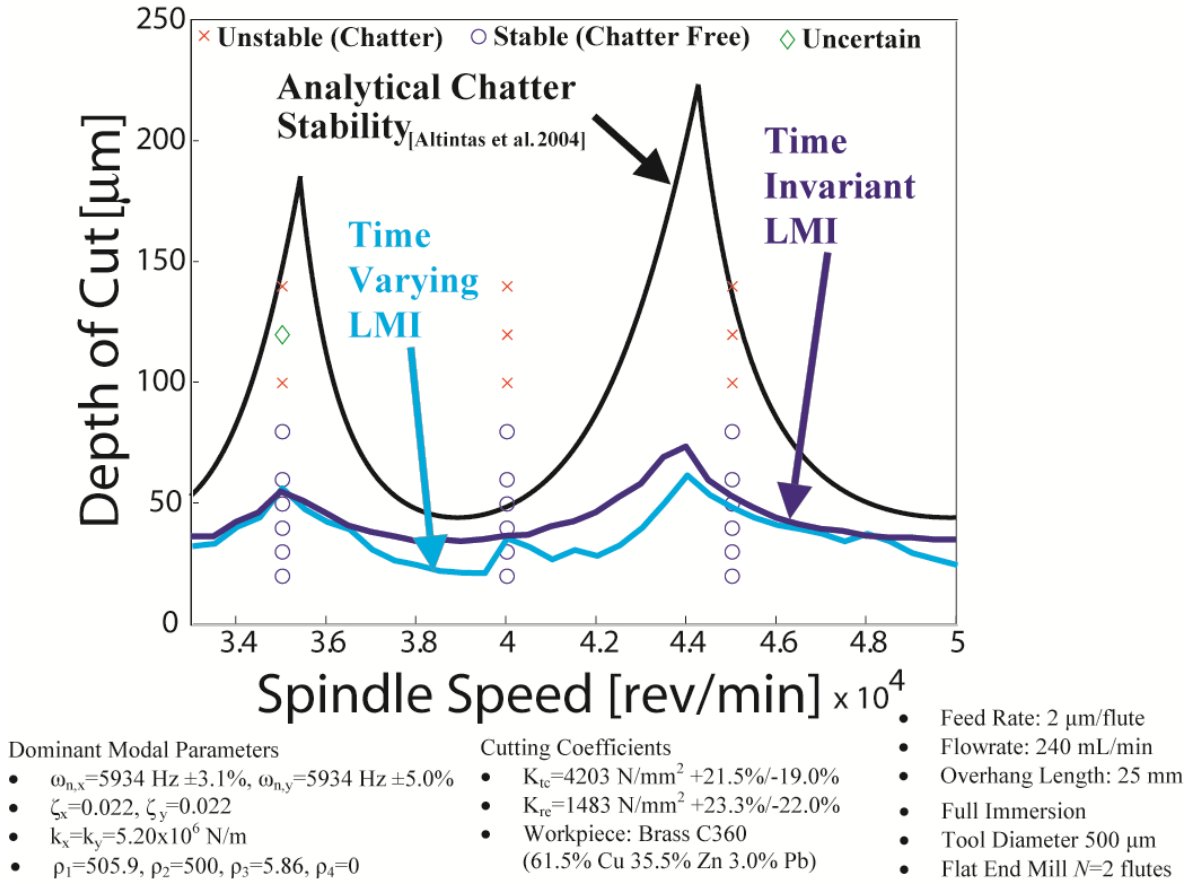

Figure 5.7 Comparison with time varying uncertainty

Figure 5.7 shows that stable points lie beneath both the two parameter case for the time invariant and time varying LMI approaches. A major limitation to the time varying LMI approach is identifying the bounds on the parameter time derivatives. For this study, the bounds were found using knowledge of the experimental system and simplifications in their calculation. The practical use of accounting for time variations in the uncertain parameters is also questionable since it requires considerably more computational time and resources. The experimental evidence indicates that the time invariant LMI, Equation 5.16, provides a sufficient prediction.

An important aspect when implementing robust methods is to consider the balance between modeling accuracy and computational time. While including more uncertain parameters and time varying effects more accurately reflect the real system, increased complexity adds to the computational resources required. Familiarity of the milling system, the robust method, and its limitations is required to facilitate a suitable level of modeling accuracy and enable computation to take place in a timely manner.

5.4 Summary

In this chapter, a robust chatter stability formulation based on a novel matrix approach using LMIs was investigated. The 2-DOF milling stability was described in state space form using a Pade approximation of the time delay. Three different robust LMI systems, based on Lyapunov quadratic stability theory, were implemented and solved using numerical convex optimization solvers in Matlab^{TM}. The robust LMI lobes considering three varying parameters were compared to the Edge theorem approach described in Chapter 4 and experimental conditions. Quadratic stability required the least amount of computational resources, however it gave a highly conservative prediction and its usage is limited depending upon the extent of the uncertain parameter intervals. Both a time invariant and time varying LMI systems based upon parameter dependent Lyapunov functions were used to predict stability based on the experimental conditions. The time invariant case closely matched the Edge theorem approach using the experimental parameters and gave an identical prediction in a simulated comparison for small uncertainty intervals. The time varying LMI set also gave a conservative prediction of stability for the case of two uncertain parameters. However, it required considerably more computational time and additional effort to identify bounds on parameter variations.

CHAPTER 6. CONCLUSIONS

Regenerative chatter presents a serious limitation to productivity and can cause damage to cutting tools and machine. While chatter stability lobe diagrams can be used to select optimal cutting depths and spindle speeds to avoid the occurrence of chatter, variations in parameters can cause inaccuracies. This thesis presented a first attempt at accounting for three uncertain parameters in chatter stability prediction for micro milling operations using robust stability theorems. This chapter presents a summary of the work conducted and the novel contributions of this study. A discussion of the limitations and assumptions of the robust methods and experiments are presented and future works are suggested at the end of the chapter.

6.1 Thesis Summary

Chatter is a dynamic phenomenon that resulting from an oscillating chip thickness and leads to self-excited vibrations. Chatter is highly detrimental to the quality of machined components and overall productivity of machining operations. Poor dimensional accuracy, poor surface finishes, wasted time and resources all result from unstable machining. Many researchers have studied many different methods of predicting and minimizing chatter, and the easiest and most viable method is to utilize chatter stability lobe diagrams. Conventional chatter models combined with experimentally identified parameters are used to predict stability lobes which outline regions where certain combinations of cutting depth and spindle speed are stable and unstable. Stability lobe diagrams can be used as an effective tool for selecting optimal machining parameters prior to the machining process.

The effects of parameter uncertainties are the primary drawback of using the stability lobe approach. Analytical models are limited in accuracy due to simplifications, and many assume that parameters are constant when in reality they can never be known exactly. Tool dynamics are subject to variations due to dynamic phenomena at the spindle and are acquired through modal testing performed on stationary machine tool setups. Cutting coefficients are dependent upon the interaction between the cutting edge and the workpiece material and many different factors can contribute to changes in cutting forces and chip formation.

Cutting coefficients were obtained by micro milling free machining brass with a 500 μm diameter, 2 fluted carbide end mill on an ultra precision micro milling machine Cutting forces were measured using a table dynamometer, and optimized with a linear cutting force model to obtain nominal coefficient values. Variations needed to reach the maximum and minimum bounds of the experimental data were identified. Receptance coupling was used to identify modal parameters at the tool tip. The frequency response function (FRF) of a blank end mill was found using impact hammer testing. The FRF of the tool tip was obtained with a finite element model utilizing Timoshenko beam theory. The two FRFs were combined mathematically, and curve fitted to identify the modal parameters. Variations in the dynamics were introduced through a liquid reservoir system attached to a 3-axis micro milling system which could be filled and emptied via a peristaltic pump to adjust the overall mass of the spindle structure during chatter tests. Hammer testing on the spindle structure was performed at full and empty reservoirs, for a range of spindle speeds to identify the largest uncertainty intervals. Chatter tests were performed at different cutting depth and spindle speed combinations and a FFT of AE signals provided a means for determining the occurrence of chatter. Large peaks in AE signals are shown near dominant tooltip natural frequencies when chatter occurs.

Two different robust stability approaches for finding stable, chatter free regions were presented and compared while accounting for three uncertain parameters. The two degree of freedom (2-DOF) chatter stability model for milling is extended with both a parametric approach and a modern LMI formulation. By accounting for parameter uncertainty, stable cutting regions can be guaranteed and the negative aspects of chatter minimized. The proposed robust chatter stability models are supported by chatter experiments where parameter uncertainties were artificially introduced and the bounds quantified. Comparisons were made with the conventional chatter models and measured chatter points.

6.2 Novel Contributions

A robust stability analysis has never been performed using the 2-DOF analytical stability model for milling first presented by Altintas et al. [1995]. This model is widely used and regarded to be the most viable model for predicting chatter stability in milling. The novel contributions of this research are:

i. *Considered three varying parameters in micro milling operations:*

Parameter variations in micro milling operations primarily occur in both the dynamic and cutting coefficient parameters. This study investigated changes in three parameters, natural frequency, damping ratio, and cutting coefficients. High spindle speeds can cause uncertainty in dynamics of the tool, thermal expansion at the spindle bearings are known to cause variations, and measurements acquired on stationary machine tool setups can differ from dynamics during actual operations. Uncertainty in cutting coefficients can arise depending upon tool geometry, friction, material uniformity, and switching cutting mechanisms between ploughing and shearing dominant. For

accurate chatter stability prediction, parameter variations must be taken into account for micro milling operations.

Micro milling of free machining brass C360 introduced uncertainties into the cutting coefficients. Cutting forces were measured at different feed rates between 0.25 and 6 μm/flute and optimized with a linear mechanistic cutting force model to identify nominal cutting coefficients. Variations in nominal coefficients needed to match the maximum and minimum experimental data were found. Tangential cutting coefficient was found to be 4203 N/mm^2 and vary between +21.5% and -19.0%. The radial cutting coefficient was identified as 1483 N/mm^2 and varies between +23.3% and -22.0%. Edge coefficients do not contribute to chatter stability due to their static nature. Since the edge radius of the tool is comparable in size to the microstructure and chip thickness, variations were assumed to be dominated by cutting of grain boundaries, material defects, friction, and ploughing effects.

Variations were introduced into the dynamics using a liquid reservoir system. A combination of EMA and RC methods were used to identify vibrational modes of the spindle structure and tooltip over a range of spindle speeds and at empty and full reservoirs. In the *x* direction, the natural frequencies were found to vary between ±3.1% and the damping ratios to vary between ±16.0%. In the *y* direction the natural frequencies were found to vary between ±5.0% and the damping ratios between ±10.6%.

Time invariant parameter uncertainty assumes the rate at which parameters change during milling is negligible. In addition to the bounds on the uncertain parameters, bounds on the rates of parameter variation are needed to account for time varying effects. Based upon the operating limitations of the experimental equipment

used, simplifications were made to estimate the upper and lower bounds on the time derivatives of the natural frequency and cutting coefficients.

ii. *Extension of Edge theorem approach for 2-DOF chatter stability:*

Previous works have applied the Edge theorem and Zero Exclusion approach to the pseudo SDOF models which may not always be suitable for milling stability [Park et al. 2007, Park et al. 2010]. While the 2-DOF chatter stability model is more accurate for milling operations, it still assumes that system parameters are constant and for micro milling operations parameter variations must be taken into account. In addition, these previous works also only considered two uncertain parameters in their formulations.

Time variant parameter uncertainty can be accounted for using the combination of the Edge theorem and the Zero Exclusion condition. Through evaluation of the characteristic equation over a range of chatter frequencies, extreme polynomials can be expressed as functions of the extreme uncertain parameter combinations. These extreme vertex polynomials can be used to build edges and by applying the Zero Exclusion condition to graphically check whether the origin lies inside or outside these boundaries can establish stability. With each iteration, a 100 to 6500 Hz frequency range was swept to include all dominant tooltip modes of milling system. The cutting depth of the robust chatter lobe boundaries are found using a bisection method at a given spindle speed. Total computational time for the algorithm presented was reduced using parallel computing. In comparison to the conventional 2-DOF stability model which does not consider parameter variations, the robust stability lobes give a conservative prediction of chatter stability. The robust predictions were verified experimentally by comparing to measured chatter conditions for a real micro milling system. Chatter tests were performed

at various spindle speed and cutting depth combinations at full immersion conditions at a feed of 2 μm/flute. Compared with the experimental chatter tests, robust lobes do not capture all potential stable points, but can be used to guarantee chatter stability.

iii. *Formulation of robust 2-DOF chatter stability involving Lyapunov theory and LMIs:*

Many problems can be formulated in terms of linear matrix inequalities (LMI) and can be solved using convex optimization techniques. Lyapunov stability theory is applicable to many different types of complex systems, and can be expressed as a LMI. Stability can be established by using convex optimization to find a suitable matrices that satisfies the Lyapunov equation. A state space formulation of the 2-DOF chatter was presented and three different robust LMI formulations were compared.

Quadratic stability requires the least amount of computational resources and time, but only one Lyapunov matrix needs to be found. This produces a highly conservative stability lobe prediction that was not realizable using the experimental data due to the wide extent of the uncertain intervals of the parameters. A LMI formulation based upon parameter dependent Lyapunov functions while considering three uncertain parameters proved to be sufficient in providing a stability prediction similar to that of the Edge theorem approach. The Edge theorem approach was computationally faster; however, the formulation depends upon a straight edged approximation of the value set. This makes the LMI approach less sensitive to mathematical formulation since it is sufficient condition based on finding stability of system states.

The effects of including time varying uncertainty into robust stability models was investigated using a parameter dependent Lyapunov LMI formulation originally derived by Montagner et al. [2003]. Time varying effects cannot be implemented into the Edge

theorem and Zero Exclusion approach. By including the effects of time varying uncertainty, the robust chatter prediction become more conservative and further guaranteed stability. However due to limitations on computational resources, the time varying case was only investigated for two uncertain parameters, the natural frequency and cutting coefficients. While this study showed a successful prediction of robust stability which accounted for time varying uncertainty, the practical use is limited due to the required computational time and difficulty in accurately estimating bounds on the parameter variations.

6.3 Discussions

This study investigated the prevention of chatter using robust stability formulations of the 2-DOF milling analytical stability model. Chatter is highly detrimental; however, in micro milling operations, the effects of parameter uncertainty cannot be ignored. Due to the miniature size of the cutting tools, high spindle speeds are needed, which can alter the spindle and tool dynamics. The relative size of the cutting edge with the workpiece can significantly affect the interaction between the cutting edge and the workpiece and lead to changes in cutting coefficient values. Robust stability theorems provide a possible means of addressing the issue of parameter uncertainty. There are several assumptions behind the robust methods and experimental work presented.

6.3.1 Assumptions

The conventional linear shearing force model was optimized over a range of experimental forces to identify cutting coefficients with variations. During micro milling operations, different cutting regimes are present depending upon the uncut chip thickness [Malekian et al. 2009]. At

higher feed rates, a shearing dominant region exists where cutting forces can be modeled using a linear force model. Below a critical chip thickness value, ploughing dominant cutting exists where the edge radius of the cutting tool is comparable to the uncut chip thickness. The effects of elastic recovery of the material in this region typically cannot be ignored and instead of modeling the cutting and ploughing forces in each regime separately, linear cutting coefficients were used. It was assumed that the identified coefficients with variations quantified the effects of ploughing and material uniformity. This led to relatively wide uncertainty intervals in the cutting coefficients. Since each cutting flute goes through both ploughing and shearing cutting mechanisms, the rate of change in cutting coefficients were assumed to be linearly related to immersion angle for the time varying uncertainty case. The bounds on the rate of change of the cutting coefficient parameters was then estimated by relating to the spindle speed limitations of the spindle.

The tooltip dynamics were assumed to be the same in both directions due to relative symmetry of a cylindrical flat end mill. In reality, the dynamics will be slightly different in each direction. Due to the difficulty in influencing and measuring the tooltip dynamics directly, variations were assumed to be due entirely to variations in spindle dynamics. This was motivated by much of the background literature, which indicates that high rotational speeds have an effect in determining tool dynamics. Dynamic effects due to high spindle speeds and thermal expansion in spindle bearings have been identified as major contributors to dynamic variations [Abele et al. 2010]. Joint dynamics between tool and clamping conditions of the spindle can also influence chatter frequencies, however these were not included [Shi et al. 2012]. Time varying effects in the natural frequencies was also assumed to be due entirely to the mass flow rate of the fluid.

Estimation on the bounds of the rate of change in the natural frequency was found by relating to the flow rate range of the pump used.

There are also some assumptions associated with the robust modeling. While the robust methods presented can be implemented for any number of uncertain parameters, only three were considered, the natural frequency, cutting coefficients, and damping ratios. This study also only considers the 2-DOF chatter stability. Utilizing a different analytical model which includes effects such as more degree of freedoms, accounting for time varying effects, and including more uncertain parameters, could make the robust model to more representative of a real system.

The effects of nonlinearities were assumed to be within the identified extreme bounds. In reality, additional factors such as temperature changes, stage movement, dynamics of the joint between tool and spindle, and chip formation also contribute to parameter uncertainty, but were not directly included. In micro milling, size effect phenomena due to the miniature tool size, are often nonlinear [Vollersten et al. 2009]. Thermal deformations can lead to variations in dynamics of the tool and spindle and are difficult to model [Mayr et al. 2012]. Provided any parameter variations due to nonlinear behaviour remain within the extreme bounds, robust approaches can be used to establish stability without the direct need for complex modeling.

The systems used in this study were assumed to be modeled with linear delay differential equations in only two degrees of freedom and the governing characteristic equations were derived by initially considering two independent directions. Cross transfer functions were not directly considered and would have some effect on the dynamics in reality. If further extension of the model was made to include more degree of freedom or different cutter geometry with less axial stiffness and increased flexibility, then cross terms would need to be considered. The robust

approaches used were based on the nominal linear 2-DOF chatter model, which is a simplification of the real process.

The robust approaches considered only parametric uncertainties, where the physical system parameters are unknown. Dynamic uncertainties, due to neglected dynamic modes at higher frequencies, are assumed to have negligible effect in most practical cases [Fu et al. 1989]. Due to the small feed rate used (i.e. 2 μm/flute in the experiments), the tool path is assumed to be circular which differs from reality where tool paths of milling cutters are trochoidal. While this leads to differences in chip thickness, at small feeds, this difference becomes negligible [Bao et al. 2000]. The time delay at each spindle speed iteration was assumed to be constant, when in reality, imprecise tool geometry and errors in spindle speeds can cause deviations in the time delay. These assumptions may cause small errors when predicting chatter stability lobes.

6.3.2 Limitations

Using a combination of the Edge theorem and Zero Exclusion condition was shown to be a much more efficient and faster method when compared to the LMI approach. In general, the geometric computations needed are much simpler to perform as opposed to the convex optimization calculations needed to find Lyapunov matrices. One option to address this issue is to utilize more powerful computer hardware; however this would be expensive and may only be feasible in the future if further advancements in computing technology are made. The Edge theorem approach does have minor limitations when the uncertainty intervals considered are relatively large, which may render the straight edge approximation of the value set to be insufficient. This may be overcome with adjustments in modeling. At the expense of increased computational time, more uncertain parameters could be taken to widen the edge boundaries to encompass more of the value set [Bhattacharyya et al. 1995]. Alternatively, modeling of chatter

processes could be modified. For example, considering ploughing and shearing effects separately may lessen the uncertainty in cutting coefficient values.

Increase computational time is the primary limitation of using a robust approach. Total computational time depends upon the robust method used, number of uncertain parameters considered, the extent of spindle speed range required and extent of uncertainty intervals. Especially concerning the LMI formulation, depending upon the number of vibrational modes considered and the order of the Pade approximation, optimization may have to be performed over very large matrices. Finding Lyapunov matrices in general is a challenge which requires significant computational resources to solve. However, computing chatter stability lobes would be performed prior to the actual machining operation and therefore only needs to be sufficiently fast enough. In modern manufacturing, greater amounts of time are spent in pre-process planning and optimization stages. With prior knowledge of operation, the full range of chatter lobes are often not required and therefore spindle speed ranges can be restricted to further shorten the overall simulation time. The convex optimization and bisection methods may also introduce numerical errors in the robust stability lobe calculations, since they converge to an optimal value only to within a specified tolerance. Depending upon the desired precision, convergence accuracy and computational time will be inversely affected.

While robust methods can be used to ensure chatter stability, most robust stability theories are subject to a certain degree of conservatism. While this can naturally benefit a chatter stability prediction, care must be taken to avoid excess conservatism. As observed with the quadratic stability case, conservatism can depend upon the robust model selected. The number of uncertain parameters and the width of the uncertainty intervals are also important considerations as robust stability may give a prediction which is much lower than the critical depth with

additional computational time. Consideration of the number of uncertain parameters and the parameters themselves is a critical feature of uncertainty modeling. Accurate identification of the parameter and parameter variation bounds are needed to facilitate appropriate uncertainty modeling. This can require expensive sensors, such as dynamometers and impact hammers, which may not be available in real manufacturing environments. In addition, it may be difficult or time consuming to identify extreme parameter bounds, especially considering that chatter stability lobes are not unique for a given machine. Dynamic parameters can differ depending upon the type of machine, type of cutting tool, and tool-workpiece setup [Merritt 1965, Budak 2006].

A certain level of knowledge and sufficiency is required to interpret results and implement in robust stability models. In general, in order to implement in a practical system, one must consider a balance between appropriate model complexity and conservatism with available computational resources and practical requirements. The objectives of the robust methods presented are to ensure system stability for all possible values of the uncertain parameters. Alternative control approaches to avoiding chatter while considering uncertainties have been investigated. These either include a probabilistic robust modelling approach or implementing an adaptive procedure.

For some applications, determining definite bounds on the uncertain parameters may not be feasible or meaningful. Alternatively, uncertain systems can be modelled using a probabilistic approach where uncertain parameters have associated probability density functions, which can be a more realistic description [Tempo et al. 2013]. The central difficulty with applying a probabilistic method to a real system is identifying the probability density functions. This requires a large number of time consuming experimental tests to be performed in order to find a

statistical distribution that matches the occurrence of a given uncertain parameter. In addition, the extent these methods would only ensure robust stability for most uncertain parameter values; there would be a small risk that uncertainty may lie outside the measure of probability used.

Prediction of chatter stability lobe diagrams is an offline approach, performed prior to the actual milling operation; however, many researchers have investigated alternative active methods of eliminating chatter in the presence of uncertainties that are performed during the operation. Utilizing sensors to detect the occurrence of chatter in real time, an adaptive control approach can be used to either eliminate chatter using actuators and active dampers, or avoid chatter by adjusting machining parameters to shift the process towards stable cutting regions [Altintas et al. 2004]. In micro milling, the micro sized features makes adaptive techniques challenging to implement due to the difficulty in sensing changes in the cutting conditions, and often additional equipment is needed facilitate an adaptive approach [Chae et al. 2006]. Sensor and signal processing requirements, and the dynamic bandwidth of control loop, are also important considerations is the response time of adaptive feedback loops. If the latency of the response is too slow after chatter is detected, damage to machine or tool will result, rendering the technique useless [Quintana et al. 2011]. An experimental analysis of the machine-tool setup is still required to implement adaptive techniques, which can be time consuming. Due to these disadvantages, predicting stability lobe diagrams has remained a prominent approach to chatter avoidance.

6.4 Future Works

While considering uncertain parameters other than the natural frequency, damping ratios, and cutting coefficients could potentially guarantee stability for micro milling operations, there is still many much work to be done. While this study mainly focussed on the effects of three

uncertain parameters, the robust methods presented could be extended to include other parameters which were neglected. Stiffness can also change at high spindle speeds and in addition the time delay between flutes can also vary due to non exact spindle speeds and geometrical inaccuracies of the cutting tool.

While this study employed methods to deliberately introduce parameter uncertainties which could be quantified, identifying parameter variations due to specific effects is more challenging. Investigation into how parameter variations due to nonlinear behaviour, such as material behaviour during chip formation, and thermal effects affect chatter stability could also be performed. Finding experimental methods to either identify uncertainties of these more complex processes or simplify current time consuming methods of parameter identification may also be warranted.

The issues of computational time and conservatism could be addressed by investigation into either different robust models or computer software. The LMI formulations could be extended to include the delay term directly without a Pade approximation. LMI stability theories exist which are applicable to state space formulations of time delay systems, where the most recent research in this area involves Lyapunov-Krasovskii theory [Xu et al. 2008]. Such LMI formulations can also be solved using convex optimization techniques, however, their applicability to the chatter problem and issues of conservatism would need to be investigated.

REFERENCES

Abele, E., Altintas, Y., Brecher, C., 2010, "Machine tool spindle units", CIRP Annals - Manufacturing Technology, Vol. 59, pp. 781-802.

Abele, E., Fiedler, U., Versch, A., Kreis, M., Weigold, M., 2003, "Online process monitoring vs. offline chatter prediction - possibilities of process stabilization in machining", Proceedings of IMECE'03 ASME International Mechanical Engineering Congress & Exposition, Washington, D.C., November.

Altintas, Y., 2012, "Manufacturing automation: Metal cutting mechanics, machine tool vibrations, and CNC design", Cambridge University Press, New York.

Altintas, Y., Verl, A., Brecher, C., Uriarte, L., Pritschowm G., 2011, "Machine tool feed drives", CIRP Annals - Manufacturing Technology, Vol. 60, pp. 779-796.

Altintas, Y., Eynian, M., Ozozuka, H., 2008, "Identification of dynamic cutting force coefficients and chatter stability with process damping", CIRP Annals, Vol. 57, pp. 371-374.

Altintas, Y., Weck, M., 2004, "Chatter stability of metal cutting and grinding", Annals of the CIRP, Vol. 53(2), pp. 619-642.

Altintas, Y., Shamoto, E., Lee, P., Budak, E., 1999, "Analytical prediction of stability lobes in ball end milling", Transactions of the ASME, Vol. 121, pp. 586-592.

Altintas, Y., Budak, E., 1995, "Analytical prediction of stability lobes in milling", CIRP Annals - Manufacturing Technology, Vol. 44(1), pp. 357-362.

Baker, G. A., Graves-Morris, P., 1996, "Pade approximants", 2nd Edition, Cambridge University Press, New York.

Bao, W. Y., Tansel, I. N., 2000, "Modeling micro-end-milling operations. Part I: analytical cutting force model", International Journal of Machine Tools and Manufacture, Vol. 40, pp. 2155-2173.

Barmish, B.R., 1994, "New tools for robustness of linear systems", MacMilllan Publishing Company, New York, USA.

Barmish, B.R., 1989, "A generalization of Kharitonov's four-polynomial concept for robust stability problems with linearly dependent coefficient perturbations", IEEE Automatic Control, Vol. 34 (2), pp. 157-165.

Barmish, B. R., DeMarco, C. L., 1986, "A new method for improvement of robustness bounds for linear state equations", Proceedings of the Princeton Conf. Inform. Sci. Sys.

Bartlett, A. C., Hollot, C. V., Lin, H., 1987, "Root locations of an entire polytope of polynomials: It suffices to check the edges", American Control Conference, pp. 1611-1616.

Bhattacharyya, S.P., Chapellat, H., Keel, L.H., 1995, "Robust control - The parametric approach", Prentice Hall, Inc.

Boyd, S., Vandenberghe, L., 2004, "Convex optimization", Cambridge University Press, New York.

Boyd, S. El Ghaoui, L., Feron, E., Balakrishnan, V., 1994, "Linear matrix inequalities on system and control theory", Society for Industrial and Applied Mathematics, Pennsylvania.

Budak, E., Tunc, L. T., Alan, S., Ozguven, H. N., 2012, "Prediction of workpiece dynamics and its effects on chatter stability in milling", CIRP Annals - Manufacturing Technology, Vol. 61, pp. 339-342.

Budak, E., Tunc, L. T., 2010, “Identification and modeling of process damping in turning and milling using a new approach”, CIRP Annals - Manufacturing Technology, Vol. 59, pp. 403-408.

Budak, E., 2006, “Analytical models for high performance milling. Part I: Cutting forces, structural deformations and tolerance integrity”, International Journal of Machine Tools & Manufacture, Vol. 46, pp. 1478-1488.

Budak, E., 2006, “Analytical models for high performance milling. Part II: process dynamics and stability”, International Journal of Machine Tools and Manufacture, Vol. 46, pp. 1489-1499.

Calafiore, G. C., Dabbene, F., Tempo, R., 2011, “Research on probabilistic methods for control system design”, Automatica, Vol. 47, pp. 1279-1293.

Campa, F. J., Lopez de Lacalle, L., N., Celaya, A., 2011, “Chatter avoidance in the milling of thin floors with bull nosed end mills: Model and stability diagrams”, International Journal of Machine Tools and Manufacture, Vol. 51, pp. 43-53.

Cao, H., Li, B., He, Z., 2012, “Chatter stability of milling with speed varying dynamics of spindles”, International Journal of Machine Tools & Manufacture, Vol. 52, pp. 50-58.

Chae, J., Park, S. S., 2007, “High frequency bandwidth measurements of micro cutting forces”, International Journal of Machine Tools & Manufacture, Vol. 47, pp. 1433-1441.

Chae, J., Park, S. S., Freiheit, T., 2006, “Investigation of micro-cutting operations”, International Journal of machine tools & manufacture”, Vol. 46, pp. 313-332.

Chen, Y., Dong, F., 2012, “Robot machining: recent developments and future research issues”, Int. J. Adv. Manuf. Technol., pp. 1-9.

Childs, T. H. C., 2006, “Friction modelling in metal cutting”, Wear, Vol. 260, pp. 310-318.

CVX Research, Inc. CVX: MATLAB software for disciplined convex programming, version 2.0 beta.

Dasgupta, S., Chockalingam, G., Anderson, B. D. O., Fu, M., 1994, “Lyapunov functions for uncertain systems with applications to the stability of time varying systems”, IEEE Transactions on Circuits and Systems, Vol. 41, pp. 93-106.

Davis, J. R., 2001, “Copper and copper alloys”, ASM International, USA.

Duncan, G. Scott, et al., 2006, “Uncertainty propagation for selected analytical milling stability limit analyses”, Transactions of NAMRI/SME, Vol. 34.1 pp. 17-24.

Filiz, S., Conley, C. M., Wasserman, M. B., Ozdoganlar, O. B., 2007, “An experimental investigation of micro-machinability of copper 101 using tungsten carbide micro-end mills”, International Journal of Machine Tools and Manufacture, Vol. 47, pp. 1088-1100.

Francesco, A., 2006, “Robust control of linear systems subject to uncertain time varying parameters”, Spinger Berlin Heidelberg.

Franklin, G. F., Powell, J. D., Emami-Naein, A., 2002, “Feedback control of dynamic systems”, 4th Ed., Prentice Hall, Upper Saddle River, New Jersey.

Friedland, B., 1986, “Control system design: an introduction to state space methods”, McGraw-Hill, New York.

Fu, M., Olbrot, A. W., Polis, M. P., 1989, “Introduction to the parametric approach to robust stability”, IEEE Control Systems Magazine, pp. 7-11.

Fu, M. Y., Olbrot, A. W., Polis, M. P., 1989, “Robust stability for time-delay system: the edge theorem and graphical tests”, IEEE Automatic Control, Vol. 34(2), pp.813–820.

Gahinet, P., Apkarian, P., Chilali, M., 1996, "Affine parameter dependent lyapunov functions and real parametric uncertainty", IEEE Trans. of Automatic Control, Vol. 41, pp. 436-442.

Garcia, P., Rivera, S., Palacios, M., Belzunce, 2010, "Comparative study of the parameters influencing the machinability of leaded brasses", Engineering Failure Analysis, Vol. 17, pp. 771-776.

Gonzalo, O., Beristain, J., Jauregi, H., Sanz, C., 2010, "A method for the identification of the specific forces coefficients for mechanistic milling simulation", International Journal of Machine Tools and Manufacture, Vol. 50, pp. 765-774.

Grant, M., Boyd, S., 2008, "Graph implementations for nonsmooth convex programs, Recent advances in learning and control (a tribute to M. Vidyasagar)", Lecture Notes in Control and Information Sciences, Springer, pp. 95-110.

Grman, L., Rosinova, D., Kozakova, A., Vesely, V., 2003, "Robust stability conditions for polytopic systems", Int. J. Syst. Sci., Vol. 36, pp. 961-973.

Gunduz, A., Dreyer, J. T., Singh, R., 2012, "Effect of bearing preloads on the modal characteristics of a shaft-bearing assembly: Experiments on a double row angular contact ball bearings", Mechanical Systems and Signal Processing, Vol. 31, pp. 176-195.

Han, D., Ding, Y., Zhu, L., 2012, "On time-domain methods for milling stability analysis", Chinese Science Bulletin, Vol. 57, pp. 4336-4345.

Henrion, D., Arzelier, D., Peaucelle, D., Sebak, M., 2001, "An LMI condition for robust stability of polynomial matrix polytopes", Automatica, Vol. 37, pp. 461-468.

Horisberger, H. P., Belanger, P. R., 1976, "Regulators for linear, time invariant plants with uncertain parameters", Automatic Control, IEEE Transactions, Vol. 21, pp.705-708.

Huo, D., Cheng, K., 2009, "Machining dynamics", Springer Series in Advanced Manufacturing, London.

Jorgensen, B.R., Shin, Y.C., 1998, "Dynamics of spindle-bearing systems at high speeds including cutting load effects", ASME Journal of Manufacturing Science and Engineering, Vol. 120, pp. 387-394.

Kappmeyer, G., Hubig, C., Hardy, M., Witty, M., Busch, M., 2012, "Modern machining of advanced aerospace alloys - enabler for quality and performance", Procedia CIRP, Vol. 1, pp. 28-43.

Kharitonov, V.L., 1979, "Asymptotic stability of an equilibrium position of a family of systems of linear differential equations", Differential Equations, Vol. 14, pp. 1483–1485.

Kuljanic, E., Sortino, M., Totis, G., 2008, "Multisensor approaches for chatter detection in milling", Journal of Sound and Vibration, Vol. 312, pp. 672-693.

Lesaja, G., 2009, "Introducing interior point methods for introductory operations research courses and/or linear programming courses", The Open Operational Research Journal, Vol. 3, pp. 1-12.

Li, K. M., Liang, Y., 2007, "Modeling of cutting forces in near dry machining under tool wear effect", International Journal of Machine Tools & Manufacture, Vol. 47, pp. 1292-1301.

Malekian, M., Park, S.S., Jun, M., 2009, "Modeling of dynamic micro-milling cutting forces", International Journal of Machine Tools and Manufacture, Vol. 49(7-8), pp. 586-598.

Mascardelli, B., A., Park, S. S., Freiheit, T., 2008, "Substructure coupling of microend mills to aid in the suppression of chatter", Journal of Manufacturing Science and Engineering, Vol. 130, pp. pp. 011010-1-12.

Matusu, R., Prokop, R., 2011, “Graphical analysis of robust stability for systems with parametric uncertainty: An overview”, Transactions of the Institute of Measurement and Control, Vol. 33, pp. 274-290.

Mayr, J., Jedrzejewski, J., Uhlmann, E., Donmez, M. A., Knapp, W., Hartig, F., Wendt, K., Moriwaki, T., Shore, P., Schmitt, R., Brechner, C., Wurz, T., Wegener, K., 2012, “Thermal issues in machine tools”, CIRP Annals - Manufacturing Technology, Vol. 61, pp. 771-791.

Merchant, M. E. 1945, “Mechanics of the metal cutting process. II. Plasticity conditions in orthogonal cutting”, Journal of applied physics, Vol. 16.6, pp. 318-324.

Merritt, H. E., 1965, “Theory of self-excited machine tool chatter”, Transaction of ASME Journal of Engineering Industry, Vol. 87, pp. 447-454.

Mian, A. J., Driver, N., Mativenga, P. T., 2009, “Micromachining of coarse-grained multi-phase material”, Proceedings of the Institution of Mechanical Engineers, Part B (Journal of Engineering Manufacture), Vol. 223, pp. 377-385.

Montagner, V. F., Peres, P. L. D., 2004, “Robust stability and H_∞ performance of linear time-varying systems in polytopic domains”, Int. J. Control, Vol. 77, pp. 1343-135.

Montagner, V. F., Peres, P. L. D., 2003, “A new LMI condition for the robust stability of linear time varying systems”, Proceedings of the 42nd IEEE Conference on Decision and Control, pp. 6133-6138.

Movahhedy, R., Gerami, J. M., 2006, “Prediction of spindle dynamics in milling by sub-structure coupling”, International Journal of Machine Tools & Manufacture, Vol. 46, pp. 243-251.

Movahhedy, M. R., Mosaddegh, P., 2006, “Prediction of chatter in high speed milling including gyroscopic effects”, Int. J. Mach. Tool Manu., Vol. 46(9), pp. 996-1001.

Neto, A. T., 1999, “Parameter dependent lyapunov functions for a class of uncertain linear systems: an LMI approach”, Proc. of the 38th Conference on Decision and Control, Vol. 3, 2341-2346.

Opitz, H., 1969, “Investigation and calculation of the chatter behaviour of lathes and milling machines”, Annals of the CIRP, Vol. 18, pp. 335-343.

Ostertag, E., 2011, “Mono and multivariable control and estimation linear, quadratic and LMI methods”, Springer-Verlag Berlin Heidelberg.

Park, S. S., Rahnama, R., 2010, “Robust chatter stability in micro-milling operations”, CIRP Annals - Manufacturing Technology, Vol.59, pp. 391-394.

Park, S. S., Malekian, M., 2009, “Mechanistic modeling and accurate measurement of micro end milling forces”, CIRP Annals - Manufacturing Technology, Vol. 58(1), pp. 49-52.

Park, S. S., Qin, Y. M., 2007, “Robust regenerative chatter stability in machine tools”, Int. J. Adv. Manuf. Tech., Vol. 33, pp. 389-403.

Park, S. S., Altintas, Y., Movahhedy, M., 2003, “Receptance coupling for end mills”, International Journal of Machine Tools & Manufacture, Vol. 4, pp. 889–896.

Popov, K. B., Dimov, S. S., Pham, D. T., Minez, R. M., Rosochowski, A., Olejnik, L., 2006, “Micromilling: Material microstructure effects”, Proceedings of the Institution of Mechanical Engineers, Part B: Journal of Engineering Materials, Vol. 220, pp. 1807-1813.

Quintana, G., Ciurana, J., 2011, “Chatter in machining processes: A review”, Int. J. Mach. Tool Manu., Vol. 51, pp. 363-376.

Quintana, G., Campa, F. J., Ciurana, J., Lopez de Lacalle, L. N., 2010, “Productivity improvement through chatter-free milling in workshops”, Proceedings of the Institution

of Mechanical Engineers, Part B: Journal of Engineering Manufacture, Vol. 225, pp. 1163-1174.
Rahnama, R., Sajjadi, M., Park, S. S., 2009, "Chatter suppression in micro end milling with process damping", Journal of Materials Processing Technology, Vol. 209, pp. 5766-5776.
Ramos, D. C. W., Peres, P. L. D., 2002, "An LMI condition for the robust stability of uncertain continuous time linear systems", IEEE T. Automat. Contr., Vol. 47(4), pp. 675-678.
Richard, J. P., 2003, "Time-delay systems: An overview of some recent advances and open problems", Automatica, Vol. 39, pp. 1667-1694.
Safonov, M. G., 2012, "Origins of robust control: Early history and future speculations", Annual Reviews in Control, Vol. 36, pp. 173-181.
Shamoto, E., Akazawam K., 2009, "Analytical prediction of chatter stability in ball end milling with tool inclination", CIRP Annals - Manufacturing Technology, Vol. 58, pp. 351-354.
Schmitz, T. L., Smith, K. S., 2009, "Machining dynamics: Frequency response to improved productivity", Springer. New York.
Shi, Y., Mahr, F., Wagner, U., Uhlmann, E., 2012, "Chatter frequencies of micromilling processes: Influencing factors and online detection via piezoactuators", International Journal of Machine Tools and Manufacture, Vol. 56, pp. 10-16.
Shin, Y.C., 1992, "Bearing nonlinearity and stability analysis in high speed machining", Journal of Engineering for Industry, Translations of the ASME, Vol. 114, pp. 23-30.
Stepan, G., 2001, "Modeling nonlinear regenerative effects in metal cutting", Philosophical Transaction of the Royal Society A, Vol. 359, pp. 739-757.
Tempo, R., Calafiore, G., Dabbene, F., 2013, "Randomized algorithms for analysis and control of uncertain systems", Springer London, pp. 71-91.
Teti, R., Jemielniak, K., O'Donnell, G., Dornfeld, D., 2010, "Advanced monitoring of machining operations", CIRP Annals - Manufacturing Technology, Vol. 59, pp. 717-739.
Tlusty, J., 2000, "Manufacturing processes and equipment", Prentice Hall. New York.
Tlusty, J., 1993, "High speed machining", CIRP Annals, Vol. 42, pp. 733-737.
Tlusty, J. 1978, "Analysis of the state of research in cutting dynamics", Annals of the CIRP Vol. 27.2, pp. 583-589.
Tlusty, J., MacNeil, P., 1975, "Dynamics of cutting forces in end milling", Annals of the CIRP, Vol. 24(1), pp. 21-25.
Tlusty, J., Polacek, M., 1963, "Stability of machine tool against self-excited vibration in machining", International Production Engineering Research Conference Proceedings, pp. 465-474.
Tobias, S. A., Fishwick, W., 1958, "Theory of regenerative machine tool chatter", The Engineer, Vol. 205, pp.199-203.
van Dijk, N. J. M., Doppenberg, E. J. J., Faasen, R. P. H., van de Wouw, N., Oosterling, J. A. J., Nijmeijer, H., 2010, "Automatic in-process chatter avoidance in the high speed milling process", Journal of Dynamic Systems, Measurement, and Control, Vol. 132, pp. 031006-1-14.
Vogler, M. P., Kapoor, S. G., DeVor, R. E., 2004, "On the modeling and analysis of machining performance in micro end milling, Part II: Cutting force prediction", Journal of Manufacturing Science and Engineering Transactions of the ASME, Vol. 126, pp. 695-705.

Vollertsen, F., Biermann, D., Hansen, H. N., Jawahir, I. S., Kuzman, K., 2009, "Size effects in manufacturing of metallic components", CIRP Annals - Manufacturing technology, Vol. 58, pp. 566-587.

Wiercigroch, M., Budak, E., 2001, "Sources of nonlinearities, chatter generation and suppression in metal cutting", Phil. Trans. R. Soc. Lond. A, Vol. 359, pp. 663-693.

Xiong, G. L., Yi, J. M., Zeng, C., Guo, H. K., Li, L. X., 2003, "Study on the gyroscopic effect of the spindle on the stability characteristics of the milling system", Journal of Materials Processing Technology, Vol. 138, pp.379-384.

Xu, S., Lam, J., 2008, "A survey of linear matrix inequality techniques in stability analysis of delay systems", International Journal of Systems Science, Vol. 39, pp. 1095-1113.

APPENDIX A. ROBUST 2-DOF CHATTER

A1. Main Matlab™ code for Robust Stability

```
%written by Eldon Graham - Main robust code for all methods
%Define parameters and uncertainties. Calculates and plots robust stability
%lobes using a parallel programming structure
clc;
clear all;
tic
%%%%%%%%%%%%%%%%%%%%        Define        Parameters        and        Uncertainties
%%%%%%%%%%%%%%%%%%%%%%
N=2;            % number of teeth
imm=3;          %define immersion condition
%Start and exit immersion angles according to the type of Immersion
if imm==1       %Half Immersion Down Milling
    phiex=pi;
    phist=pi/2;
elseif imm==2       %Half Immersion Up Milling
    phiex=pi/2;
    phist=0;
elseif imm==3       %Slotting
    phiex=pi;
    phist=0;
end

%system dynamics in x direction
fnx=[3722 4115.6 4990.5 5934]';       %natural frequency [Hz]
wnx=2*pi*fnx;                          %natural frequency [rad/s]
zetax=[0.009 0.024 0.064 0.022]';      %damping ratio
kx=[8.01e7 3.3e7 5.6e6 5.2e6]'*0.001;      %system stiffness [N/m]
%System dynamics in y direction
fny=[3722 4115.6 4990.5 5934]';
wny=2*pi*fny;
zetay=[0.009 0.024 0.064 0.022]';
ky=[8.01e7 3.3e7 5.6e6 5.2e6]'*0.001;

%Cutting Constants
Ktc=4203;       %tangential cutting coefficient [N/mm^2]
Krc=1482.5;      %radial cutting coefficient [N/mm^2]
Kr=Krc/Ktc;      %ratio of radial to tangential cutting coefficients

%percent error in paramters (must be same size as parameter vectors
deltawnxmax=0.031;
deltawnxmin=0.031;
deltawnymax=0.05;
deltawnymin=0.05;
deltazetaxmax=0.16;
deltazetaxmin=0.16;
deltazetaymax=0.106;
deltazetaymin=0.106;
deltaKtcmax=0.215;
deltaKtcmin=0.19;
deltaKrcmax=0.233;
deltaKrcmin=0.22;
```

```
%Define min/max parameters to fall within given interval
%first row=min value 2nd row=max value
wnx=[wnx.*(1-deltawnxmin) wnx.*(1+deltawnxmax) wnx];
wny=[wny.*(1-deltawnymin) wny.*(1+deltawnymax) wny];
zetax=[zetax.*(1-deltazetaxmin) zetax.*(1+deltazetaxmax) zetax];
zetay=[zetay.*(1-deltazetaymin) zetay.*(1+deltazetaymax) zetay];
Ktc=[Ktc*(1-deltaKtcmin) Ktc*(1+deltaKtcmax) Ktc];
Krc=[Krc*(1-deltaKrcmin) Krc*(1+deltaKrcmax) Krc];
Krmin=Krc(1)/Ktc(1);
Krmax=Krc(2)/Ktc(2);
alph=alpha(phist,phiex,Kr);
alphmax=alpha(phist,phiex,Krmax);
alphmin=alpha(phist,phiex,Krmin);
%%%%%%%%%%%%%%%%%%%%%%%%%%%%%%%%%%%%%%%%%%%%%%%%%%%%%
%%%%%%%%%%%%%%%%%

%%%%%%%%%%%%%%%%%%%%%Defined variables for LMI
Approach%%%%%%%%%%%%%%%%%%
%extreme state space matrices of dynamics
[A,B,C,D]=dynamicstf(wnx(:,3),zetax(:,3),kx,wny(:,3),zetay(:,3),ky,alph);
[A1,B1,C1,D1]=dynamicstf(wnx(:,2),zetax(:,2),kx,wny(:,2),zetay(:,2),ky,alphmax);
[A2,B2,C2,D2]=dynamicstf(wnx(:,2),zetax(:,1),kx,wny(:,2),zetay(:,1),ky,alphmax);
[A3,B3,C3,D3]=dynamicstf(wnx(:,1),zetax(:,2),kx,wny(:,1),zetay(:,2),ky,alphmax);
[A4,B4,C4,D4]=dynamicstf(wnx(:,1),zetax(:,1),kx,wny(:,1),zetay(:,1),ky,alphmax);
[A5,B5,C5,D5]=dynamicstf(wnx(:,2),zetax(:,2),kx,wny(:,2),zetay(:,2),ky,alphmin);
[A6,B6,C6,D6]=dynamicstf(wnx(:,2),zetax(:,1),kx,wny(:,2),zetay(:,1),ky,alphmin);
[A7,B7,C7,D7]=dynamicstf(wnx(:,1),zetax(:,2),kx,wny(:,1),zetay(:,2),ky,alphmin);
[A8,B8,C8,D8]=dynamicstf(wnx(:,1),zetax(:,1),kx,wny(:,1),zetay(:,1),ky,alphmin);
%%%%%%%%%%%%%%%%%%%%%%%%%%%%%%%%%%%%%%%%%%%%%%
%load functions needed for CVX toolbox
%CVX Research, Inc. CVX: MATLAB software for disciplined convex
%programming, version 2.0 beta.
%Grant, M., Boyd, S., 2008, "Graph Implementations for Nonsmooth Convex
%Programs, Recent Advances in Learning and Control (a tribute to M.
%Vidyasagar)", Lecture Notes in Control and Information Sciences,
%Springer, pp. 95-110.
addpath('cvx')
cvx_setup
%%%%%%%%%%%%%%%%%%%%%%%%%%%%%%%%%%%%%%%%%%%%%%
%%%%%%%%%%%%%%%%%%%%%%%%%%%%%%%%%%%%%%%%%%%%%%%%%%%%%
%%%%%%%%%%%%%%%%%%

%%%%%%%%%%%%%%%%%%Defined variables for Edge
Theorem%%%%%%%%%%%%%%%%%%%%
w=[100:40850];   %define range of chatter frequencies [rad/s]
M=length(w);
r=3;        %number of uncertain parameters
%Initialize matrices to zero to save computational time
P=zeros(M,2^r);X=zeros(M,2^r);Y=zeros(M,2^r);
judge=zeros(1,M);
%%%%%%%%%%%%%%%%%%%%%%%%%%%%%%%%%%%%%%%%%%%%%%%%%%%%%
%%%%%%%%%%%%%%%%%

%%%%%%%%General Algorithm for finding robust stability lobes%%%%%%%%%%%%
%spindle speed range
nn=33000:250:50750;
```

```
L=length(nn);
q=1;aa=zeros(L,1);
for n=1:L
   %time delay [sec]
   T=60/(N*nn(n));
   %Pade approximation of delay term
   ord=padeorder(max(max(wnx)),T);
   Ad=zeros(2*ord);Bd=zeros(2*ord,2);Cd=zeros(2,2*ord);Dd=zeros(2);
   [num_delay, den_delay]=pade(T,ord);
   [Adel,Bdel,Cdel,Ddel]=ssdata(balreal(ss(tf(num_delay,den_delay))));
   Ad(1:ord,1:ord)=Adel; Ad(ord+1:2*ord,ord+1:2*ord)=Adel;
   Bd(1:ord,1)=Bdel; Bd(ord+1:2*ord,2)=Bdel;
   Cd(1,1:ord)=Cdel; Cd(2,ord+1:2*ord)=Cdel;
   Dd(1,1)=Ddel; Dd(2,2)=Ddel;

   %initial guesses for bisection algorithm
   a_min=0;    % upper depth [mm]
   a_max=0.25;   %lower depth [mm]
   while a_max-a_min>0.001     %find upper bound
      a=(a_max+a_min)/2;
      AA=[A+0.25*(1/pi)*N*a*Ktc(3)*B*(eye(length(Dd))-Dd)*C -0.25*(1/pi)*N*a*Ktc(3)*B*Cd; Bd*C Ad];
      e=eig(AA);
      if real(e)<0
         a_min=a;
      else
         a_max=a;
      end
   end
   a2=a_min;
   %find lower bound
   stability=0;
   while stability==0
      a=0.9*a2;
      %%%%%%%%%%%%%%%%%%%%%%%%%%%
      %Call robust method
      %Edge theorem and Zero exclusion
      Edge_3Parameters;
      %Quadratic stability for time invariant parameters with common
      %Lyapunov function

      %QS_LMI;

      %Quadratic stability for time invariant parameters with parameter
      %dependent Lyapunv functions

      %TIPDQS_LMI;

      %Quadratic stability for time varying parameters with parameter
      %dependent Lyapunv functions

      %TVPDQS_LMI;
      %%%%%%%%%%%%%%%%%%%%%%%%%%%
      if b==1         % stable case
         stability=1;
      elseif b==0        % unstable case
         a2=a;
```

```
        end
    end
    %find robust boundary
    a_min=a;
    a_max=a2;
    while a_max-a_min>0.001
        a=(a_max+a_min)/2;
        %%%%%%%%%%%%%%%%%%%%%%%%%%%%%
        %Call robust method
        %Edge theorem and Zero exclusion
        Edge_3Parameters;
        %Quadratic stability for time invariant parameters with common
        %Lyapunov function

        %QS_LMI;

        %Quadratic stability for time invariant parameters with parameter
        %dependent Lyapunv functions

        %TIPDQS_LMI;

        %Quadratic stability for time varying parameters with parameter
        %dependent Lyapunv functions

        %TVPDQS_LMI;
        %%%%%%%%%%%%%%%%%%%%%%%%%%%
        if b==1          % stable case
            a_min = a;
        elseif b==0       % unstable case
            a_max = a;
        end
    end    % End of cut depth
    aa(q)=a_min;
    q=q+1;
    disp('Depth of cut:');disp(a_min);
end
%%%%%%%%%%%%%%%%%%%%%%%%%%%%%%%%%%%%%%%%%%%%%%%%%%%%%%%%%%%
%%%%%%%%%%%%%%%%%%%%
%Plot stability lobe diagram
figure;hold on;
Line1=plot(nn,aaa*1000,'--r');
set(Line1,'LineWidth',2.5);
axis([33000 50000 0 250]);
xlabel('Spindle Speed [rev/min]');
ylabel('a_l_i_m [\mum]');
toc
```

A2. Subfunction for Characteristic Polynomial

```
function P=polyE(A,w,alim,T,wnx,zetax,kx,wny,zetay,ky,N,Ktc)
%written by Eldon Graham
%evaluates extreme polynomials for eigenvalue equation in 2-DOF milling
%chatter stability
LX=length(wnx);
LY=length(wny);
WW=length(w);
s=sqrt(-1).*w;
```

```
%define eigenvalues
E = -N*alim*Ktc*(1-exp(-s.*T))/(4*pi);

%define transfer functions for multiple modes
Ixx=zeros(1,WW);Iyy=zeros(1,WW);
IX=zeros(LX,WW);IY=zeros(LY,WW);
for k=1:LX      %x direction
   IX(k,:)=((wnx(k).^2)./kx(k))./(s.^2+2*zetax(k)*wnx(k).*s+wnx(k)^2);
   Ixx=Ixx+IX(k,:);
end
for j=1:LY      %y direction
   IY(j,:)=((wny(j).^2)./ky(j))./(s.^2+2*zetay(j)*wny(j).*s+wny(j).^2);
   Iyy=Iyy+IY(j,:);
end
%define dominant mode of y direction transfer function
Iyden1=s.^2+2*zetay(4)*wny(4).*s+wny(4).^2;

%coefficients
a0=(Ixx).*(Iyy)*(A(1)*A(4)-A(2)*A(3));
a1=(A(1)*Ixx)+(A(4)*Iyy);

%eigenvalue equation
P=Iyden1.*(a0.*E.^2+a1.*E+1);
```

A3. Subfunction for Directional Factors

```
function A=alpha(phist,phiex,Kr)
%written by Eldon Graham
%computes matrix of directional cutting coefficients for 2-DOF milling
%chatter stability

axx_ex = 1/2*(cos(2*phiex)-2*Kr*phiex+Kr*sin(2*phiex));
axx_st = 1/2*(cos(2*phist)-2*Kr*phist+Kr*sin(2*phist));
axx = axx_ex-axx_st;

axy_ex = 1/2*(-sin(2*phiex)-2*phiex+Kr*cos(2*phiex));
axy_st = 1/2*(-sin(2*phist)-2*phist+Kr*cos(2*phist));
axy = axy_ex-axy_st;

ayx_ex = 1/2*(-sin(2*phiex)+2*phiex+Kr*cos(2*phiex));
ayx_st = 1/2*(-sin(2*phist)+2*phist+Kr*cos(2*phist));
ayx = ayx_ex-ayx_st;

ayy_ex = 1/2*(-cos(2*phiex)-2*Kr*phiex-Kr*sin(2*phiex));
ayy_st = 1/2*(-cos(2*phist)-2*Kr*phist-Kr*sin(2*phist));
ayy = ayy_ex-ayy_st;

A=[axx; axy; ayx; ayy];
```

A4. Subfunction for order of Pade Approximation

```
function [ord,num,den]=padeorder(wn,T)
%written by Eldon Graham
%calculates sufficient pade order to approximate delay for given
%Eigen frequency [rad/s] and delay
%matches phase at natural frequency within a given error
perc=0.005;
```

```
wn=round(wn*1000000)/1000000;
j=sqrt(-1);
ord=0;
w=0:round(2*wn);
G=exp(-j*w*T);
phase=unwrap(atan2(imag(G),real(G)));
phase=round(phase.*1000000)./1000000;

f=find(w<=wn);
f=f(length(f));
for ii=1:40
   [num,den]=pade(T,ii);
   [Mag phs W] = bode(num,den,w);
   phs=phs*pi/180;
   phs=phs-max(phs);
   phs=round(phs.*1000000)./1000000;

   if phase(f)>phs(f)*(1+perc) && phase(f)<phs(f)*(1-perc)
      ord=ii+1; %add 1 to order to be safe
      break;
   end
end
[num,den]=pade(T,ord);
```

A5. Subfunction for State Space Matrices of Dynamics

```
function [A,B,C,D]=dynamicstf(wnx,zetax,kx,wny,zetay,ky,alph)
%written by Eldon Graham
%Define state space model. Input parameters must be column vectors
Lx=length(wnx);Ly=length(wny);
Ax=zeros(2*Lx,2*Lx);
Bx=zeros(2*Lx,2);
Cx=zeros(2,2*Lx);
Ay=zeros(2*Ly,2*Ly);
By=zeros(2*Ly,2);
Cy=zeros(2,2*Ly);
for i=1:Lx
ax=[0 1; -wnx(i)^2 -2*zetax(i)*wnx(i)];
bx=[0 0; alph(1)*(wnx(i)^2)/kx(i) alph(2)*(wnx(i)^2)/kx(i)];
cx=[1 0;0 0];

Ax(2*i-1:2*i,2*i-1:2*i)=ax;
Bx(2*i-1:2*i,:)=bx;
Cx(:,2*i-1:2*i)=cx;
end
for i=1:Ly
ay=[0 1; -wny(i)^2 -2*zetay(i)*wny(i)];
by=[0 0; alph(3)*(wny(i)^2)/ky(i) alph(4)*(wny(i)^2)/ky(i)];
cy=[0 0; 1 0];

Ay(2*i-1:2*i,2*i-1:2*i)=ay;
By(2*i-1:2*i,:)=by;
Cy(:,2*i-1:2*i)=cy;
end
xx=size(Ax);yy=size(Ay);

A=[Ax zeros(xx(1),yy(2)); zeros(yy(1),xx(2)) Ay];
```

```
B=[Bx; By];
C=[Cx Cy];
D=[0 0];
```

A6. Subfunction for Edge theorem approach

```
%filename Edge_3Parameters.m
%written by Eldon Graham
%evaluates extreme polynomials and applies Zero Exclusion
%call function poly to evaluate extreme polynomials
P(:,8)=polyE(alphmin,w,a,T,wnx(1,:),zetax(1,:),kx,wny(1,:),zetay(1,:),ky,N,Ktc(1))';
P(:,7)=polyE(alphmin,w,a,T,wnx(2,:),zetax(1,:),kx,wny(2,:),zetay(1,:),ky,N,Ktc(1))';
P(:,6)=polyE(alphmax,w,a,T,wnx(2,:),zetax(1,:),kx,wny(2,:),zetay(1,:),ky,N,Ktc(2))';
P(:,5)=polyE(alphmax,w,a,T,wnx(1,:),zetax(1,:),kx,wny(1,:),zetay(1,:),ky,N,Ktc(2))';
P(:,4)=polyE(alphmin,w,a,T,wnx(1,:),zetax(2,:),kx,wny(1,:),zetay(2,:),ky,N,Ktc(1))';
P(:,3)=polyE(alphmin,w,a,T,wnx(2,:),zetax(2,:),kx,wny(2,:),zetay(2,:),ky,N,Ktc(1))';
P(:,2)=polyE(alphmax,w,a,T,wnx(2,:),zetax(2,:),kx,wny(2,:),zetay(2,:),ky,N,Ktc(2))';
P(:,1)=polyE(alphmax,w,a,T,wnx(1,:),zetax(2,:),kx,wny(1,:),zetay(2,:),ky,N,Ktc(2))';
%Real and imaginary parts of each polynomial
X=real(P);
Y=imag(P);
for i=1:M
   vertices=convhull(X(i,:),Y(i,:));
   judge(i)=inpolygon(0,0,X(i,vertices),Y(i,vertices));    %check if origin between edges
   if judge(i)==1 %reached boundary of unstable region
      break;
   end
end
if judge==0     %within stable range, dont do anything
   b=1;
else        % unstable case
  b=0;
end
```

A7. Subfunction for Quadratic Stability

```
%filename QS_LMI.m
%written by Eldon Graham
%calculates stability using quadratic stability, finds common Lyapunov
%matrix
%extreme system matrices
AAA(:,:,1)=[A1+0.25*(1/pi)*N*a*Ktc(2)*B1*(eye(length(Dd))-Dd)*C1
-0.25*(1/pi)*N*a*Ktc(2)*B1*Cd; Bd*C1 Ad];
AAA(:,:,2)=[A2+0.25*(1/pi)*N*a*Ktc(2)*B2*(eye(length(Dd))-Dd)*C2
-0.25*(1/pi)*N*a*Ktc(2)*B2*Cd; Bd*C2 Ad];
AAA(:,:,3)=[A3+0.25*(1/pi)*N*a*Ktc(2)*B3*(eye(length(Dd))-Dd)*C3
-0.25*(1/pi)*N*a*Ktc(2)*B3*Cd; Bd*C3 Ad];
AAA(:,:,4)=[A4+0.25*(1/pi)*N*a*Ktc(2)*B4*(eye(length(Dd))-Dd)*C4
-0.25*(1/pi)*N*a*Ktc(2)*B4*Cd; Bd*C4 Ad];
AAA(:,:,5)=[A5+0.25*(1/pi)*N*a*Ktc(1)*B5*(eye(length(Dd))-Dd)*C5
-0.25*(1/pi)*N*a*Ktc(1)*B5*Cd; Bd*C5 Ad];
AAA(:,:,6)=[A6+0.25*(1/pi)*N*a*Ktc(1)*B6*(eye(length(Dd))-Dd)*C6
-0.25*(1/pi)*N*a*Ktc(1)*B6*Cd; Bd*C6 Ad];
AAA(:,:,7)=[A7+0.25*(1/pi)*N*a*Ktc(1)*B7*(eye(length(Dd))-Dd)*C7
-0.25*(1/pi)*N*a*Ktc(1)*B7*Cd; Bd*C7 Ad];
AAA(:,:,8)=[A8+0.25*(1/pi)*N*a*Ktc(1)*B8*(eye(length(Dd))-Dd)*C8
-0.25*(1/pi)*N*a*Ktc(1)*B8*Cd; Bd*C8 Ad];
```

```
nAA=size(AAA(:,:,1),1);
setlmis([])
P = lmivar(1,[nAA 1]);
lmiterm([1 1 1 P],1,AAA(:,:,1),'s')   % PAA+AA'P
lmiterm([2 1 1 P],1,AAA(:,:,2),'s')
lmiterm([3 1 1 P],1,AAA(:,:,3),'s')
lmiterm([4 1 1 P],1,AAA(:,:,4),'s')
lmiterm([5 1 1 P],1,AAA(:,:,5),'s')
lmiterm([6 1 1 P],1,AAA(:,:,6),'s')
lmiterm([7 1 1 P],1,AAA(:,:,7),'s')
lmiterm([8 1 1 P],1,AAA(:,:,8),'s')
lmiterm([-9 1 1 P],1,1)        % P
lmisys = getlmis;
[copt,xopt] = feasp(lmisys1);
if copt>=0
   b=0;  % unstable case
else
   b=1;  % stable case
end
```

A8. Subfunction for Time Invariant Parameter Dependent Quadratic Stability

```
%filename TIPDQS_LMI.m
%written by Eldon Graham with collaboration by Dr. Nagamune
%calculates stabiltiy using time invariant parameter dependent quadratic
%stability case
%extreme system matrices
AAA(:,:,1)=[A1+0.25*(1/pi)*N*a1*Ktc(2)*B1*(eye(length(Dd))-Dd)*C1
-0.25*(1/pi)*N*a1*Ktc(2)*B1*Cd; Bd*C1 Ad];
AAA(:,:,2)=[A2+0.25*(1/pi)*N*a1*Ktc(2)*B2*(eye(length(Dd))-Dd)*C2
-0.25*(1/pi)*N*a1*Ktc(2)*B2*Cd; Bd*C2 Ad];
AAA(:,:,3)=[A3+0.25*(1/pi)*N*a1*Ktc(2)*B3*(eye(length(Dd))-Dd)*C3
-0.25*(1/pi)*N*a1*Ktc(2)*B3*Cd; Bd*C3 Ad];
AAA(:,:,4)=[A4+0.25*(1/pi)*N*a1*Ktc(2)*B4*(eye(length(Dd))-Dd)*C4
-0.25*(1/pi)*N*a1*Ktc(2)*B4*Cd; Bd*C4 Ad];
AAA(:,:,5)=[A5+0.25*(1/pi)*N*a1*Ktc(1)*B5*(eye(length(Dd))-Dd)*C5
-0.25*(1/pi)*N*a1*Ktc(1)*B5*Cd; Bd*C5 Ad];
AAA(:,:,6)=[A6+0.25*(1/pi)*N*a1*Ktc(1)*B6*(eye(length(Dd))-Dd)*C6
-0.25*(1/pi)*N*a1*Ktc(1)*B6*Cd; Bd*C6 Ad];
AAA(:,:,7)=[A7+0.25*(1/pi)*N*a1*Ktc(1)*B7*(eye(length(Dd))-Dd)*C7
-0.25*(1/pi)*N*a1*Ktc(1)*B7*Cd; Bd*C7 Ad];
AAA(:,:,8)=[A8+0.25*(1/pi)*N*a1*Ktc(1)*B8*(eye(length(Dd))-Dd)*C8
-0.25*(1/pi)*N*a1*Ktc(1)*B8*Cd; Bd*C8 Ad];
nAAA = size(AAA,1);
NN = size(AAA,3);
cvx_precision best
cvx_solver sdpt3
tol = sqrt(eps);
cvx_begin sdp
variable P(nAAA,nAAA,NN) symmetric
for j=1:NN
   P(:,:,j)*AAA(:,:,j)+AAA(:,:,j)'*P(:,:,j)<-eye(nAAA);
   P(:,:,j)>tol*eye(nAAA);
end
for j=1:NN-1
   for k=j+1:NN
```

```
      P(:,:,k)*AAA(:,:,j)+AAA(:,:,j)'*P(:,:,k)...
         +P(:,:,j)*AAA(:,:,k)+AAA(:,:,k)'*P(:,:,j)<2/(NN-1)*eye(nAAA);
   end
end
cvx_end
if cvx_optval<eps          % stable case
   b=1;
else                    % unstable case
   b=0;
end
```

A9. Subfunction for Time Varying Parameter Dependent Quadratic Stability

```
%filename TVPDQS_LMI.m
%written by Eldon Graham with collaboration by Dr. Nagamune
%calculates stabiltiy using time varying parameter dependent quadratic case
%only consider two varying parameters
[A1,B1,C1,D1]=dynamicstf(wnx(:,2),zetax(:,3),kx,wny(:,2),zetay(:,3),ky,alphmax);
[A2,B2,C2,D2]=dynamicstf(wnx(:,2),zetax(:,3),kx,wny(:,2),zetay(:,3),ky,alphmin);
[A3,B3,C3,D3]=dynamicstf(wnx(:,1),zetax(:,3),kx,wny(:,1),zetay(:,3),ky,alphmax);
[A4,B4,C4,D4]=dynamicstf(wnx(:,1),zetax(:,3),kx,wny(:,1),zetay(:,3),ky,alphmin);
%extreme system matrices
AAA(:,:,1)=[A1+0.25*(1/pi)*N*a*Ktc(2)*B1*(eye(length(Dd))-Dd)*C1
-0.25*(1/pi)*N*a*Ktc(2)*B1*Cd; Bd*C1 Ad];
AAA(:,:,2)=[A2+0.25*(1/pi)*N*a*Ktc(1)*B2*(eye(length(Dd))-Dd)*C2
-0.25*(1/pi)*N*a*Ktc(1)*B2*Cd; Bd*C2 Ad];
AAA(:,:,3)=[A3+0.25*(1/pi)*N*a*Ktc(2)*B3*(eye(length(Dd))-Dd)*C3
-0.25*(1/pi)*N*a*Ktc(2)*B3*Cd; Bd*C3 Ad];
AAA(:,:,4)=[A4+0.25*(1/pi)*N*a*Ktc(1)*B4*(eye(length(Dd))-Dd)*C4
-0.25*(1/pi)*N*a*Ktc(1)*B4*Cd; Bd*C4 Ad];
nAAA = size(AAA,1);
NN = size(AAA,3);
cvx_precision default
cvx_solver sdpt3
tol = sqrt(eps);
cvx_begin sdp
variable P(nAAA,nAAA,NN) symmetric
%   feasibility problem
for j=1:NN
   for jj = 0:2^NN-1
      pmtmp = dec2bin(jj,NN);
      coef = ((-1).^(pmtmp)).*rhovec;
      Psum = zeros(nAAA);
      for jjj=1:NN
         Psum = Psum+coef(jjj)*P(:,:,jjj);
      end
      P(:,:,j)*AAA(:,:,j)+AAA(:,:,j)'*P(:,:,j)+Psum...
         <-tol*eye(nAAA);
      if j<NN
         for k=j+1:NN
            P(:,:,k)*AAA(:,:,j)+AAA(:,:,j)'*P(:,:,k)...
               +P(:,:,j)*AAA(:,:,k)+AAA(:,:,k)'*P(:,:,j)+2*Psum...
               <-tol*eye(nAAA);
         end
      end
   end
```